Regulation of Membrane Traffic at the Golgi Apparatus by Rab GTPases and their GAPs

Dissertation

zur Erlangung des

Doktorgrades der Naturwissenschaften

(Dr. rer. nat.)

der Fakultät für Biologie der

Ludwigs-Maximilians-Universität München

vorgelegt von

Evelyn Fuchs

München 2007

Dissertation eingereicht am: 30. August 2007

Tag der mündlichen Prüfung: 22. Februar 2008

Erstgutachter: Prof. Dr. Erich Nigg

Zweitgutachterin: PD Dr. Angelika Böttger

Ehrenwörtliche Versicherung und Erklärung über frühere Promotionsversuche

Hiermit versichere ich, Evelyn Fuchs, ehrenwörtlich, dass die vorgelegte Dissertation von mir selbständig und ohne unerlaubte Hilfe angefertigt ist. Desweiteren erkläre ich, dass die vorgelegte Dissertation weder ganz noch in wesentlichen Teilen einer anderen Prüfungskomission vorgelegt wurde. Ich habe mich anderweitig keiner Doktorprüfung unterzogen.

München, 19. August 2007

Evelyn Fuchs

Table of contents

Summary

Rab family GTPases together with their regulators define specific pathways of membrane traffic within eukaryotic cells. Dependent on the bound nucleotide, they exist in an inactive (GDP) and active (GTP) state. In their active state, Rab GTPases are able to recruit specific effector proteins required for vesicle motility and membrane fusion. Guanine nucleotide exchange factors (GEFs) and GTPase-activating proteins (GAPs) control the activation state of the Rab GTPase and therefore the functional relationship with effector proteins.

The first part of this work focuses on the Golgi localised GTPase Rab6. Rab6 interacts with the dynein-dynactin microtubule motor complex, through the p150[glued] subunit and the coiled-coil proteins Bic-D1 and Bic-D2 (Matanis et al., 2002; Short et al., 2002). In this way, Rab6 facilitates the minus-end-directed transport of vesicles along microtubules. However, many details of this Rab6 pathway remain unclear. Therefore, a screen for novel Rab6 effector proteins was carried out. This led to the identification of PIST as a Rab6 binding protein. Biochemical and cell biological analysis showed that PIST is a strong and specific binding partner of Rab6 in vitro and in vivo. However, PIST localised to Golgi membranes independently of Rab6 and was not affected in cells with altered Rab6 protein levels. Thus, the function of PIST as a Rab6 binding protein remains unclear.

In the second part of this work the family of Rab GTPase-activating proteins (GAPs) was investigated. The 39 predicted human GAPs were tested for their ability to interfere with the trafficking of Shiga toxin from the cell surface to the Golgi apparatus, and with the transport of the epidermal growth factor (EGF) from the cell surface to endosomes. The screen identified 6 GAPs (EVI5, RN-tre, TBC1D10A-C, and TBC1D17) as specific regulators of Shiga toxin, but not EGF uptake. Biochemical assays showed that Rab43 is the target of RN-tre, and is required for Shiga toxin uptake. In contrast, RabGAP-5, a Rab5 GAP, was unique amongst the GAPs tested and reduced uptake of EGF but not Shiga toxin. These results suggest that Shiga toxin trafficking to the Golgi is a multi-step process controlled by a number of Rab GAPs and their target Rabs, and that this process is discrete from ligand-induced EGF-receptor trafficking.

1 Introduction

1.1 The Golgi apparatus: Processing and sorting station along intracellular transport routes

1.1.1 The Golgi apparatus in a cell biological view

A defining characteristic of eukaryotic cells is their compartmentalisation into physically separated and functionally distinct organelles. This is reflected in the specific subset of proteins and lipids present in the lumen or in the enclosing lipid bilayer of each organelle. Therefore, the maintenance of the structural and functional organisation of a eukaryotic cell requires an efficient transport system for newly synthesised proteins and lipids from their site of production to their final destination within or outside the cell.

At the centre of this intracellular transport system is the Golgi apparatus, linking the endoplasmic reticulum (ER) with endosomes and the plasma membrane. First described by Camillo Golgi in the year 1898 as an "internal reticular apparatus" in neurons (Bentivoglio and Mazzarello, 1998; Golgi, 1898), we now know that the Golgi apparatus is a ubiquitous organelle present in every cell type except for red blood cells and conserved from yeast to mammals. Dependent on the organism and on the particular needs of specialised cells, the Golgi apparatus can vary in shape and size. A common feature, however, is the modification and sorting of protein and lipid cargo within the Golgi membrane system. A general overview of the mammalian Golgi apparatus structure and function, as well as mechanisms and routes determining intracellular transport will be provided in the next chapters.

1.1.2 Structure and function of the Golgi apparatus

The mammalian Golgi apparatus consists of a series of overlapping flattened membrane-enclosed cisternal structures. Several cisternae are arranged in layers and build a so-called stack. Golgi stacks can be interconnected by membrane tubules and associated with vesicular structures (Farquhar and Palade, 1981). How the cisternae are hold together in stacks without fusing with one another is not yet fully understood. It has been proposed that a proteinaceous matrix shapes and organises Golgi cisternae, by linking membranes to each other and to the cytoskeleton. Key components of this Golgi matrix are long coiled-coil proteins termed Golgins, regulated by the Rab family of small GTPases. Together with actin filaments or microtubules and associated motor proteins, these proteins may play a

role in maintaining Golgi architecture and in directing membrane trafficking (Gillingham and Munro, 2003; Short et al., 2005).

Within the cell the Golgi apparatus is located in the perinuclear region close to the centrosome. This positioning is microtubule dependent. Upon depolymerisation of microtubules using the drug nocodazole, the ribbon-like structure of the Golgi apparatus breaks apart into smaller individual stacks distributed throughout the cytoplasm (Robbins and Gonatas, 1964; Rogalski et al., 1984). Thus, the complex Golgi membrane system is not randomly oriented in the cytoplasm but closely linked to the cytoskeleton. This is important for regulated secretion in polarised cells, e.g. at the leading edge of migrating cells. Stimulated by intracellular signalling processes involving kinases of the Ste20 family, PAK4 and protein kinase D family members (Preisinger and Barr, 2005), the Golgi apparatus polarises together with the centrosome towards the site of membrane protrusion and delivers membrane cargo to the outgrowing side of the cell (Corthesy-Theulaz et al., 1992; Kupfer et al., 1982; Preisinger et al., 2004).

At the onset of mitosis the Golgi stack breaks down into small vesicles (mitotic haze), which become partitioned between the forming daughter cells. This process is also linked to intracellular signalling cascades. Phosphorylation of Golgi structural proteins by Cdk1-cyclin B, polo-like and mitogen-activated kinases, induces the reorganisation of Golgi stacks during mitosis (Acharya et al., 1998; Lowe et al., 1998; Preisinger and Barr, 2005; Sutterlin et al., 2001). Whether the Golgi apparatus keeps its own identity and remains discrete in vesicular shape, or whether Golgi components redistribute to the ER and are inherited as a merged compartment before Golgi stacks reform from newly established ER exit sites in telophase, is currently debated (Altan-Bonnet et al., 2006; Axelsson and Warren, 2004; Pecot and Malhotra, 2004; Pecot and Malhotra, 2006).

As the central organelle of the secretory pathway the Golgi apparatus exhibits a defined polarity. The *cis* side of the stacks faces the ER and defines the site of lipid and protein cargo input arriving from ER exit sites. The opposite side of the Golgi apparatus, where lipid and protein sorting to other organelles or to the plasma membrane occurs, is referred to as *trans* Golgi, flanked by a tubular-vesicular network called *trans* Golgi network (TGN).
Besides cargo sorting and secretion the main function of the Golgi apparatus is to catalyse complex lipid and protein modifications, like N- and O-linked glycosylation or sulfation. This is accomplished by a variety of enzymes residing in discrete Golgi cisternae, dependent on their order of action more towards the *cis* or *trans* face of the Golgi apparatus. As lipids and proteins become modified in a serial manner the

temporal and spatial organisation of these enzymes is crucial for the correct pattern of modification (Spiro, 2002). Like all post-translational modifications, glycosylation is an important means of creating functional diversity in lipids and proteins. Errors in the glycosylation pattern can result in severe diseases such as the congenital disorders of N-glycosylation caused by mutations in genes required for glycosylation and Golgi function (Aridor and Hannan, 2002; Olkkonen and Ikonen, 2006).

All trafficking steps to, from and within the Golgi apparatus and thus the Golgi cisternae themselves are highly dynamic and need to be regulated in a complex way. The full details of membrane trafficking through the Golgi apparatus are not yet known but the importance of the Golgi apparatus as central sorting and modifying station along intracellular and secretory transport routes can be seen clearly in the long list of diseases linked to Golgi dysfunction (Aridor and Hannan, 2000; Aridor and Hannan, 2002).

1.1.3 Molecular mechanisms of intracellular transport

Intracellular traffic between compartments occurs through membrane vesicles or tubules budding off from a donor membrane and fusing with an acceptor membrane downstream of the transport process (Figure 1.1). These vesicle fission and fusion processes are facilitated by a number of molecules, which are either integral transmembrane proteins or peripheral membrane proteins recruited from the cytoplasm.
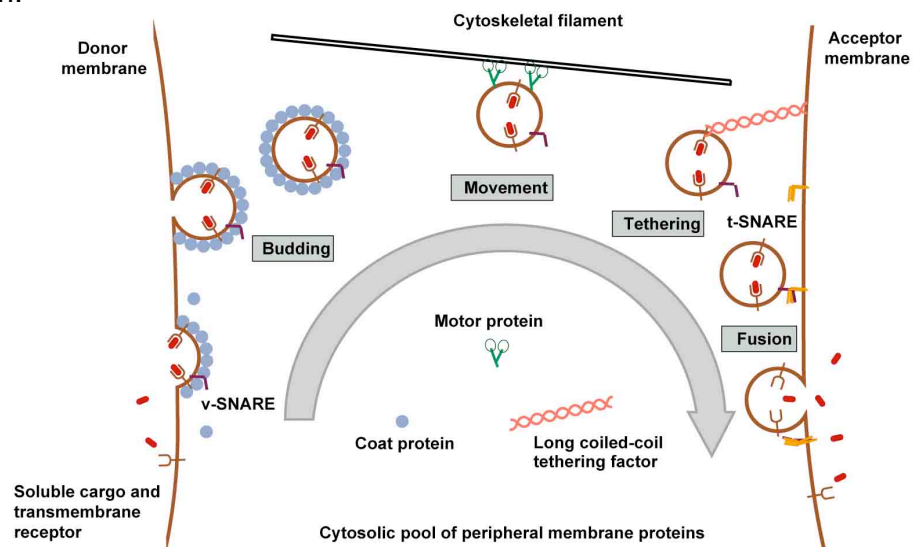
Figure 1.1 The four main steps of vesicular transport, which involve budding of the vesicle from the donor membrane, movement along microtubule or actin filaments, tethering to the acceptor membrane and fusion of vesicular and acceptor membrane. Proteins that facilitate these processes are either integral membrane proteins (e.g. cargo receptors, SNAREs), or recruited from the cytoplasm (e.g. coat proteins, motor proteins, tethering factors). Figure adapted from (Behnia and Munro, 2005).

Coat proteins play a vital role in vesicle budding. Together with adaptor proteins and transmembrane cargo receptors, they associate with the donor membrane. The coated membrane region gets curved and adapts a ball-like structure, which finally pinches off as a free vesicle. Three different coat machineries are known so far: Clathrin coated vesicles budding from the plasma membrane, endocytic structures and *trans* Golgi regions, COPI coated vesicles in intra Golgi and retrograde transport and COPII coated vesicles carrying cargo from ER exit sites to the *cis* Golgi network (Bonifacino and Glick, 2004). Also GTPases, like dynamin, Arf or Sar1 are involved in coat formation and vesicle fission (Bonifacino and Glick, 2004). One class of proteins, the CtBP/BARs, was just recently discovered to convey membrane curvature and induce the formation of membrane tubules, which can be important for vesicle formation and abscission (Corda et al., 2006). It is hard to imagine that only three different coat machineries accomplish the full variety of vesicular transport steps. Despite the fact that the COPI and COPII machinery can adjust its exact composition of protein components according to the kind of sorting process within the vesicle, one speculates that there are more, so far unknown coats and also uncoated mechanisms of vesicle budding (Bonifacino and Glick, 2004).

Once the vesicle has budded off the donor compartment, the coat proteins dissociate and the vesicle gets transported to the acceptor compartment. Interaction with motor proteins facilitates transport along microtubules or actin filaments (Matanis et al., 2002; Seabra and Coudrier, 2004; Short et al., 2002). At the acceptor membrane tethering factors, usually long coiled-coil proteins, can help to bring vesicles close to the target membrane. Tethering factors are recruited from the cytosol by small GTPases of the Rab family, which are anchored in the membrane through a C-terminal lipid modification (Pfeffer, 2001; Zerial and McBride, 2001). The actual fusion reaction is driven by the interaction of SNARE proteins. A specific v-SNARE on the vesicle interacts with the t-SNAREs of the target membrane, inducing a conformational shift in these proteins, which generates the force necessary to merge two membranes (Chen and Scheller, 2001; Pelham, 2001).

The variety of compartments and the high number of different forward and retrograde transport routes within the cell require that both, donor and acceptor membrane are well defined and can be specifically recognised by the respective transport machinery. Many of the proteins that mediate transport between organelles are cytosolic proteins and need to be recruited to the cytosolic face of the membrane. The unique identity of a membrane domain is conferred, on the one hand by transmembrane proteins, like cargo receptors or SNAREs, and on the other

hand by activated Rab GTPases and specific lipids, such as phosphoinositides. Four forms of phosphatidylinositol are known to localise to different organelles. PI(4)P is generated in Golgi membranes and in the plasma membrane, whereas PI(4.5)P_2 is found only in the plasma membrane. PI(3)P is predominantly found in early endosomes, PI(3,5)P_2 in late endosomes and lysosomes (Behnia and Munro, 2005). Specific lipid kinases and phosphatases regulate the transformation of phosphatidylinositol forms and are therefore important players in organelle identity and intracellular transport (Choudhury et al., 2005). Out of 60 human Rabs only a handful have been shown to localise to distinct membrane compartments and to be involved in specific transport routes. The best characterized is Rab5 which is involved in the homotypic fusion of early endosomes. Less is known about the Rab co-factors for nucleotide exchange and GTP-hydrolysis, the GEFs and GAPs (see 1.3). So, the puzzle of membrane identity and specificity in intracellular transport is far away from being solved.

1.1.4 Anterograde transport and Exocytosis

Anterograde transport is the transport of lipids and proteins from their site of production in or at the ER to various destinations within the cell or secretion outside of the cell. Cargo to be sorted or secreted leaves the ER at so called ER exit sites in COPII coated vesicular or tubular structures (Duden, 2003; Klumperman, 2000). ER exit sites are marked by the absence of ribosomes and the presence of the ER integral membrane protein Sec12p, which acts as an exchange factor for the GTPase Sar1. Thereby, Sar1 is locally activated and initiates COPII coat formation at ER exit sites (Pfeffer, 2003). Transmembrane proteins to be transported are enclosed directly into a COPII vesicle whereas soluble cargo binds transmembrane cargo receptors such as ERGIC53 to be enriched in the lumen of the forming vesicle (Appenzeller-Herzog and Hauri, 2006). In general, only proteins, which have passed the ER quality control for correct folding, can be transported. For that reason chaperones like BiP or Calnexin can be found in ER exit sites. Vesicles or tubular structures leaving ER exit sites are believed to fuse shortly after to form vesicular-tubular clusters (VTCs) or the ER-to-Golgi intermediate compartment (ERGIC) (Appenzeller-Herzog and Hauri, 2006). VTCs are the first stations for lipid and protein sorting in the anterograde pathway. ER resident proteins are recycled back to the ER in COPI coated vesicles. Many of them carry signal sequences, which make them visible for retrograde sorting receptors, like the KDEL sequence is recognised by the KDEL-receptor. ER resident transmembrane proteins carry a C-

terminal basic sequence (KKXX) which is recognised by the COPI machinery for retrograde sorting (Pelham, 1996).

Cargo proteins destined for forward transport or secretion are transported further in COPII vesicles, which fuse then with the *cis* face of the Golgi apparatus. Subsequently cargo gets transported within the Golgi apparatus and modifications (glycosylation, sulfation) are carried out along this pathway. There is a debate going on whether cargo transport within the Golgi is facilitated via vesicles budding from one cisterna and fusing with the anterograde cisterna of the Golgi stack (vesicular transport model) or whether the Golgi cisternae themselves mature while enzymes along the biosynthetic pathway of carbohydrate and other modifications get recycled back in a retrograde fashion (cisternal maturation model) (Pelham, 2000). In reality it could be well true that a mixture of both pathways exists and that the vesicular transport is the fast track for small cargo whereas larger cargo has to take the slower route of cisternal maturation.

Finally, after cargo has got the full set of modifications, it reaches the *trans* Golgi region and the TGN. The TGN is primarily sorting station for arriving cargo. Vesicles are budding from the TGN as clathrin coated vesicles and are either destined for the endocytic membrane system or for the plasma membrane, where transmembrane proteins and lipids get incorporated into the plasma membrane and soluble cargo secreted to the extracellular space. Clathrin assembly at the TGN is regulated by Arf GTPases, activated locally by their GEFs, and by GGA-proteins, which are able to bind to the cytosolic side of cargo receptors. Some proteins carry a molecular tag for sorting. The N-linked oligosaccharide mannose-6-phosphate for example is an identification tag for lysosomal proteins and is recognised by a specific transmembrane receptor (mannose 6-phosphate receptor, MPR) shuttling between TGN and late endosomes/ lysosomes (Ghosh and Kornfeld, 2004). Other sorting signals for soluble and transmembrane proteins are less well understood (Rodriguez-Boulan and Musch, 2005).

1.2 Endocytosis and retrograde transport

1.2.1 Endocytic vesicle formation at the plasma membrane

Endocytosis is the process by which a cell takes up membrane components, receptor-associated ligands and soluble molecules from outside to various destinations within the cell. Endocytic trafficking is closely linked to signalling processes and is therefore necessary for cell growth and communication. In principle endocytosis is the opposite process to secretion and is also mediated by

vesicular membrane transport. Endocytic vesicles invaginate and pinch off from specific domains at the plasma membrane. Based on the requirement for coats and other proteins and lipids, different types of endocytic vesicle formation can be discriminated (Figure 1.2) (Nichols, 2003).
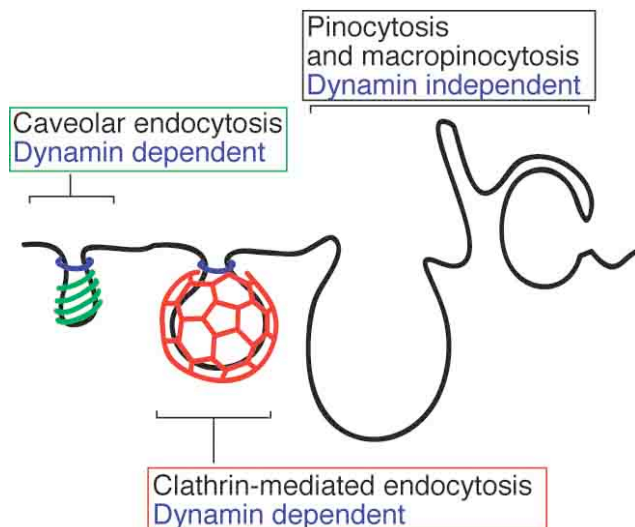
Figure 1.2 Endocytic vesicle formation at the plasma membrane. Both, clathrin-mediated and caveolar endocytosis require the GTPase dynamin for vesicle abscission, whereas other types of endocytosis don't. Due to its cage-like structure clathrin coated vesicle formation is well characterised. In contrast, it is not clear how many mechanisms of clathrin-independent endocytosis besides caveolar endocytosis exist. Figure taken from (Nichols, 2003).

Due to their unique cage-like structure in electron micrographs, clathrin coated pits were observed very early in cell biological research and belong to the best-studied processes in endocytosis (Roth, 2006). Clathrin is recruited to the plasma membrane by the multisubunit adaptor complex AP2 in cooperation with several other adaptor proteins, like Epsin or Eps15. Epsin is able to bind $PI(4,5)P_2$, a phosphoinositide generated mainly in the plasma membrane and in the TGN. By interaction with Eps15, Epsin recruits AP2 and clathrin subunits and additionally acts in curving the membrane for vesicle formation. AP2 and probably other adaptor proteins mediate the assembly of the clathrin cage around the forming vesicle (Mousavi et al., 2004). It should be noted that $PI(4,5)P_2$ alone is not sufficient to determine the site for clathrin coat formation on the plasma membrane. In order to be recruited to the membrane, AP2 seems to require also specific integral membrane proteins like synaptotagmin or cell surface receptors, which define membrane microdomains in clathrin coated pit formation (Mousavi et al., 2004). For the abscission of the coated vesicle the action of dynamin, a high-molecular-weight GTPase, is needed. Dynamin forms ring-like oligomers around the neck of the

budding vesicle, which constrict the membranes by conformational change upon GTP-hydrolysis. Because dynamin is also able to bind actin-modifying proteins, it may be involved in regulating actin polymerisation at the site of vesicle fission (Mousavi et al., 2004).

Clathrin-independent vesicle formation is less well understood. One example is caveolae-mediated endocytosis, characterised by the protein caveolin and a lipid compositon different from the surrounding membrane region, called lipid rafts. Lipid rafts are membrane microdomains enriched in cholesterol, glycosphingolipids, phospholipids, GPI-anchored proteins and integral membrane proteins. Caveolin binds cholesterol and is extremely resistant to detergent extraction (Nichols, 2003). Like clathrin-mediated endocytosis, caveolar endocytosis requires the activity of the GTPase dynamin. Yet, other clathrin-independent, mainly uncharacterised pathways exist that are dynamin-independent (Glebov et al., 2006; Nichols, 2003).

1.2.2 Endocytic sorting pathways

After budding endocytic vesicles fuse with each other to form the early endosomal compartment. This homotypic fusion process is regulated by the small GTPase Rab5 and its effector protein EEA1 (early endosomal antigen 1). EEA1 is a coiled-coil protein that dimerises and acts as a tethering factor to bring two membranes in close contact. EEA1 is recruited to the endosomal membrane by both, PI(3)P and active Rab5. Additionally EEA1 interacts with the SNARE Syntaxin13, which is important for the actual membrane fusion step (Woodman, 2000). The early endosome is the first sorting station within endocytic routes and is therefore also called sorting endosome. The entire endosomal system is extremely complex, therefore only the main endocytic routes are depicted in Figure 1.3 and will be described below.

The major determinant in early sorting steps is whether cargo is meant to be recycled back to the plasma membrane or to be further transported to intracellular destinations. One assumes that, by default, membrane and components like integral membrane proteins take the recycling pathway, whereas solute cargo is destined for the intracellular route. This is achieved by "geometry-based sorting", where membrane components are enriched in narrow endosome tubules from which vesicles bud off towards the plasma membrane, and solute cargo is left behind in the main lumen of the endosome (Maxfield and McGraw, 2004).
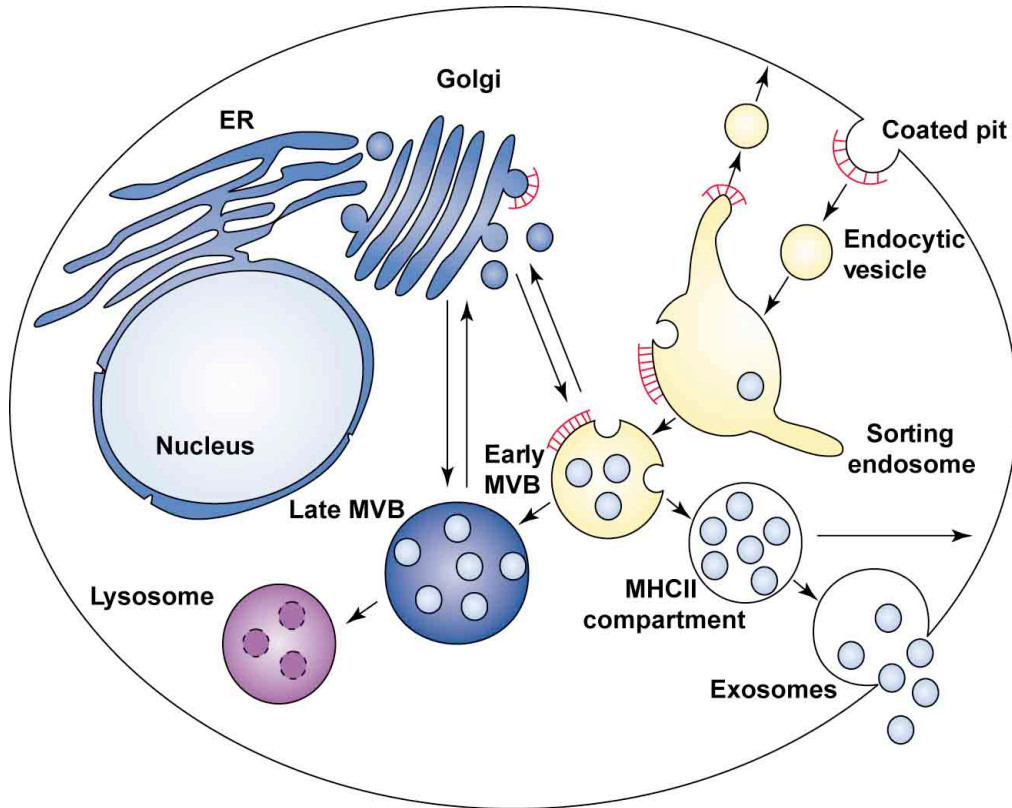
Figure 1.3 Main endocytic routes. Endocytic vesicles fuse to form the sorting endosome, from which cargo gets either recycled back to the plasma membrane or transported further to the late endosome/ early MVB (multivesicular body). In specialised cells, like antigen presenting cells, the early MVB can mature to form exosomes. In general, early MVBs are in exchange with the Golgi apparatus and can mature to form late MVBs and lysosomes, where protein degradation takes place. Clathrin is indicated in red and is involved in vesicle formation at the plasma membrane, in endocytic compartments and in the TGN. Figure adapted from (Raiborg et al., 2003).

An example for the recycling pathway is transferrin receptor (TfR), which transports iron bound to the carrier protein transferrin and shuttles between plasma membrane and sorting endosome. While the standard recycling route is taken by many nutrient receptors, activated mitogenic receptors, like the epidermal growth factor (EGF) receptor are marked for degradation by monoubiquitination and actively sorted into the internal vesicles of multivesicular bodies (see below) (Mukhopadhyay and Riezman, 2007; Urbe, 2005). Ligands are usually released in the sorting endosome due to the low pH (approx. pH6) and the receptor becomes free for another round of ligand uptake or for degradation in the lysosome. This first sorting step involving budding tubules and vesicles for recycling goes along with maturation of the core sorting endosome to form the late endosome. The maturation is accompanied by the exchange of key regulatory proteins, Rab7 is replacing Rab5, and by the transport towards the cell center along microtubules. The latter is mediated by the minus-end directed motor protein dynein (Bananis et al., 2004; Driskell et al., 2007;

Valetti et al., 1999). Late endosomal membranes can invaginate and create intralumenal vesicles. These multivesicular bodies (MVBs) can serve as storage intermediates for secretory lysosomes, like the MHCII compartment in antigen-presenting cells or function in receptor down-regulation (Raiborg et al., 2003). By sequestering the cytosolic signalling domain of transmembrane receptors to the luminal side of MVBs, any signalling cascade gets terminated prior to degradation of the receptor in the lysosome. In the past few years the molecular details of the MVB sorting machineries have elucidated. Networks of the multisubunit ESCRT (endosomal sorting complex required for transport) complexes recognise ubiquinated transmembrane receptors and drive their internalisation into lumenal vesicles of MVBs (Hurley and Emr, 2006; Williams and Urbe, 2007). Receptor-downregulation is a very important intracellular process to terminate extracellular signalling events. In the case of EGF receptor, whose activation leads to a stimulation of cell proliferation, MVB formation can even be referred to as a tumor suppressor pathway (Alexander, 1998; Dikic, 2003).

The endocytic system is in cross talk with other membrane systems like the Golgi apparatus. Late endosomes and MVBs can fuse with Golgi-derived vesicles carrying newly synthesised lysosomal hydrolases to build lysosomes for lipid and protein degradation. Apart from the exchange of lysosomal enzymes and the transport of their receptors (MPRs) back to the Golgi (see 1.1.4), other retrograde recycling pathways between endosomes and the Golgi apparatus exist, yet they are not well characterised. Most data on this subject were obtained from work with Shiga toxin and other bacterial toxins, which exploit existing cellular pathways in order to intoxicate the cell.

1.2.3 Retrograde transport of Shiga toxin

Shiga toxins and Shiga-like toxins are produced by *Shigella dysenteria* and some enterohaemorrhagic *E. coli* strains (EHEC). Infection with these bacteria occurs in most cases through poisoned food or water and causes severe diarrhoea and fatal complications like haemorrhagic uremic syndrome (HUS). Shiga toxin producing bacteria colonise and associate with the large intestinal mucosa, which causes severe inflammation and intestinal damage leading to diarrhoea and dehydration. Active toxin is secreted into the lumen of the gut and is able to enter the systemic circulation by translocation through the epithelial layer of the gut from the apical to the basolateral sides of the cells. Once circulating Shiga toxin intoxicates endothelial cells leading to microvascular thrombosis and organ damage mainly in the gastrointestinal tract, brain and kidney (O'Loughlin and Robins-Browne, 2001).

Similar to the bacterial Cholera toxin or the plant toxin ricin, Shiga toxin is a two subunit protein containing an enzymatically active A-subunit (32 kDa) and a pentameric B-subunit (7.7 kDa per monomer) that is important for binding and transport of the toxin into target cells (Figure 1.4 A). Both subunits are non-covalently linked to form the AB holotoxin. The five identical B-monomers build a doughnut-shaped structure that binds to the membrane glycolipid globotriasoyl ceramide (Gb3) on the cell surface of Shiga toxin sensitive cells (Sandvig et al., 2002). Cells deficient of the Shiga toxin receptor Gb3 are resistant to Shiga toxin. However, non-Gb3 mediated transport of the toxin seems to exist as human colon cancer cell lines devoid of Gb3 were shown to internalise Shiga toxin. The purpose of such a pathway could be the entry of the toxin into the systemic circulation without destroying the epithelial cell layer of the gut (O'Loughlin and Robins-Browne, 2001).
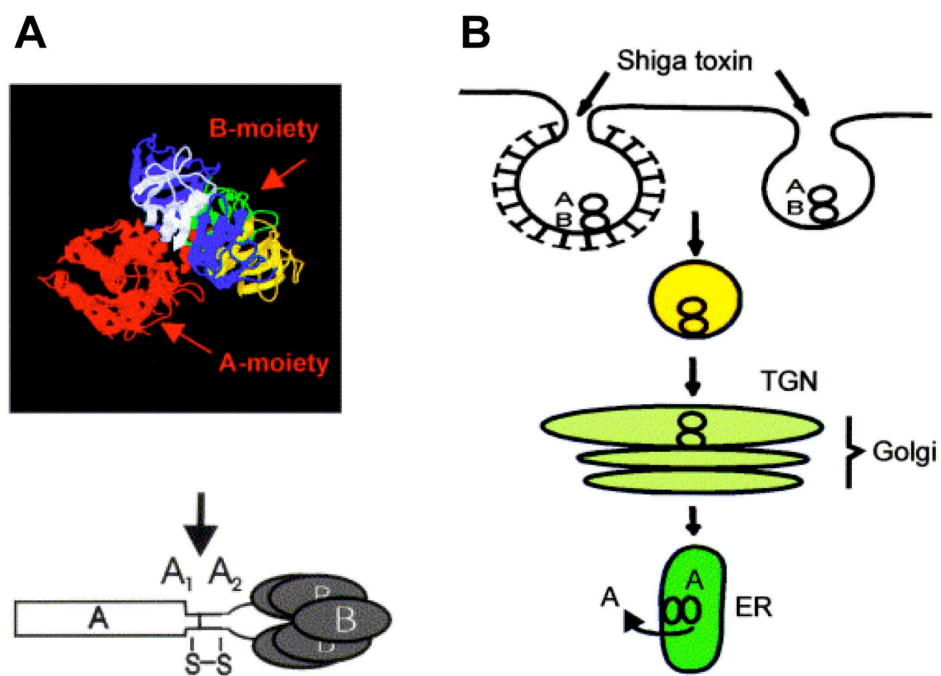
Figure 1.4 Structure and transport pathway of Shiga toxin. The full toxin comprises an enzymatically active A-subunit and a pentameric B-subunit, which is important for binding the toxin to the glycolipid Gb3 on the cell surface. In early endosomes, the A-subunit is cleaved into A_1 and A_2 but remains linked by a disulfide bond (A). After binding to the surface of Gb3 positive cells, Shiga toxin is endocytosed by clathrin-dependent and –independent mechanisms and transported to the Golgi apparatus. From there Shiga toxin is transported in a retrograde fashion to the ER, where the A-subunit is translocated to the cytosol (B). Figure adapted from (Sandvig and van Deurs, 2002).

After binding to Gb3 through its B-subunit Shiga toxin becomes endocytosed by clathrin-dependent and clathrin-independent (e.g. caveolae) pathways (Figure 1.4 B) (Sandvig and van Deurs, 2002). In early and recycling endosomes the

endopeptidase furin cleaves the A-subunit of Shiga toxin into disulphide linked A1 (29 kDa) and A2 (3 kDa) chains. This proteolytic cleavage transforms the non-toxic pro form of Shiga toxin into an active form, which is able to inhibit protein synthesis in target cells. From early and recycling endosomal compartments the toxin is transported to the trans Golgi network (TGN). This pathway depends on the function of clathrin and dynamin (Lauvrak et al., 2004), on the SNAREs Syntaxin5 and Syntaxin16 (Amessou et al., 2007), on the small GTPase Arl1 and its effector protein Golgin-97 (Lu et al., 2004), on the lipid phosphatase OCRL1 (Choudhury et al., 2005) and on Rab6 and its effector proteins (White et al., 1999). From the TGN the toxin is transported in a retrograde fashion through the Golgi apparatus to the ER. Unlike other bacterial toxins (e.g. *Pseudomonas* exotoxin A) Shiga toxin does not contain a KDEL sequence for efficient retrieval to the ER. It was shown that retrograde trafficking of Shiga toxin is COPI-independent (Girod et al., 1999) and relies on an alternative mechanism involving Rab6 (White et al., 1999). After arrival in the ER, the toxin A-subunit enters the cytosol by retro-translocation, probably subverting the ER-associated degradation pathway (ERAD) (Spooner et al., 2006; Yu and Haslam, 2005). Usually, retro-translocation is a quality control mechanism by which misfolded proteins are transported from the ER lumen to the cytosol where they are degraded by the ubiquitin-proteasome system (Tsai et al., 2002). Having arrived in the cytosol the toxin A-subunit is not degraded but refolds and inhibits protein synthesis by inactivating the ribosome. In detail, Shiga toxin A-subunit cleaves a specific N-glycosidic bond within the 28S rRNA, which leads to the release of a conserved adenine base in the position of the aminoacyl-tRNA acceptor site and consequently to a block in peptide chain elongation (O'Loughlin and Robins-Browne, 2001).

Although the basic steps of Shiga toxin transport and the mechanism of toxicity are known, the full molecular details of retrograde toxin trafficking remain obscure. Elucidation of intracellular processes required for efficient transport of Shiga toxin is not only of great medical interest but would also answer many cell biological questions concerning endogenous routes within the endocytic and secretory membrane system.

1.3 Rab GTPases: Molecular switches regulating membrane traffic

1.3.1 The Rab family of small GTPases

The human Ras superfamily of small GTPases comprises more than 150 human members and is divided in 5 family branches according to sequence and functional similarities: Ras, Rho, Rab, Ran and Arf. With 63 known members, the family of human Rab GTPases represents the biggest branch in the Ras superfamily of monomeric G proteins (Wennerberg et al., 2005). Like all small GTPases Rab proteins function as GDP/GTP-regulated molecular switches. While some Rabs are cell type or tissue specific, many are ubiquitously expressed (Pereira-Leal and Seabra, 2001). For instance, in melanocytes Rab27a regulates the trafficking of the pigment-containing melanosomes (Bahadoran et al., 2001; Hume et al., 2001; Wu et al., 2001), whereas Rab1 is a ubiquitous Rab defining ER to Golgi transport (Allan et al., 2000; Moyer et al., 2001).

Rab GTPases are localised to distinct membrane compartments and are regulators of secretory and endocytic intracellular transport pathways. They play a role in vesicle docking and fusion with target membranes and in vesicle motility through the recruitment of motor proteins, and some have also been implicated in receptor cargo selection and vesicle formation (Pfeffer, 2005a; Zerial and McBride, 2001). However, only a handful of Rabs and their effector proteins are characterised in detail and the impact of the majority of Rabs is largely unknown. Examples for well-established Rab functions are Rab1, which recruits the p115 tethering factor to ER-derived vesicles to mediate targeting and fusion to *cis* Golgi membranes (Allan et al., 2000; Moyer et al., 2001; Weide et al., 2001) or Rab9 and its effector protein TIP47, which is important for the selection of the mannose 6-phosphate receptor (MPR) to late endosomal vesicles for recycling of MPR to Golgi membranes (Aivazian et al., 2006; Carroll et al., 2001).

Rab GTPases are conserved from yeast to human. While the human genome contains more than 60 Rab genes, the fission yeast *Schizosaccharomyces pombe* possesses only seven and the budding yeast *Saccharomyces cerevisiae* only 12 Rab (or Ypt) genes (see Figure 1.5). In yeast, gene disruptions of either Rab results in lethality or in a severe phenotype concerning membrane trafficking (Pereira-Leal and Seabra, 2001). The yeast Rabs have homologues within the human Rab family and the members of this group are considered the "ancestral" Rabs, such as scYpt1/ hsRab1 regulating ER to Golgi trafficking. The increased number of Rab genes in humans might correspond to the functional diversification and cellular specialisation in a multicellular organism.
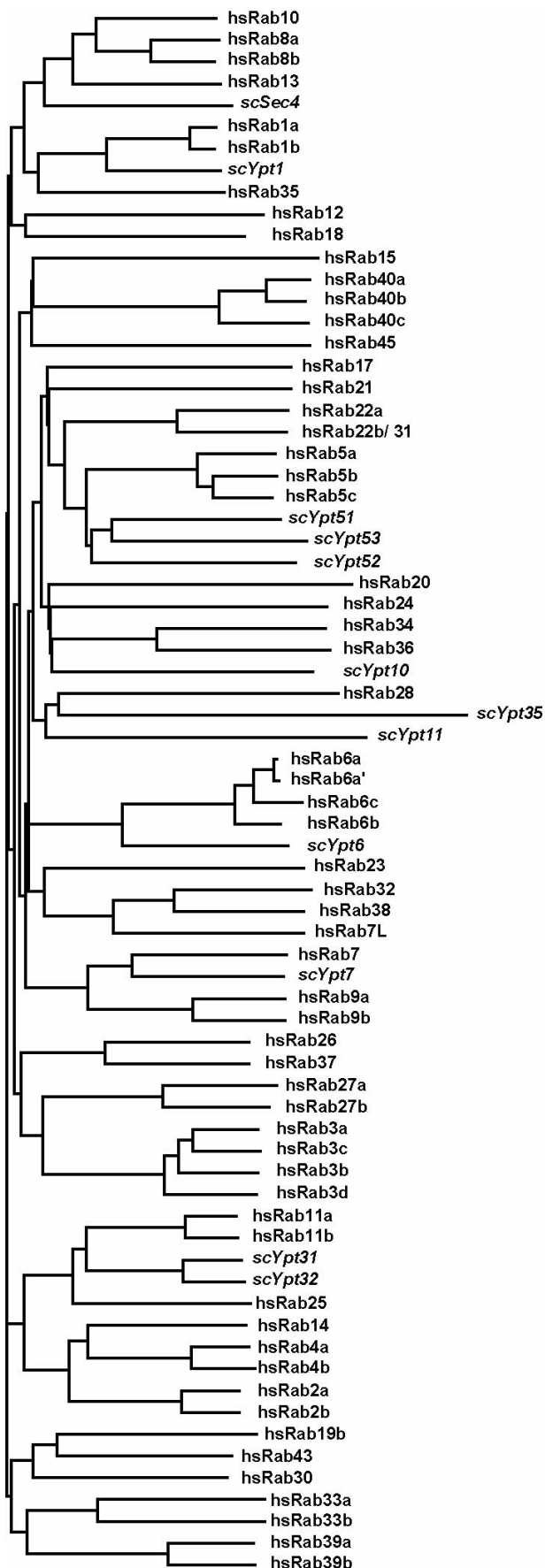
Figure 1.5 Phylogenetic tree of 60 human and 12 yeast Rabs/ Ypts. The Ypts from *Saccharomyces cerevisiae* are shown in italics.

All Rabs share a 20 kDa globular GTPase domain with conserved structure and biochemical properties. The G-domain is folded into a six-stranded β-sheet (β1 - β6) surrounded by five α-helices (α1 – α 5). Within the G-domain there are two regions that change their conformation dependent on the bound nucleotide GDP or GTP. They are located between α1 and β 2 and between β3 and β 4 and are called switch I and switch II regions (Ostermeier and Brunger, 1999; Pfeffer, 2005b). In and around these switch regions there are five Rab family specific motifs (RabF1 – RabF5) that determine the identity of a Rab and most likely the interface of effector and regulator binding. In addition, within clusters of related Rabs, there are sequence motifs that show higher identity than other regions. They are termed Rab subfamily motifs (RabSF1 – RabSF4) and define Rab isoforms, which share more than 70 % overall sequence identity, such as Rab1a and Rab1b (Pereira-Leal and Seabra, 2000).

Outside of the globular G-domain Rab GTPases exhibit a C-terminal hyper-variable region, which is unstructured and variable in length (approx. 30 – 40 amino acids). This sequence stretch together with other domain determinants is thought to be essential for Rab localisation in the target membrane (Pfeffer, 2005b). At the very C-terminus there are usually two cysteines, which are geranylgeranylated by geranylgeranyltransferase II. This post-translational lipid modification is needed to anchor the Rab in the membrane. In the cytosol a protein called GDI chaperones the double prenylated Rab in its GDP bound conformation. Structural studies show that the Rab GTPase sits on the side of GDI whereas the prenyl groups lie at the bottom of GDI, the first one deep inside a binding pocket, the second prenyl group more towards the surface of GDI (Pylypenko et al., 2006). The C-terminal hypervariable region stretches over the surface of GDI and represents a polypeptide linker between the globular GTPase domain and prenylation site. This extension could also be important for Rab function within the membrane, by positioning the active G-domain in distance to the lipid bilayer and therefore holding it available for cytosolic effector proteins.

1.3.2 The Rab GTPase cycle

Rab GTPases bind both, GDP and GTP with high affinities and usually exhibit low intrinsic GDP/GTP exchange rates. However, to act as molecular switches, the spatial and temporal control of GDP-bound, inactive and GTP-bound, active Rab conformation is necessary. So, the Rab GTPase itself is not sufficient to fulfil its role as a membrane organiser, and a whole set of other proteins is needed to initiate and control the Rab GTPase cycle (Figure 1.6).
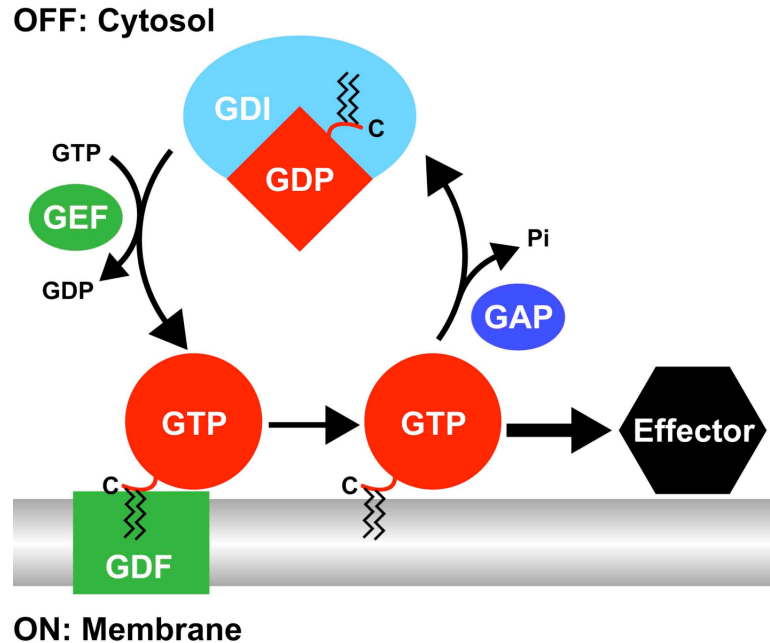
Figure 1.6 The Rab GTPase cycle. GDP bound prenylated Rab (red rhombus) is chaperoned in the cytosol by GDI. Upon membrane delivery, GDI is displaced by GDF and the Rab is inserted into the membrane by both prenyl groups at the C-terminus. A GEF catalyses the exchange of GTP for GDP and the Rab switches to its active state (red circle). Only in its active state a Rab can bind effector proteins, which can fulfill various functions within intracellular transport. Effector binding is terminated when the Rab switches back to its inactive, GDP-bound state. GTP-hydrolysis and the release of free phosphate is catalysed by GAP proteins.

In the cytoplasm, inactive Rab proteins in their GDP conformation are chaperoned by GDI (see above). Rab-GDI complexes were shown to contain all of the information needed to deliver the Rab to its target membrane. Within the membrane so-called GDI displacement factors (GDFs) can bind the Rab-GDI complex (Sivars et al., 2003). Upon this binding, conformational changes sequentially release both prenyl groups of the Rab from the GDI binding site and allow them to insert into the membrane. Once anchored in the membrane, the Rab protein is released from GDI and can start its functional cycle (Pylypenko et al., 2006). While GDI is a general factor and recognises all Rabs in their prenylated, GDP-bound state, there seem to exist several GDFs with distinct membrane localisation and selectivity for certain Rabs. The Golgi/ endosome localised transmembrane protein Yip3 has been shown to have GDI displacement factor activity for endosomal Rabs. According to BLAST searches and expression profiles there are 12 ubiquitously expressed members of the human Yip family, but only two have been shown to act as GDFs (Pfeffer and Aivazian, 2004).

In order to be activated, GDP must be exchanged for GTP in the Rab G-domain. A class of proteins called GEFs (guanine nucleotide exchange factors) catalyse this reaction by complex formation with the GDP-bound Rab. A subsequent

structural rearrangement in Switch I and Switch II within the Rab G-domain disrupts the interaction of Switch I with GDP and facilitates the release of GDP (Delprato et al., 2004; Dong et al., 2007; Sato et al., 2007). Because the concentration of GTP in the cytoplasm is far higher than that of GDP, nucleotide free Rab proteins are loaded preferentially with GTP. In their GTP-bound state Rabs change to their active conformation, which can be recognised and bound by effector proteins with high affinity. Rab effector proteins can have a variety of functions. They can be tethering factors for vesicle fusion or linkers to motor protein function (Grosshans et al., 2006; Zerial and McBride, 2001). Initially, Rab effectors were considered independent proteins recruited by a specific Rab in order to fulfil their function, but it turned out that some Rab effectors can even influence the stability and localisation of a Rab such as TIP47 stabilises Rab9 on late endosomal membranes (Ganley et al., 2004). Thus, effector proteins can play a role in recruitment of specific Rabs to specialised membrane micro-domains and therefore in defining membrane identity. The active state of Rab GTPases is turned off by hydrolysis of the bound GTP to GDP with release of free phosphate. Most Rabs exhibit a very slow intrinsic GTP-hydrolysis rate and need GTPase activating proteins (GAPs) for efficient enzymatic cleavage of the γ-phosphate group. Once in the inactive GDP-bound form the Rab protein gets either activated again by the GEF for another round of activity or retrieved to the cytosol through the interaction with GDI.

While GEFs for Rho or Ras GTPases are well characterised, relatively little is known about GEFs acting on Rab GTPases. So far, only a few GEFs for Rabs and their yeast homologues Ypts were identified. The best understood are Vps9/Rabex-5 which acts on Rab5, and the Sec2p GEF for the Sec4p GTPase in yeast (Dong et al., 2007) which belongs to the class of coiled-coil GEFs. In general, Rab GEFs are structurally unrelated and can be part of larger protein complexes, like the yeast TRAPP complex, regulating transport from the ER to the Golgi (Jones et al., 2000; Kim et al., 2006; Kim et al., 2005). Therefore, the systematic identification of putative GEFs by homology search is rather difficult. In contrast, Rab GAPs share a conserved domain, defining a family of about 40 human Rab GAP candidates.

1.3.3 Catalytic mechanism and members of the human Rab GAP family

Human Rab GAPs were identified through a conserved domain which was first defined in yeast GAPs for Ypts (Gyps). Because of its homology to regions in the Tre-2 oncogene and in the yeast mitotic regulators Bub2 and Cdc16 the domain was called TBC (Tre-2/Bub2/Cdc16) domain (Richardson and Zon, 1995). The TBC

domain is between 200 and 400 amino acids long and consists of six conserved sequence motifs (A-F) (Figure 1.7).

Figure 1.7 The TBC domain. The conserved sequence motifs IxxDxxR with the catalytic arginine (red R) and YxQ with the catalytic glutamine (red Q) for the dual-finger mechanism are given below the six conserved sequence motifs A-F.

Crystal structural analysis of the yeast Gyp1 in complex with human Rab33 showed that Rab GAPs act by a dual-finger mechanism (Pan et al., 2006). Similar to the "arginine finger" in Ras or Rho family GAPs a conserved arginine residue of the TBC domain inserts into the GTP binding pocket of the G-domain and mediates hydrogen-bonding with oxygen of the γ- and β-phosphate group of GTP. This interaction compensates the accumulation of negative charge at the β-phosphate group during the hydrolysis reaction. Concomitantly the TBC domain provides a conserved glutamine residue to coordinate the water molecule for the nucleophilic attack of the γ-phosphate (Pan et al., 2006). Before, it has been assumed that the coordination of the water molecule was mediated by a conserved glutamine (DxxGQ motif) of the Rab GTPase itself. This was the basis for constitutively active Rab QL mutants where GTP cannot be hydrolysed. From the structural study of (Pan et al., 2006) we now know that the conserved glutamine of the Rab instead mediates the interaction with a tyrosine residue and the amino group of the glutamine of the active site of the GAP. The motifs for the arginine and glutamine fingers in the TBC domain of the GAP are IxxDxxR (in motif B) and YxQ (in motif C) respectively. As both motifs are conserved throughout all yeast Gyps and in about 70 % of all known human Rab GAPs the dual-finger mechanisms seems to be the general principle of GTP hydrolysis catalysed by Rab GAPs. Based on the B and C active site motifs of the characterised yeast Gyps a database search for human homologues identified 39 potential human RabGAPs (Figure 1.8) (Francis Barr and Alexander Haas, unpublished results). Whereas some candidates comprise more or less only the TBC domain, many other contain other functional domains (RUN, GRAM, PH, PTB, SH3) that may regulate their activity or localisation.

```
              *     *    *
BUB2      Y Q K I K N D T S R T F Q T D P N F R N

AAH68496  D R Q I E V D I P R C H Q Y D E L L S S
EVI5      E K L I R R D I A R T Y P E H N F F K E
KIAA1055  S K Q I E L D L L R T L P N N K H Y S C
NP_060222 T E E I E R D L R R S L P - - E H P A F
NP_060779 Q N T I H K D C L Q F I D Q L S V P E E
NP_660288 E K L I R R D I A R T Y P E H E F F K G
NP_942568 T E E I E R D L H R S M P - - E H P A F
RN-tre    I R Q I D L D V N R T F R D H I M F R D
RUTBC1    - - - I D K D V Q R C D R - N Y W Y F T
RUTBC2    - - - I E K D V Q R C D R - N Y W Y F T
RUTBC3    A K Q I E K D L L R T M P S N A C F A S
TBC1D01   Q H A I L I D L G R T F P T H P Y F S A
TBC1D02   A R Q I E L D L N R T F P N N K H F T C
TBC1D03A  I Q Q M D L D V S G T L R R H I F F R D
TBC1D03B  I Q R I D R D V S G T L R K H I F F R D
TBC1D04   Q H A I L V D L G R T F P T H P Y F S V
TBC1D05   R S M I E Q D V K R T F P E M Q F F Q -
TBC1D06   E D A I R T D L N R T F P D N V K F R K
TBC1D07   - K E Q Y L D V L H A L K V V R F V S D
TBC1D08   T E E I E R D L H R S L P - - E H P A F
TBC1D10A  L D V I E R D L H R Q F P F H E M F V S
TBC1D10B  L D V I E K D L H R Q F P F H E M F A A
TBC1D10C  M E T I G R D L H R Q F P L H E M F V S
TBC1D11   D S A I T R D I N R T F P A H D Y F K D
TBC1D12   L E L I K L D I S R T F P S L Y I F Q -
TBC1D13   L L Q I D K D V R R L C S S L N E Y E V
TBC1D14   L E L I K L D I S R T F P N L C I F Q -
TBC1D15   R S L I E K D V N R T D R T N K F Y E G
TBC1D16   Q F T V D K D V V R T D R N N Q F F R G
TBC1D17   R S L I E R D V S R T D R T N K F Y E G
TBC1D18   E S V I T R D I H R T F P A H D Y F K D
TBC1D19   L Y Q V L L C F S R D T S V L S H F A F
TBC1D20   Y Q Q V L L D V R R S L R R F P P G M P
TBC1D21   R N N I A R D I Q K I Y D K D P L G N V
TBC1D22A  Y R Q I H I D I P R M S P E A - L I L Q
TBC1D22B  Y R Q I H I D I P R T N P L I P L F Q Q
USP6      I H H I D L D V R T T L R N H V F F R D
XM_037557 G I Q I V K D L H R T G C S - - S Y C G
XP_093895 T E E I E R D L H R S L P - - E H P A F
XP_370928 C L P L P E F V D N T Q V P S Y C L N A
Consensus     I e r D L   R T   p         f
```

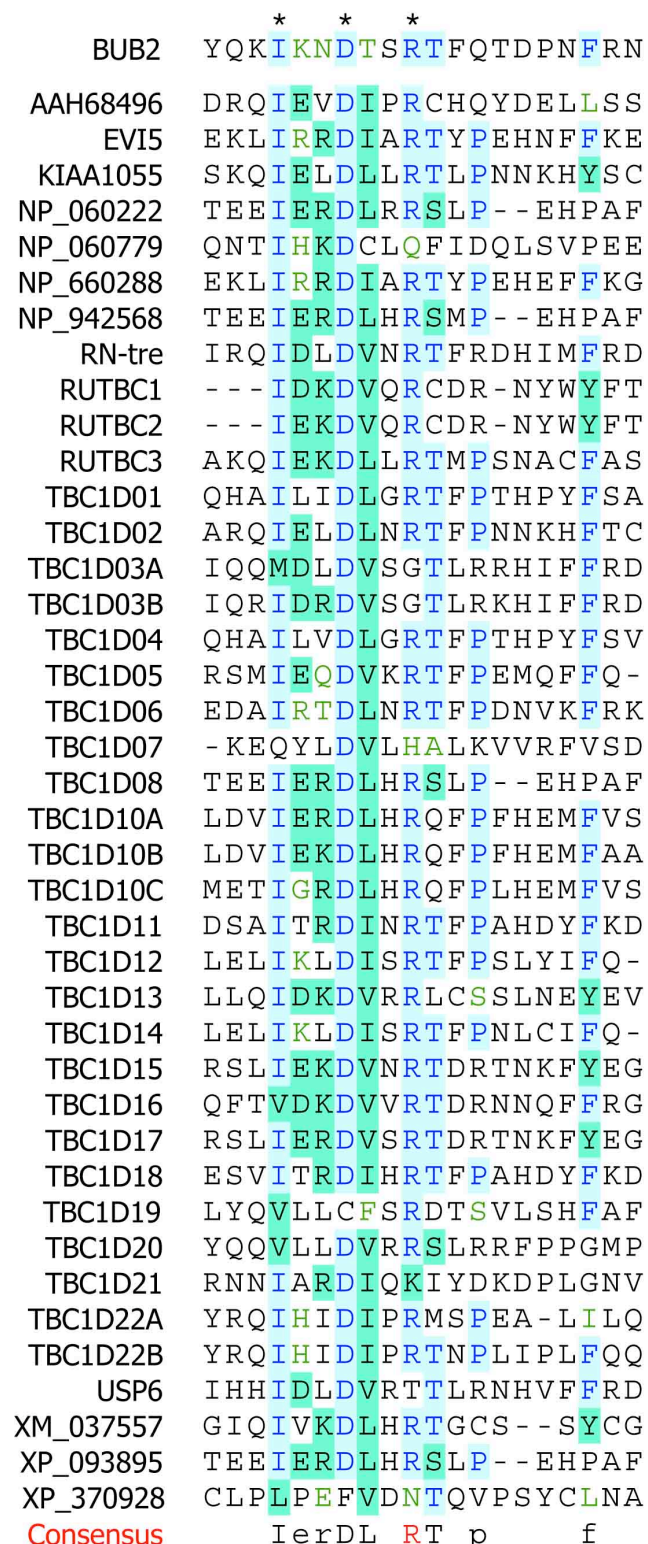**Figure 1.8 Alignment of the core B-motif of human TBC domain proteins with the yeast protein Bub2. Stars at the top indicate the conserved residues within the catalytic motif. At the bottom the consensus sequence containing the IxxDxxR arginine finger motif is depicted. Human TBC domain proteins are either shown with their full name according to the TBC nomenclature, or with their protein database accession number.**

1.4 Rab6: Role of a Golgi localised Rab

1.4.1 Isoforms and features of Rab6

Rab6 is a Golgi localised GTPase (Goud et al., 1990) and was one of the first human Rabs to be cloned (Zahraoui et al., 1989). There are three isoforms of Rab6, named Rab6a, Rab6b and Rab6c. Rab6a was found to exist in two isoforms Rab6a and Rab6a', which are generated by alternative splicing of a duplicated exon within the Rab6 gene. Both, Rab6a and Rab6a' are ubiquitously expressed and differ only in three amino acids (Echard et al., 2000). Rab6b is encoded by a different gene and exhibits 91 % amino acid sequence identity with the Rab6a protein. Rab6b also localises to the Golgi apparatus and interacts with known Rab6a effector proteins, but seems to be expressed in a tissue-specific manner, predominantly in brain (Opdam et al., 2000). The third Rab6 isoform, Rab6c, was described to play a role in multidrug resistance in the human breast cancer cell line MCF7/AdrR (Shan et al., 2000). However, it is unclear whether Rab6c functions as a classical Rab GTPase in terms of membrane anchoring and GTPase cycle. Whereas Rab6a and Rab6b are both 209 amino acids long and end at their C-terminus with two cysteines as prenylation sites, Rab6c contains a C-terminal extension of 46 amino acids, therefore lacks the C-terminal prenylation sequence needed for membrane attachement.

Rab6a is the best-characterised Rab6 isoform and is also the subject of this work. Unless otherwise stated Rab6a will be referred to as Rab6. In terms of intrinsic GTP hydrolysis Rab6 represents a special member of the Rab family. Bergbrede et al., 2005 showed that recombinant Rab6, purified from *E. coli*, is extremely stable in its GTP bound state and displays a very slow intrinsic GTP hydrolysis rate. The rate of GTP hydolysis was in the case of Rab6 5.0×10^{-6} s^{-1}, which is very slow compared to other Rab GTPases (Rab5: 5.5×10^{-4} s^{-1}, Rab7: 4.5×10^{-5} s^{-1}) Therefore, Bergbrede et al., 2005 were able to crystallise, for the first time, a wild-type Rab (Rab6) together with bound GTP instead of using Rab mutants or complexes of wild-type Rab with non-hydrolysable GTP analogues. The structural data obtained from these Rab6 crystals could explain the slow GTP hydolysis rate of Rab6. First, Rab6 has a very flexible Switch II region, which is important for the catalytic mechanism of GTP hydrolysis, and more efficient when more constrained as in the case of Rab5. Second, a bulky tyrosine residue in Switch I forms hydrogen bonds with the γ-phosphate of GTP, thus shielding the active site like a lid. This tyrosine residue is absent in the fast hydrolysing Rab5, and could be important for a slow intrinsic hydrolysis rate.

Although Rab6 itself is well characterised, there is no GEF for Rab6 known to date and the circumstances of Rab6 activation remain obscure. Also the mechanism of Rab6 inactivation by GTP hydrolysis in coordination with a GAP is not fully understood. Some years ago, a protein called GAPCenA was published to act as Rab6 GAP on wild-type Rab6 (Cuif et al., 1999). However, functional in vivo data are missing and there are no follow-up studies confirming the role of GAPCenA as a Rab6 GAP.

1.4.2 Rab6 function in membrane transport

The role of Rab6 in membrane traffic has been studied intensively for more than ten years, yet there is some controversy within the published data. Whereas the majority of groups claim a function of Rab6 in retrograde transport, there are also publications in favour of Rab6 regulating forward transport. Most studies rely on the overexpression of Rab6 mutants, like Rab6^{Q72L} (GTP restricted "active" mutant, which cannot hydrolyse GTP) and Rab6^{T27N} (GDP restricted "inactive" mutant, which inhibits the GTP exchange reaction) (see also 1.3.2 and 1.3.3 and (Martinez et al., 1994)). Following the trafficking of a soluble secreted form of alkaline phosphatase (SEAP) and of the membrane protein hemagglutinin of influenza virus (HA) in co-expression with Rab6 wild-type and mutants Martinez et al., 1994 obtained the first hints for a role of Rab6 in maintaining Golgi morphology and membrane traffic within the Golgi stack. However, it was not clear from their data whether Rab6 acts rather by inhibiting forward or promoting retrograde transport. The same group showed some years later that Golgi resident proteins, like the trans Golgi enzyme β-1,4-galactosyltransferase, become relocated to the ER upon over-expression of Rab6 wild-type and Rab6^{Q72L} (Martinez et al., 1997), which would rather speak for a positive regulation of retrograde transport by Rab6.

Another approach to elucidate the function of Rab6 was taken by Mayer et al., 1996 where the authors used Rab6 specific antibodies in a cell free Golgi membrane system. The authors found a block in *cis* to *medial* Golgi transport of the marker protein vesicular stomatitis virus protein G protein (VSV-G) when inhibiting Rab6 function by antibodies and therefore concluded that Rab6 plays a role in promoting forward transport through the Golgi apparatus. In contrast, the study of Girod et al., 1999 provides evidence for a Rab6 dependent Golgi to ER recycling pathway that is utilised by Golgi resident enzymes and Shiga toxin. Both, Golgi enzyme and Shiga toxin retrograde transport to the ER was blocked in Rab6^{T27N} expressing cells. These data were supported by live cell fluorescent studies of White et al., 1999. Fluorescent-protein tagged Rab6 was expressed in HeLa cells and monitored

together with the retrograde cargo Shiga toxin. From the accumulation of Shiga toxin in Rab6 positive structures, which then fused with ER membranes, the authors concluded, that Rab6 defines special Golgi to ER retrograde transport carriers. These Rab6 positive transport carriers seem to act independently of the COPI machinery as proteins containing a KDEL-sequence were retrieved to the ER independently of Rab6 through the classical COPI-dependent retrograde pathway (Girod et al., 1999; White et al., 1999). The plant toxin Ricin, however, was reported to use neither the COPI nor the Rab6 dependent retrograde pathway to reach the ER (Chen et al., 2003), which leaves the question of how many different routes from the Golgi apparatus back to the ER exist.

Another complication of the Rab6 story came along with the detection of a Rab6a splice variant that differs from Rab6a only by three amino acids and was called Rab6a' (Echard et al., 2000). Whereas Mallard et al., 2002 proposed that Rab6a' is functionally distinct from Rab6a, and regulates endosome to Golgi transport, Young et al., 2005 saw no functional difference between the two isoforms. The latter data were obtained using small interfering RNAs directed against either Rab6a or Rab6a', while the study of Mallard et al., 2002 was based on over-expression of mutant Rab6a and 6a' proteins. The latest comparative study of Rab6a and 6a' (Del Nery et al., 2006), though using sequence specific siRNA as well, comes to the conclusion that Rab6a and 6a' fulfil different tasks in membrane trafficking. The authors suggest that, in contrast to earlier publications, Rab6a is dispensable in membrane traffic and Rab6a' is the important splice variant regulating Golgi to ER trafficking, and additionally cell cycle progression in HeLa cells (Del Nery et al., 2006; Miserey-Lenkei et al., 2006).

1.4.3 Rab6 effector proteins

A link between Rab6 regulated transport processes and the cytoskeleton was provided by two independent research groups (Matanis et al., 2002; Short et al., 2002). Both groups found that Rab6 binds the two mammalian homologues of *Drosophila* Bicaudal-D, Bic-D1 and Bic-D2. The coiled-coil proteins Bic-D1/2 have been shown to bind the dynein-dynactin motor complex through interaction with the dynamitin subunit of dynactin (Hoogenraad et al., 2001). Furthermore, Rab6 can interact directly with p150^{glued}, a core component of the dynactin complex (Short et al., 2002). These findings suggest that Rab6 can interact with dynactin directly via p150^{glued} or indirectly via Bic-D1/2. Hence, Rab6 together with Bic-D proteins may be involved in the dynein-dynactin dependent capture and movement of Golgi derived vesicles along microtubules.

Recently, the protein OCRL1 has been shown to bind several Rabs and interact strongest with the endosomal Rab5 and with the Golgi localised Rabs Rab1 and Rab6 (Hyvola et al., 2006). OCRL1 is an inositol polyphosphate 5-phosphatase and regulates the levels of different phosphoinositides at different places within the cell. Mutation of OCRL1 causes the x-chromosome linked disease oculocerebrorenal syndrome of Lowe, which underlines the importance of correct lipid signalling and regulation by lipid kinases and phosphatases. Interaction with Rab5 and Rab6 is required for OCRL1 localisation to endosomes and to the Golgi apparatus, respectively. Interestingly, Rab5 and Rab6 can also stimulate the phosphatase activity of OCRL1 after membrane recruitment (Hyvola et al., 2006) and over-expression of an inactive form of OCRL1 changes endosome and Golgi morphology (Choudhury et al., 2005). This highlights, that regulation of membrane trafficking goes far beyond pure protein-protein interactions but also involves lipid-signalling pathways.

Several other Rab6 binding proteins have been identified by yeast-2-hybrid screening or pulldown assays (Echard et al., 1998; Fridmann-Sirkis et al., 2004; Liewen et al., 2005; Monier et al., 2002; Rosing et al., 2007; Teber et al., 2005). Yet, their specificity and functional relationship with Rab6 remains to be explored. Rab6 could play a role in various processes along Golgi related transport routes by recruiting different effector proteins. The best characterised Rab6 effector complexes to date are Bic-D1/2 and p150[glued] as linker to motor protein function for vesicle motility and OCRL1 as lipid phosphatase giving membrane identity to the Golgi complex and other organelles.

2 Identification and Characterisation of PIST as a novel Rab6 effector protein

2.1 Aim of the work

Rab6 is a Golgi localised Rab GTPase that can interact with the dynein-dynactin microtubule motor complex, either directly through the p150^{glued} subunit or indirectly through the coiled-coil proteins Bic-D1 and Bic-D2 (Matanis et al., 2002; Short et al., 2002). In this way, Rab6 facilitates the minus-end-directed transport of vesicles along microtubules. However, the nature of these Rab6 regulated transport vesicles and the exact function of minus-end-directed movement is unclear. In general, Rab GTPases act as molecular on/off switches for protein interactions. Only in their active GTP-bound state Rabs are able to recruit effector proteins, which then provide the functional properties needed. To find out more about the function of a specific Rab means at the same time to get to know its effector proteins. The aim of this part of the work was therefore to identify and characterise novel Rab6 effector proteins in order to elucidate the molecular mechanisms underlying Rab6 function.

2.2 Results

2.2.1 Identification of PIST as a putative Rab6 effector

To identify novel Rab6 effector proteins a GST-pulldown experiment from rat liver cytosol was performed. The liver is an organ where extensive secretion takes place. Hence, liver cells are enriched in Golgi membranes and represent an ideal source for Golgi associated proteins. A simple membrane fraction procedure can be used to isolate two fractions, the Golgi membranes enriched in tightly associated Golgi membrane and peripheral membrane proteins, and a cytosolic fraction with more loosely associated and soluble Golgi proteins. For the GST-pulldown experiment, either the active GTP-restricted point mutant of human Rab6 (Rab6^{Q72L}), or as a control the inactive GDP-restricted mutant Rab6^{T27N}, were immobilised on glutathione sepharose. Both proteins were purified from *E. coli* as 6xHisGST fusion proteins using Ni-NTA agarose. Rab effector proteins are expected to bind preferentially the active GTP-bound conformation of a Rab (see 1.3). Coomassie brillant blue (CBB) staining of the eluates showed several bands in the pulldown with Rab6^{Q72L}, which could not be seen in the control lane (Figure 2.1 A). MALDI-TOF mass spectrometric analysis identified known Rab6 interaction partners p150^{glued} and Bic-D2 (Matanis et al., 2002; Short et al., 2002), as well as a protein named PIST (PDZ domain protein interacting specifically with TC10). Tryptic

peptides derived from this protein were not found in the corresponding gel region of the control pulldown with Rab6^{T27N}, suggesting that PIST may be a GTP-dependent binding protein of Rab6.
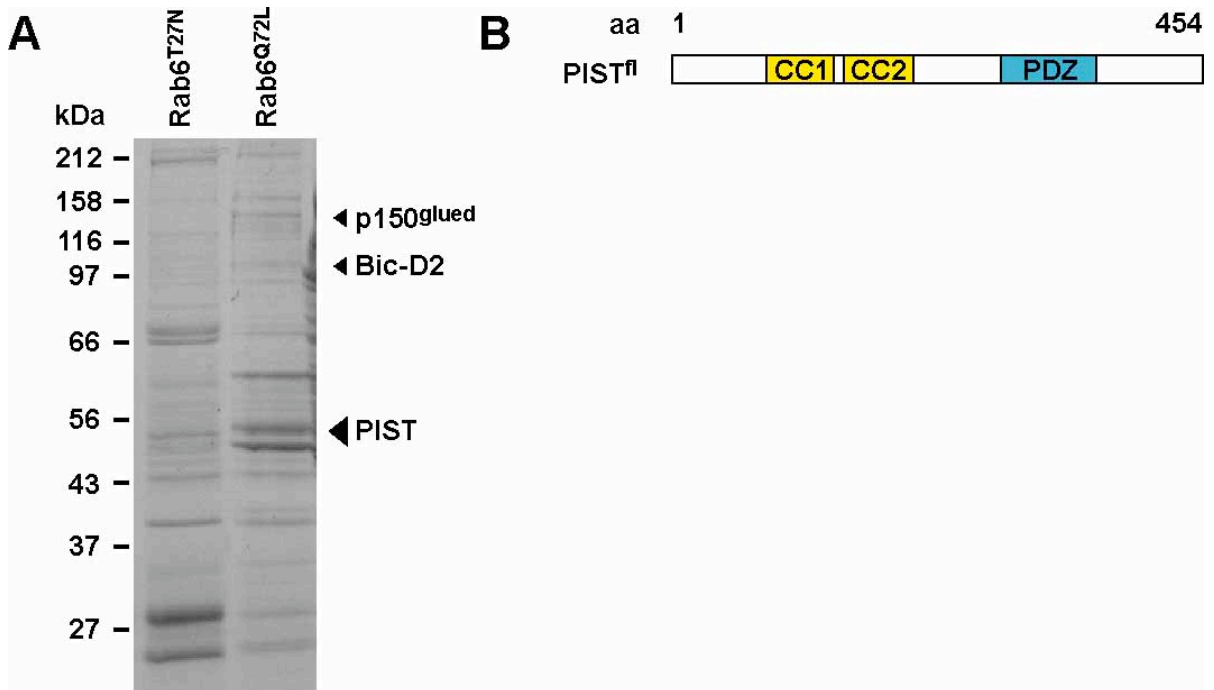
Figure 2.1 Identification of PIST as a Rab6 interacting protein from rat liver cytosol. (A) CBB staining of the GST-pulldown experiment with Rab6^{T27N} and Rab6^{Q72L}. (B) Domain structure of the human 454 amino acid protein PIST with two coiled-coil (CC) regions and PDZ domain.

PIST is a ubiquitously expressed 55 kDa protein also known as GOP/C (<u>Go</u>lgi associated <u>P</u>DZ and <u>c</u>oiled-coil motif containing protein), FIG (<u>f</u>used <u>i</u>n <u>g</u>lioblastoma) and CAL (<u>C</u>FTR <u>a</u>ssociated <u>l</u>igand) (Charest et al., 2003; Cheng et al., 2002; Neudauer et al., 2001; Yao et al., 2001). PIST is not evolutionary conserved and is only found in mammals and primates. The rat protein discovered in the pulldown experiment exhibits approx. 90 % sequence identity with the human homologue. In humans there are two different isoforms of PIST (Entrez protein accession numbers NP_065132 (isoform A 462 aa's) and NP_001017408 (isoform B 454 aa's)).

For cloning and subsequent biochemical and cell biological analysis, the nucleotide sequence encoding the PIST protein was amplified from a human liver cDNA library. Nucleotide sequence analysis showed that only the cDNA encoding the shorter isoform of the protein could be obtained. The shorter isoform lacks 8 amino acids within the N-terminal coiled-coil region of the protein, but so far there are no data available about functional differences between the two isoforms of the PIST protein.

PIST has a simple two domain architecture, and consists of two coiled-coil regions in the N-terminal half of the protein and a C-terminal PDZ domain (Figure 2.1 B). Coiled-coil protein folding motifs are thought to form extended rod-shaped structures, which can be both, rigid or highly dynamic and therefore fulfil various functions within the cell (Burkhard et al., 2001; Gillingham and Munro, 2003). The PDZ domain is a classical protein-protein interaction domain that binds C-terminal or internal peptide sequences in target proteins (Ponting et al., 1997). Often, PDZ domains are involved in scaffolding and assembly of multi-protein complexes. PIST was shown to bind via its PDZ domain the Wnt ligand receptor frizzled (Yao et al., 2001), the plasma membrane chloride channel CFTR (Cheng et al., 2002), the neural transmembrane protein CALEB/NGC (Hassel et al., 2003) and the Rho effector Rhotekin (Ito et al., 2006) and could be involved in intracellular trafficking of these proteins. Furthermore, PIST was shown to interact with the Rho-family GTPase TC10 (Neudauer et al., 2001) and with the SNARE syntaxin6 (Charest et al., 2001). Still, the exact function of PIST remains obscure. PIST knock-out mice are viable and show no defects except infertility in male mice due to a lack in acrosome formation (Yao et al., 2002).

2.2.2 Generation and validation of a PIST specific antibody

In order to further investigate the Rab6 binding capacity of PIST and also the functional relationship of this interaction, a rabbit polyclonal antibody was generated. Full-length 6xHis-tagged human PIST was purified from *E.coli* and sent to Charles River Laboratories for immunisation (see 5.4.7). PIST specific antibodies were purified from the final bleed out. Figure 2.2 shows the characterisation of the purified antibody. R-α-PIST recognises recombinant 6xHis-PIST as well as endogenous PIST from HeLa extract in Western blotting (Figure 2.2 A). Also in immunoprecipitation (IP) from HeLa extract the antibody, but not the pre-immune serum, gives a clean and strong signal (Figure 2.2 B), which could be confirmed to be PIST by mass spectrometric analysis of a CBB stained immunoprecipitated band in a similar experiment (see Figure 2.12).
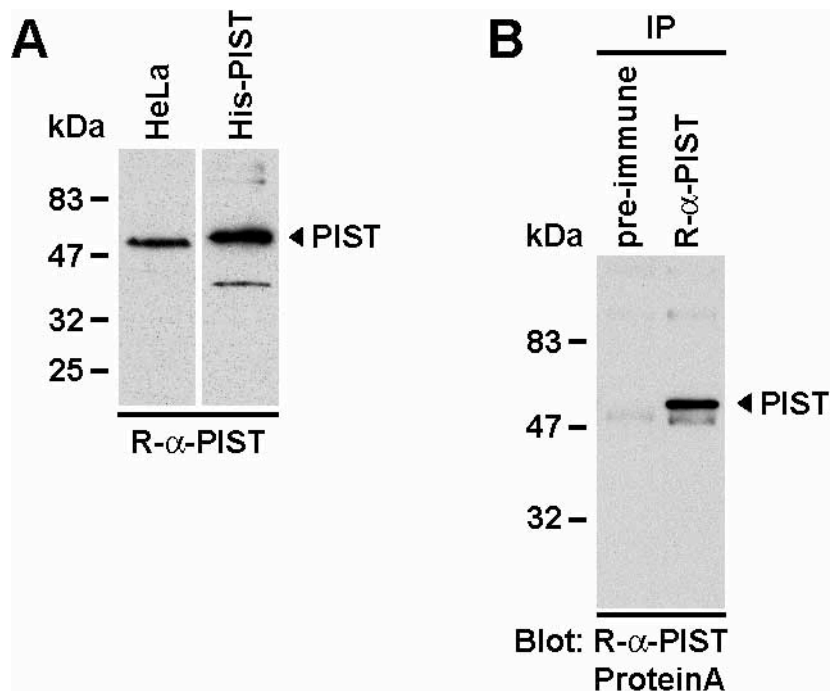
Figure 2.2 Characterisation of the purified PIST antibody in Western blotting (A) and immunoprecipitation (B). (A) R-α-PIST was tested on 20 μg HeLa extract and on 20 ng recombinant 6xHis-PIST. (B) An immunoprecipitation experiment was performed using either pre-immune serum or purified R-α-PIST. Precipitated PIST was detected on a Western blot by R-α-PIST and HRP-coupled proteinA.

2.2.3 PIST binds Rab6 in a GTP-dependent fashion

The rat homologue of PIST was identified in a large-scale Rab6 pulldown from rat liver cytosol. To confirm the interaction of human PIST with Rab6 a pulldown experiment from HeLa cell extract was performed and probed with the validated PIST specific antibody. Bacterially expressed GST-tagged Rab6 was used as wild-type, active GTP-restricted mutant and inactive GDP-restricted mutant. Rab effector proteins are expected to bind the active pool of a Rab in its GTP-bound conformation, which is mimicked by the QL mutant and also represented by a fraction of wild-type Rab. On the contrary, effectors should not bind the GDP-bound conformation of the Rab, mimicked by the TN mutant (see 1.3).

In Figure 2.3 this is true for the known Rab6 interactors p150^{glued} and Bic-D1 (Matanis et al., 2002; Short et al., 2002). p150^{glued}, a dynactin core component, is precipitated with Rab6^{wt} and Rab6^{Q72L}, but not with Rab6^{T27N}. Compared to the input lane relatively little p150^{glued} is in complex with Rab6. This can be explained by the fact that p150^{glued}/dynactin has various functions and binding partners within the cell (Habermann et al., 2001; Vaughan et al., 2002; Watson et al., 2005; Watson and Stephens, 2006) and obviously only a small proportion functions together with Rab6

at the Golgi apparatus. Also Bic-D1 is precipitated by Rab6^{Q72L}, but only very little by wild-type Rab6, which cannot be explained at this point. Unspecific signals in the Rab6^{T72N} pulldown, marked by asterisks, are most likely cross-reactions with impurities in the Rab6^{T72N} protein preparation.

PIST shows the same pattern of Rab6 binding like p150^{glued} in the same pulldown experiment and is bound by Rab6^{wt} and Rab6^{Q72L} but not Rab6^{T27N}. The coiled-coil protein p115, known to interact with Rab1 at the cis-Golgi (Allan et al., 2000; Moyer et al., 2001), served as a negative control and could not be detected in the Rab6 pulldown. Therefore it can be concluded that the GST-pulldown was specific for Rab6 binding proteins and that human PIST binds Rab6 in a GTP-dependent manner.
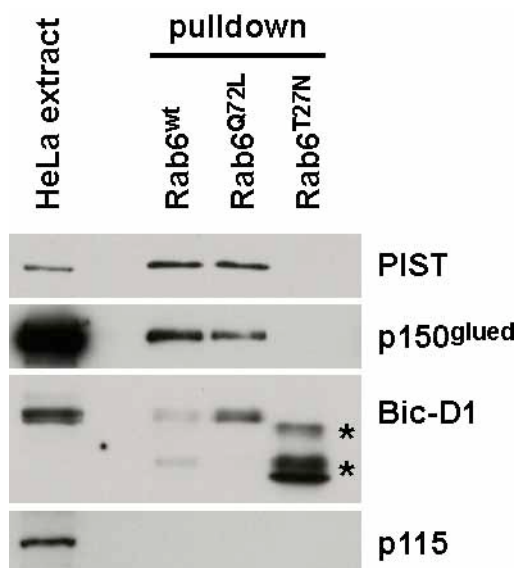
Figure 2.3 PIST binds Rab6 in a GTP-dependent fashion. Pulldown experiment from HeLa cell lysate with recombinant GST-tagged Rab6 wild-type (wt) and active (Q72L) and inactive (T27N) mutant. The Western blot containing the input of HeLa extract and the pulldown reactions was probed for PIST, p150^{glued}, Bic-D1 and p115. Asterisks mark unspecific signals of the Bic-D1 antibody in the Rab6^{T27N} pulldown.

2.2.4 PIST is a specific binding partner of Rab6 and not of TC10

PIST was reported to interact with the Rho family GTPase TC10 in yeast two-hybrid and in an in vitro binding assay (Neudauer et al., 2001). However, the authors did not examine the full-length protein but only a fragment of PIST (amino acids 155-320), which corresponds to the second coiled-coil, a bit of the PDZ domain and the sequence inbetween these domains.

To clarify the point whether full-length PIST is able to bind TC10 or Rab6, or both GTPases to the same extent, the nucleotide sequence encoding the TC10 protein was amplified from a human fetus cDNA library. First, primers were

designed and used according to the mRNA sequence corresponding to the TC10 protein described in Neudauer et al., 2001 (Entrez nucleotide accession number AF498976). However, even several PCRs did not produce amplified DNA of the expected length. After an extensive search of expressed sequence tags (ESTs) for the respective TC10 sequence, AF498976 turned out to be wrong. Instead, in all corresponding ESTs, an insertion of two nucleotides after the putative TC10 start codon shifted the reading frame and turned the second ATG into the real start codon. In summary, the originally described TC10 protein used in Neudauer et al., 2001 was 8 amino acids too long at the N-terminus and therefore an artefact. The new TC10 gene sequence was published recently as Ras homolog gene family member Q (ARHQ) under the Entrez number NM_012249.

In order to address the question of specificity of the PIST-Rab6 interaction a comprehensive yeast two-hybrid analysis with full-length PIST against a representative set of Rab GTPases and against TC10 was carried out (Figure 2.4). The nucleotide sequence encoding the PIST protein was fused to the nucleotide sequence of the activation domain of the GAL4 promotor (GAL4 AD) in the vector pAct2, and the nucleotide sequences encoding the respective GTPases were fused to the nucleotide sequence of the GAL4 binding domain (GAL4 BD) in the vector pFBT9. The resultant fusion proteins were screened for interaction in the host strain PJ69-4A allowing for growth on QDO medium lacking the amino acids leucin, tryptophan, adenin and histidin. Tested against 52 Rab GTPases in their GTP-restricted conformation (QL mutants) PIST interacted with Rab6a and Rab6b only (Figure 2.4). At the same time PIST did not interact with TC10^{Q67L} (Figure 2.4), suggesting that among the tested GTPases full-length PIST is specific for Rab6 in yeast two-hybrid.
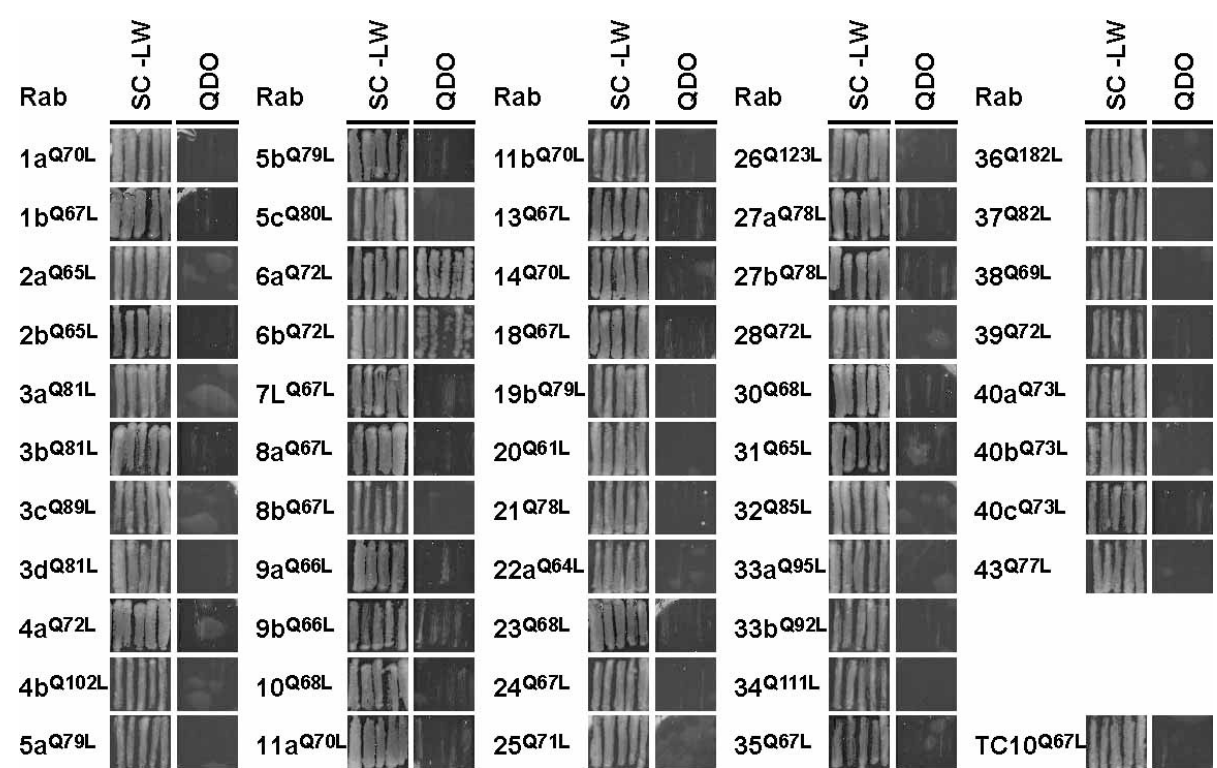
Figure 2.4 PIST is a specific binding partner of Rab6 in yeast two-hybrid. Yeast two-hybrid interaction of full-length PIST against a set of human Rabs and the Rho GTPase TC10 in the active conformation (QL mutant). Transformants were grown on synthetic complete medium lacking leucin and tryptophan (SC –LW) and interaction was screened on quadrupel drop-out medium (QDO) lacking the amino acids leucin, tryptophan, adenin and histidin.

In Neudauer et al., 2001 the authors claim that recombinant PIST(155-320) binds TC10 in vitro. However, this result could not be verified using full-length PIST in an in vitro binding assay with GST-tagged TC10 (Figure 2.5). 6xHis-tagged PIST was binding GST-Rab6^{wt} and GST-Rab6^{Q72L} but not GST-Rab6^{T27N}, confirming a GTP-dependency of the interaction. No binding at all could be observed to GST-TC10 protein, neither to wild-type nor to the active QL mutant. The recovery of GTPase was comparable for all binding reactions (bound) except for TC10^{T23N}. This can be neglected because effector proteins are not expected to bind the inactive TN mutant anyway. The fact that there is no visible band of PIST in the TC10 binding reactions with wild-type and active TC10 (TC10^{Q67L}) supports the conclusion that PIST is not interacting with TC10 in vitro. Compared to the loading of PIST (1 μg) Rab6-bound PIST was in the μg range, suggesting a stable binding of these proteins. Furthermore, the direct binding experiment showed that the interaction of PIST with Rab6 is direct and not mediated by other proteins.
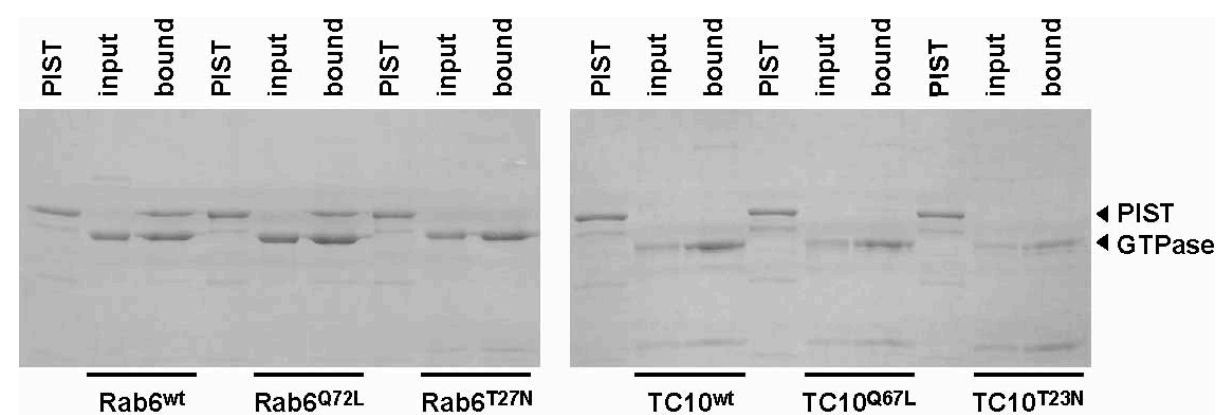
Figure 2.5 PIST does not bind TC10 but Rab6 in vitro. CBB staining of an in vitro binding assay of 6xHis-tagged PIST with GST-tagged Rab6 or TC10 GTPase as wild-type, active mutant (QL) and inactive mutant (TN). For comparison 1 µg of PIST and of the GTPase (input) is shown next to the binding reaction (bound).

2.2.5 PIST is a Golgi localised protein

Rab6 is a *trans* Golgi localised GTPase and the interaction of active Rab6 with PIST should therefore take place at the Golgi apparatus. Immunofluorescence staining with the purified PIST specific antibody R-α-PIST showed, that PIST localises to the perinuclear region of HeLa cells (Figure 2.6). Co-staining with the Golgi markers GM130, Golgin97 and TGN46 revealed that PIST is a Golgi localised protein.

TGN46, like its rat homologue TGN38, is an extensively glycosylated type 1 membrane protein which localises primarily to the *trans* Golgi network (TGN) (Luzio et al., 1990; Ponnambalam et al., 1996). Also Golgin97 was shown to be a TGN localised protein (Griffith et al., 1997), whereas GM130 is a *cis*-Golgi localised Golgi matrix protein (Nakamura et al., 1995). As there is a better overlap of PIST staining with the *trans* Golgi markers Golgin97 and TGN46 than with the *cis* Golgi marker GM130, PIST is supposed to be a protein associated with the *trans* Golgi compartments.

Because the only available antibody against Rab6 is a rabbit polyclonal antibody, cells could not be stained for PIST and Rab6 at the same time. However, in its active state Rab6 is anchored in Golgi membranes and could therefore be regulating the recruitment of PIST to the Golgi apparatus. PIST does not contain any transmembrane regions or lipid modifications for membrane anchoring and is therefore regarded a cytosolic protein (Charest et al., 2001). How PIST is recruited to the Golgi was therefore examined further.
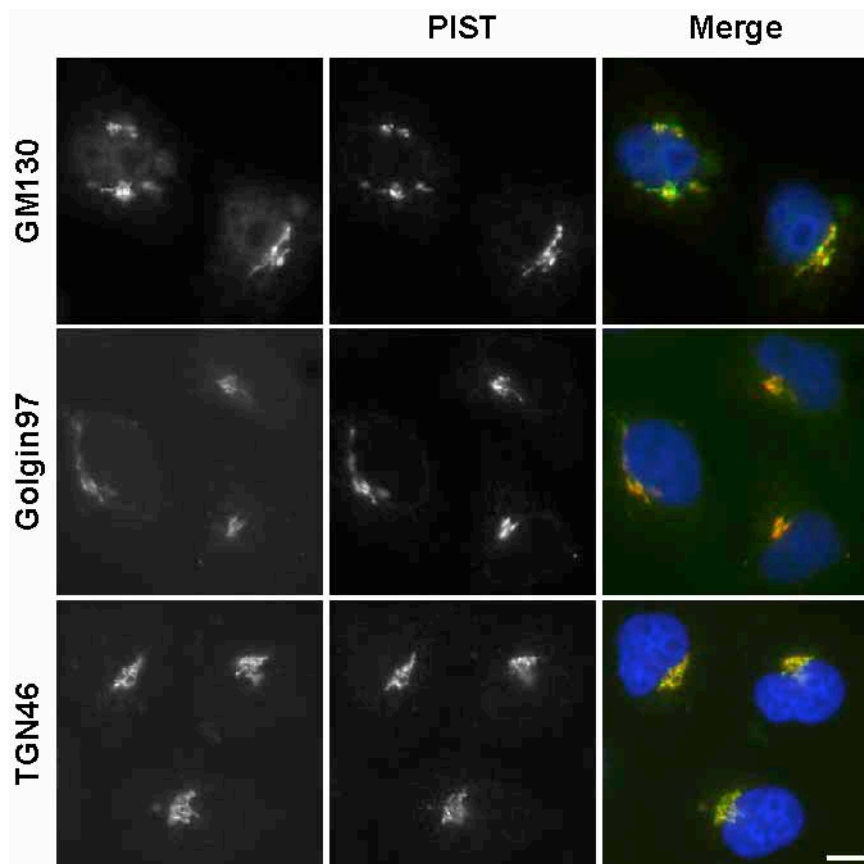
Figure 2.6 PIST is a Golgi localised protein. Immunofluorescent staining of HeLa cells with purified R-a-PIST (red), costained for the Golgi markers GM130, Golgin97 and TGN46 (green). DNA was visualised with DAPI (blue). Bar indicates 10 μm in all panels.

2.2.6 Domain specific Rab6 binding and Golgi localisation of PIST

In addition to a PDZ domain in the C-terminal region PIST possesses two coiled-coil stretches in the N-terminal half. Coiled-coil proteins have been shown before to interact with small GTPases of the Rab and Arl family to be recruited to membrane domains (reviewed in Barr and Short, 2003 and Short et al., 2005). Thus, the question was, which domain in PIST mediates Rab6 binding and whether the interaction with Rab6 is a prerequisite for the Golgi targeting of PIST.

For this purpose five different fragments of PIST were generated representing different combinations of the first and second coiled-coil domain (CC1 and CC2) and the PDZ domain (Figure 2.7 A). In yeast two-hybrid analysis with Rab6^{Q72L} only PIST fragments containing CC1, that is PIST^{fl}, PIST$^{1-255}$ and PIST$^{1-141}$, were able to interact with Rab6, detected by growth on QDO (Figure 2.7 A). This result could be reproduced with recombinant proteins in an in vitro binding experiment using 6xHis-tagged PIST and GST-tagged Rab6 proteins. Whereas proteins with CC1 bound the GTP-restricted mutant Rab6^{Q72L} (Figure 2.7 B, closed triangles), proteins with CC2

and/ or the PDZ domain were not able to bind Rab6 in vitro (Figure 2.7 B, open triangles). One construct (PIST$^{142-255}$) containing CC2 could not be expressed in *E. coli* and was therefore not tested in this assay. However, this PIST fragment did not interact with Rab6 in yeast two-hybrid and is furthermore represented by the longer fragment PIST$^{142-454}$, which did not bind Rab6 in vitro. All Rab6 binding PIST fragments (PIST^{fl}, PIST$^{1-255}$ and PIST$^{1-141}$) exhibit specificity for the active Rab6 mutant (Rab6^{Q72L}) and do not bind inactive Rab6^{T27N}. Therefore the first coiled-coil region of PIST is required for GTP-dependent Rab6 binding.
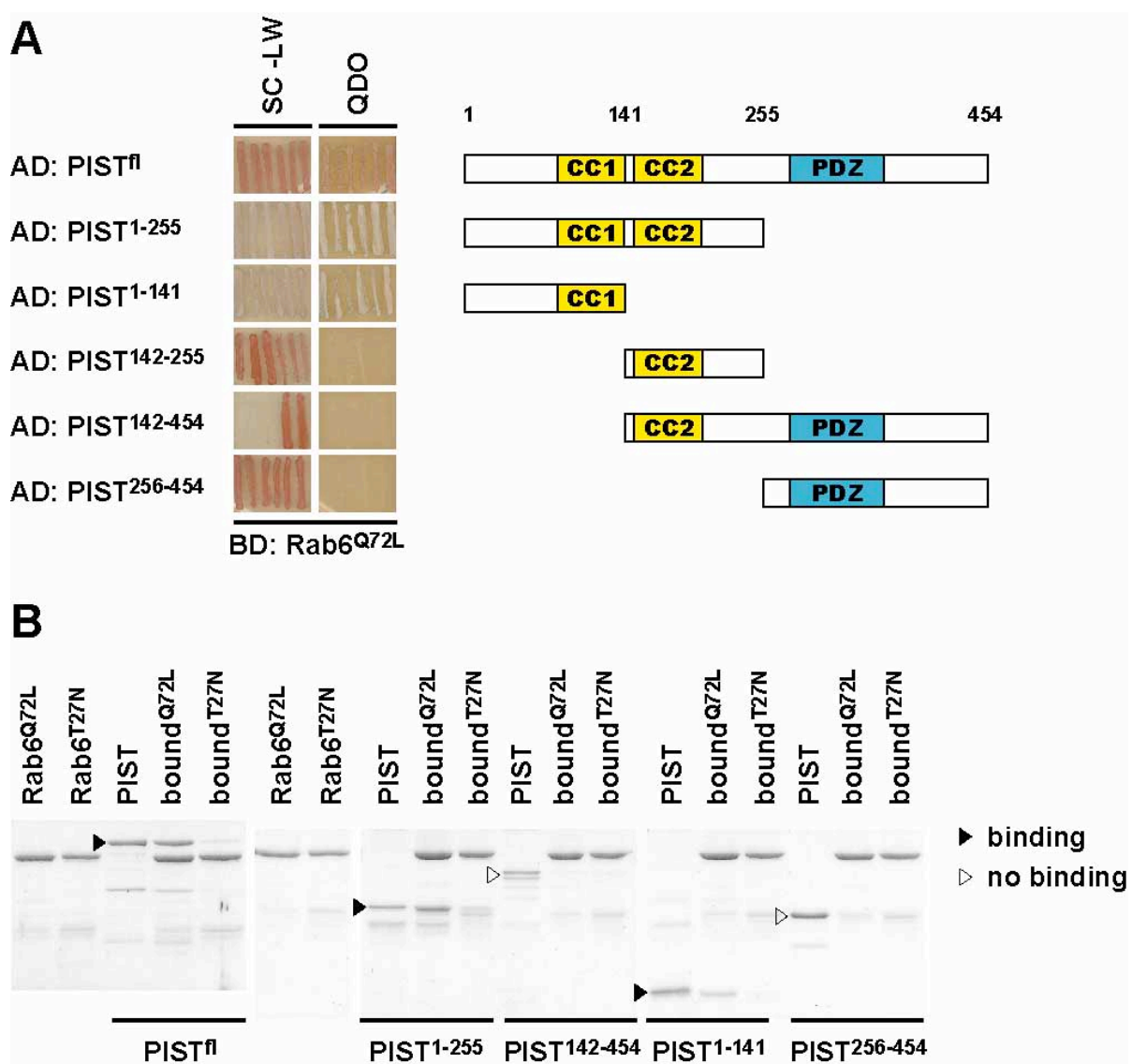
Figure 2.7 The first coiled-coil domain of PIST is required for Rab6 binding. (A) Yeast two-hybrid analysis of interaction of GAL4 AD-PIST fusion proteins with the GAL4 BD-Rab6^{Q72L} fusion protein. Also shown is the schematic of dissecting full-length PIST into fragments. (B) CBB staining of an in vitro binding assay of 6xHis-tagged PIST fragments with GST-tagged Rab6, highlighting bound PIST with closed and unbound PIST with open triangles.

As PIST carries no structural features for direct membrane insertion or association, its localisation to Golgi membranes is most likely dependent on protein-protein or protein-lipid interactions. Whether Rab6 binding is required to target PIST to the Golgi apparatus should be addressed by overexpression of GFP-tagged PIST fragments in HeLa cells (Figure 2.8). In untreated HeLa cells the GFP signal of PIST^{fl} and PIST$^{1-255}$ was found almost exclusively in the perinuclear region whereas the signal of PIST$^{142-255}$ and PIST$^{142-454}$ was less clear at the Golgi and showed cytosolic background staining. PIST$^{1-141}$ and PIST$^{256-454}$ were targeted mainly to the nucleus. However, coiled-coil regions as well as PDZ domains tend to dimerise and PIST has been previously shown to form homodimers (Neudauer et al., 2001). In order to make sure that Golgi targeting of GFP-PIST is not due to dimerisation with the endogenous protein, the localisation of GFP-PIST fragments was also determined in HeLa cells depleted of PIST by siRNA prior to transfection with GFP-constructs (see Figure 2.15 for PIST siRNA). Because the siRNA duplex was directed against a sequence within the PDZ domain of PIST the GFP signal of PIST^{fl}, PIST$^{142-454}$ and PIST$^{256-454}$ was silenced and only PIST$^{1-255}$, PIST$^{1-141}$ and PIST$^{142-255}$ could be detected in the siRNA background. Out off these three, PIST$^{1-255}$ (CC1 and CC2) showed Golgi targeting and PIST$^{142-255}$ (CC2) a less prominent perinuclear signal with high cytosolic background, similar to the result seen with control cells. PIST$^{1-141}$ (CC1) was again not able to target to the Golgi and was mainly nuclear as in control cells.

These results suggest that the second coiled-coil domain of PIST is sufficient to localise the protein at Golgi membranes. However, a better targeting is achieved when both coiled-coils are present. In contrast, CC1 alone is not enough for Golgi localisation of PIST while the PDZ domain seems to have no impact on the intracellular targeting of the protein.

Taken together, these results show that the Golgi localised protein PIST is able to bind Rab6 via its first coiled-coil domain, as shown in Figure 2.7. However, the interaction with Rab6 seems not to be the critical step for the localisation of PIST to Golgi membranes, because in overexpression experiments another part of the protein, the second coiled-coil region is required for Golgi targeting (Figure 2.8). A summary of both, Rab6 binding and Golgi targeting of the various PIST fragments is shown in Figure 2.9.
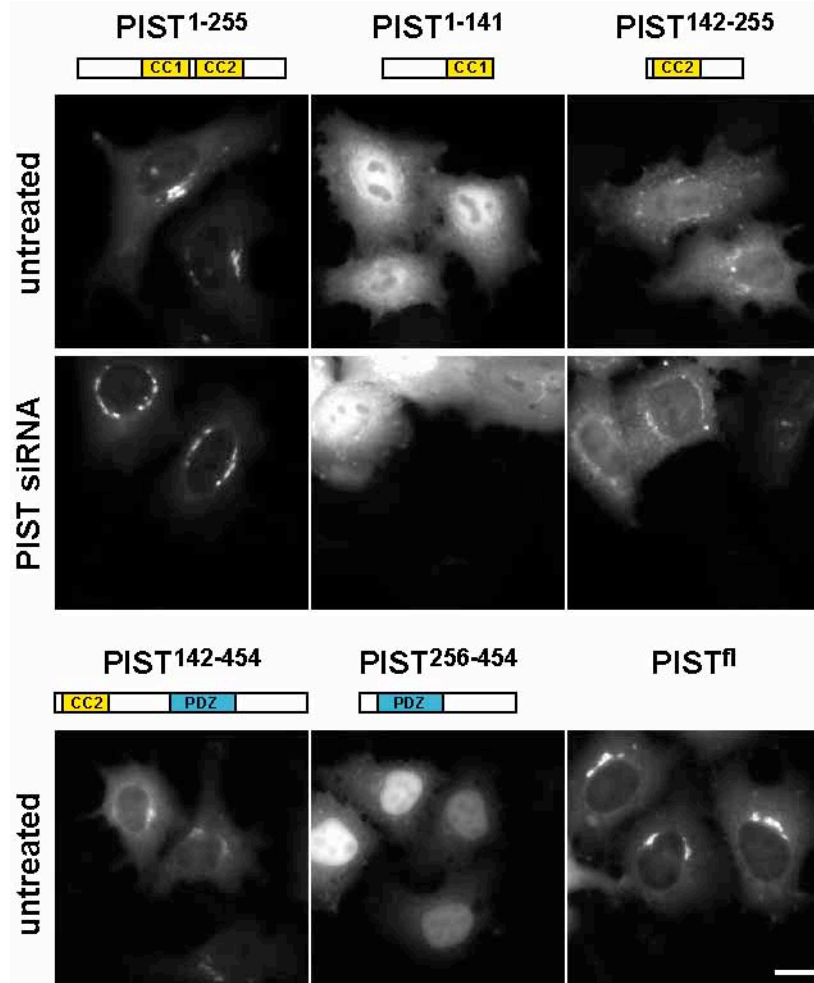
Figure 2.8 PIST targets to the Golgi apparatus via CC2. HeLa cells, either untreated or depleted of PIST by siRNA, were transfected with GFP-PIST constructs for 24 hours and fixed. Bar indicates 10 μm in all panels.

	1	141	255	454	Y2H interaction with Rab6Q72L	Direct binding to Rab6Q72L	Golgi localisation HeLa cells
PISTfl		CC1	CC2	PDZ		+	+	+
PIST1-255		CC1	CC2			+	+	+
PIST1-141		CC1				+	+	-
PIST142-255			CC2			-	n.d.	+
PIST142-454			CC2	PDZ		-	-	+
PIST256-454				PDZ		-	-	-

Figure 2.9 PIST binds Rab6 via CC1 and targets to the Golgi via CC2. Depicted here is a summary of the results from Figure 2.7 and Figure 2.8.

2.2.7 Interfering with Rab6 levels does not affect PIST at the Golgi

The data from chapter 2.2.6 indicate that PIST localises to Golgi membranes independently of Rab6. To further test this, the role of Rab6 in PIST targeting was characterised in more detail. If PIST's localisation is indeed independent of Rab6, altering levels of Rab6, especially decreasing active membrane bound Rab6, should not affect the distribution of PIST at the Golgi.

Over-expression of Rab mutants is one tool to interfere with the endogenous level of active GTPase. The pool of active Rab is increased by over-expression of the GTP-restricted QL mutant whereas the pool of inactive Rab is elevated by over-expression of the GDP-restricted TN mutant. Over-expression of wild-type Rab controls general effects, generated by increased Rab levels independent of the mutation. Rab effector interactions occur with the active state of the GTPase and should in theory be titrated out by the inactive TN mutant. If an effector protein requires the interaction with active Rab for its membrane localisation, its localisation should be altered in cells expressing inactive Rab.

Figure 2.10 displays the over-expression of GFP-Rab6^{wt}, GFP-Rab6^{Q72L} and GFP-Rab6^{T27N} in HeLa cells. Co-staining with the transmembrane protein TGN46 proves that the Golgi morphology was normal in transfected and untransfected cells and that GFP-Rab6^{wt} and GFP-Rab6^{Q72L} localised to the Golgi, whereas GFP-Rab6^{T27N} was mainly distributed in the cytosol and in the nucleus. Golgin160, a peripheral Golgi membrane protein (Fritzler et al., 1993; Misumi et al., 1997), was unaltered in all Rab6 transfected cells. Also PIST did not change its Golgi localisation irrespective of which Rab mutant was over-expressed, consistent with the idea that PIST targets to the Golgi independently of Rab6. However, Bic–D1, another Rab6 effector protein which was described to target to the TGN in a Rab6 dependent fashion (Matanis et al., 2002), was not displaced from the Golgi by the over-expression of the inactive mutant GFP-Rab6^{T27N}. This is an unexpected result and weakens the significance of the over-expression experiment.
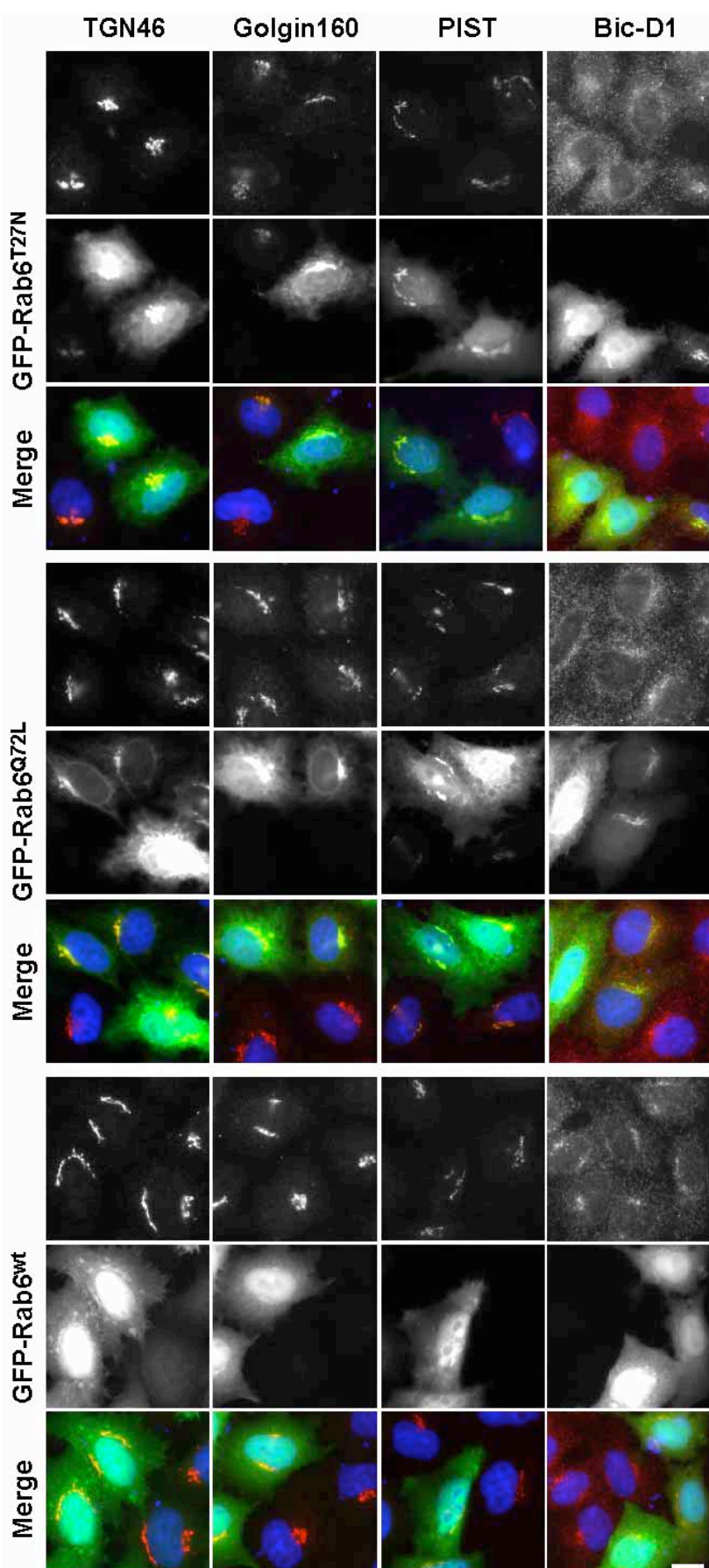
Figure 2.10 Rab6 over-expression has no effect on the Golgi localisation of PIST. HeLa cells were transfected for 24 hours with GFP-Rab6wt, GFP-Rab6Q72L and GFP-Rab6T27N (green), fixed and stained for Bic-D1, PIST, Golgin160 and TGN46 (red). DNA was visualised with DAPI (blue). Bar indicates 10 μm in all panels.

The limitation of over-expressing Rab mutants in cells is probably the presence of the endogenous Rab, which could mask any effects of the mutant proteins. Thus, another approach was taken to analyse the influence of Rab6 on the Golgi locali-sation of PIST, depletion of Rab6 from cells using small interfering RNA (siRNA).

The result of this approach is depicted in Figure 2.11. Compared to control cells depleted of the nuclear envelope protein LaminA (Elbashir et al., 2001) Rab6 staining was gone after 72 hours of Rab6 siRNA while the staining pattern for TGN46 and p115 was unaltered, representing a normal Golgi morphology in HeLa cells. The polyclonal antibody against Rab6 exhibits a high cytosolic and nuclear background staining, but the Golgi localised pool of Rab6 was clearly reduced in Rab6 siRNA, suggesting that little or no active GTPase was left. Under these conditions PIST was unchanged, and it localised to the normal Golgi structure marked by TGN46 as in control cells. On the other hand, Bic-D1 staining was clearly lost from the Golgi in Rab6 depleted cells suggesting that Bic-D1 indeed needs to bind Rab6 to be targeted to Golgi membranes whereas PIST relies on other binding partners or mechanisms for Golgi localisation.
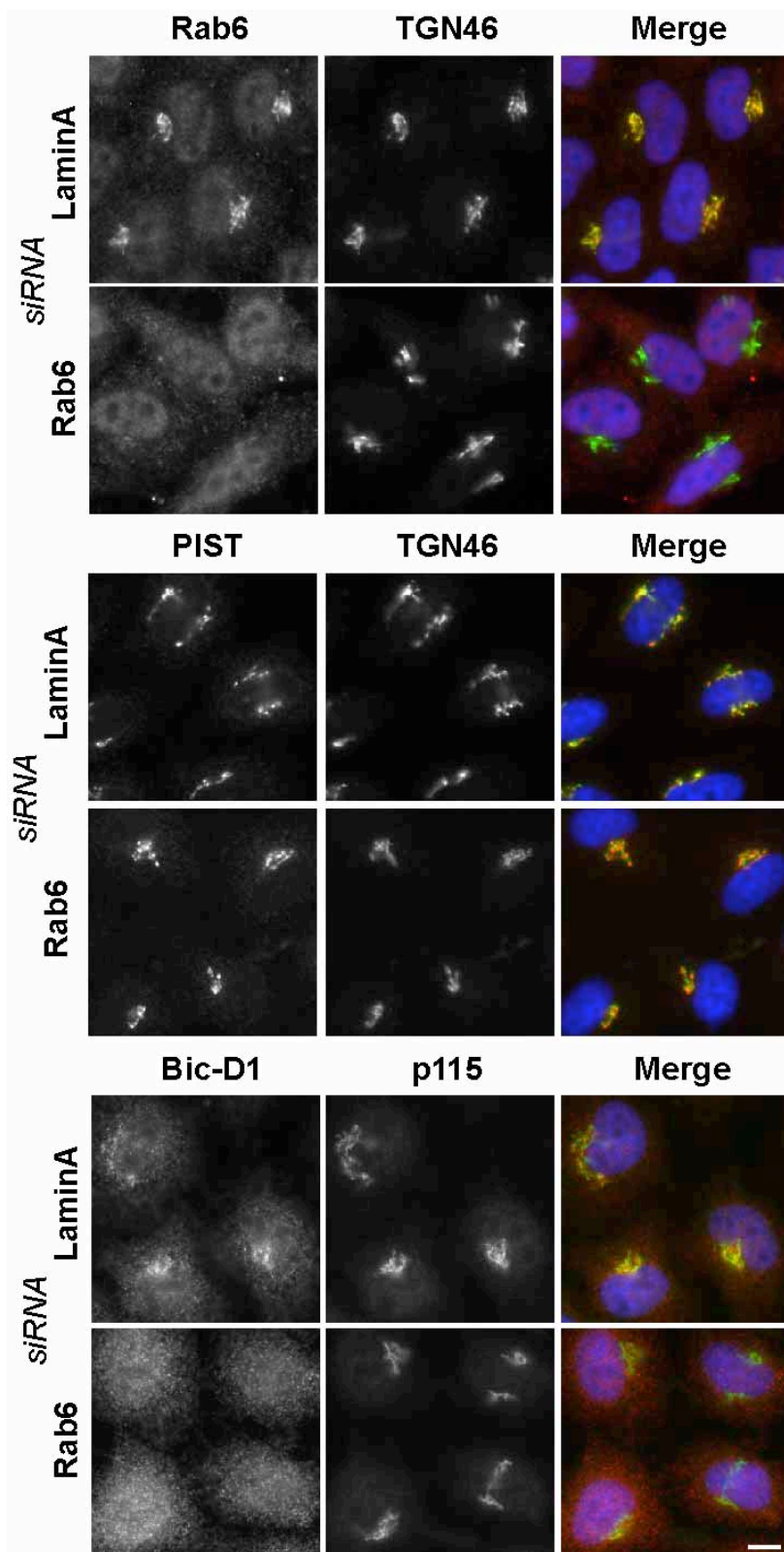
Figure 2.11 Depletion of Rab6 by siRNA redistributes Bic-D1 off the Golgi but has no effect on the localisation of PIST. HeLa cells were transfected with either Rab6 or LaminA siRNA duplexes for 72 hours, fixed and stained for Rab6, PIST or Bic-D1 (red) and TGN46 or p115 (green). DNA was visualised with DAPI (blue). Bar indicates 10 μm in all panels.

2.2.8 Golgin160 is a binding partner of PIST

Known binding partners of PIST are so far restricted to its PDZ domain and seem to be cargo proteins instead of targeting factors for PIST (Cheng et al., 2002; Hassel et al., 2003; Ito et al., 2006; Wente et al., 2005; Yao et al., 2001). Therefore, identifying proteins important for recruitment of PIST to the Golgi could help explaining the function of PIST and of Rab6. In order to identify so far unknown binding partners for PIST a large-scale immunoprecipitation (IP) was performed (Figure 2.12). Assay buffer or 293T total cell lysate was incubated with either pre-immune serum as unspecific control or the purified R-α-PIST antibody to precipitate PIST specific binding proteins. Bands visible also in the buffer control, originating from the antibody preparation itself, were ignored and only bands visible in the IP with R-α-PIST from 293T extract were excised. A gel piece of the corresponding position and size in the lane of the IP with pre-immune serum was excised as well to serve as a background control for mass spectrometric analysis. A faintly staining band in the molecular weight region of 160 – 180 kDa was identified by MALDI-TOF as the known Golgi localised protein Golgin160 (Fritzler et al., 1993; Misumi et al., 1997). The strongly staining band above the antibody heavy chain (about 55 kDa) turned out to be PIST itself.
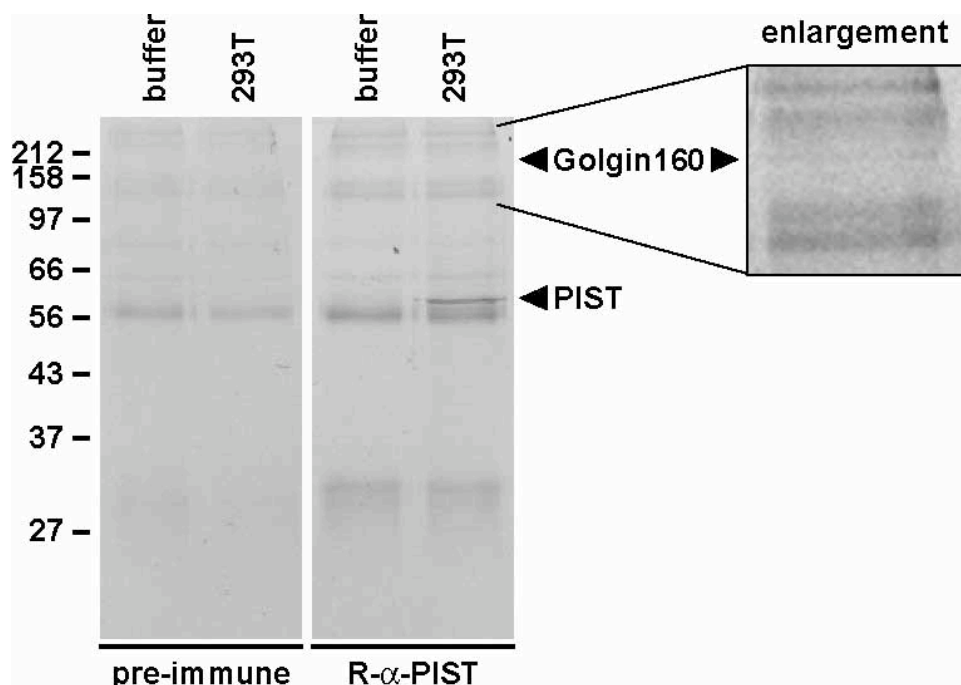
Figure 2.12 CBB staining of a large-scale immunoprecipitation (IP) from 293T extract, leading to the identification of Golgin160 as a binding partner of PIST.

Golgin160 is a peripheral membrane protein at the cytoplasmic face of Golgi membranes. Hicks and Machamer, 2002 showed that its N-terminal head domain is required for Golgi targeting, but the exact mechanism is unknown. The C-terminal two thirds of the protein are made of coiled-coil regions. Thus, Golgin160 belongs to the family of golgins, which are implicated in the maintenance of Golgi structure and integrity of membrane trafficking pathways (Barr and Short, 2003). Interestingly, the head of Golgin160 is cleaved by caspase-2 during apoptosis. The cleavage is required for the efficient disassembly of the Golgi and the propagation of apoptotic signals (Maag et al., 2005; Mancini et al., 2000). Interactions with Golgin160 at the Golgi could therefore be important for the structural integrity of Golgi membranes. The nature and functional relationship of the interaction of PIST with Golgin160 should be examined further.

Golgin160 could be confirmed as a binding partner for PIST via yeast two-hybrid analysis and immunoprecipitation from HeLa extract (Figure 2.13). In yeast two-hybrid analysis, full-length Golgin160 interacted strongly with PIST^{fl} and PIST$^{142-454}$ but not with the other fragments of PIST (Figure 2.13 A). The binding region within PIST might be positioned in-between the second coiled-coil and the PDZ domain because neither PIST$^{142-255}$, containing CC2, nor PIST$^{256-454}$, containing PDZ, gave a signal with Golgin160 in yeast two-hybrid analysis. In an immunoprecipitation experiment Golgin160 could be co-precipitated together with PIST by the PIST specific antibody R-α-PIST (Figure 2.13 B). Compared to the amount of PIST in total cell extract, the bulk of the protein was precipitated by the antibody and nothing at all by pre-immune serum. Golgin160 was co-precipitated, however, relatively little compared to the amount of protein in the loaded HeLa extract. Still, both proteins bound each other and the question remained whether Golgin160 could be the targeting factor for PIST being localised at the Golgi.
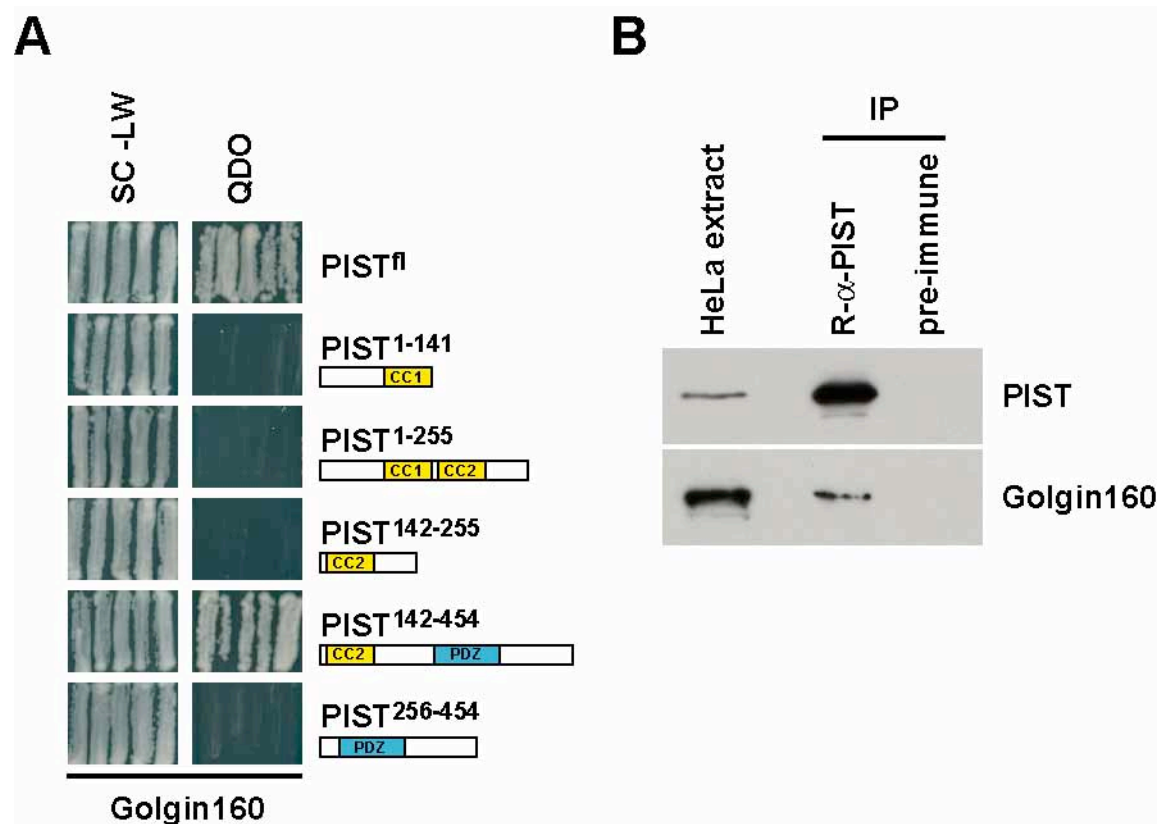
Figure 2.13 Golgin160 is a binding partner of PIST. (A) Yeast two-hybrid analysis of full-length Golgin160 against PIST full-length and PIST fragments, screening for interaction on QDO medium. **(B)** Co-immunoprecipitation of PIST and Golgin160 from HeLa extract by R-a-PIST.

2.2.9 PIST is unaltered in Golgin160 depleted cells

To address the role of Golgin160 in terms of PIST targeting and function Golgin160 was depleted from HeLa cells using siRNA. After 72 hours of siRNA Golgin160 protein levels dropped below the detection threshold in western blotting (Figure 2.14 A). GM130 and PIST levels remained the same in LaminA control siRNA and Golgin160 siRNA. Equal tubulin levels are shown as a loading control for equal total protein amounts on the blot. When Golgin160 depleted cells were stained for TGN46 a partial breakdown of the Golgi ribbon structure into ministacks was observed (Figure 2.14 B). PIST, and also Rab6, remained Golgi localised in these ministacks, as seen by the overlap with the TGN46 signal.

These results suggest that Golgin160 has no impact on the localisation of PIST at Golgi membranes. However, Golgin160 seems to function in maintaining the ribbon-like structure of the Golgi as in cells without detectable Golgin160 the ribbons break apart to form ministacks.
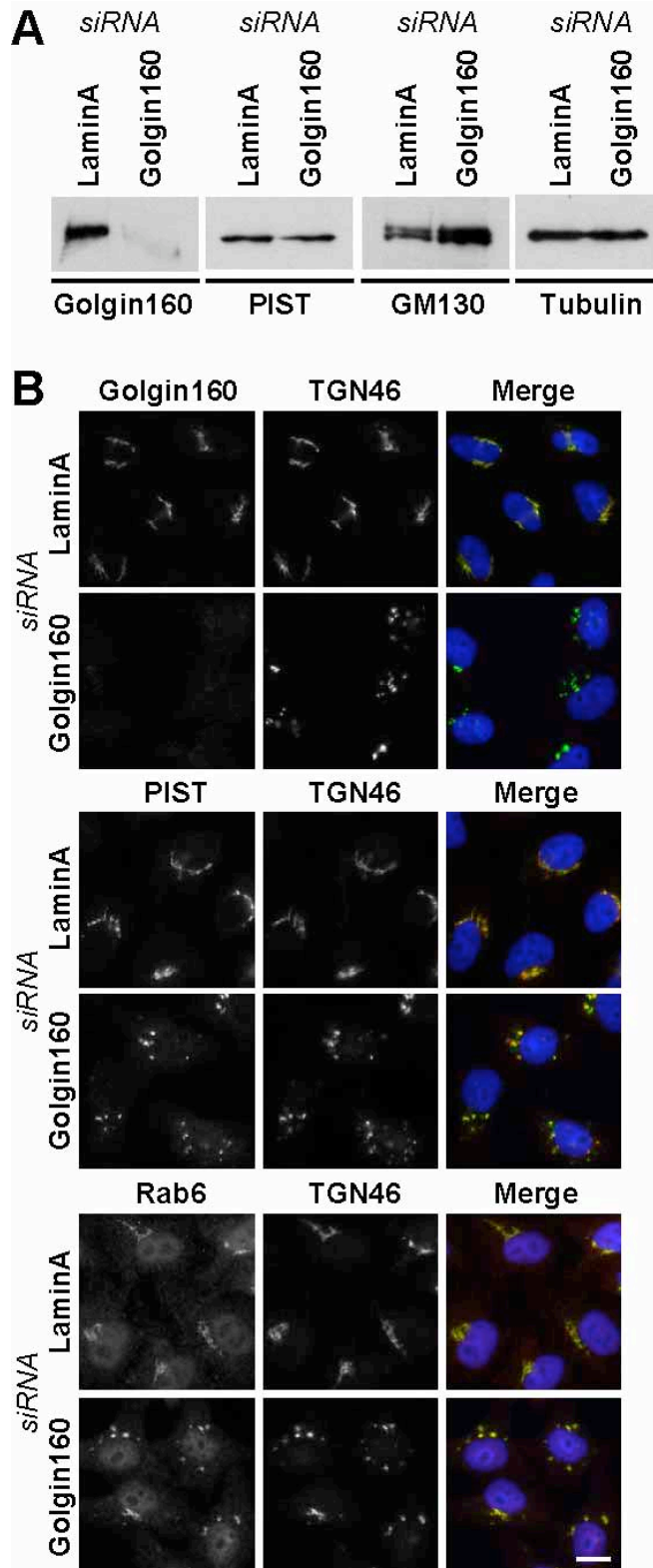
Figure 2.14 Depletion of Golgin160 by siRNA has no effect on the Golgi localisation of PIST. (A) Western blot of LaminA and Golgin160 siRNA cells probed for Golgin160, GM130, PIST and Tubulin. (B) Immunofluorescence of LaminA and Golgin160 siRNA cells, stained for Golgin160, Rab6 or PIST (red) and TGN46 (green). DNA was visualised with DAPI (blue). Bar indicates 10 μm in all panels.

2.2.10 Depletion of PIST does not have an effect on Golgi structure

So far it is unclear how and why PIST is targeted to Golgi membranes. As a coiled-coil protein it might also fulfil structural functions within the Golgi stack, like many other coiled-coil proteins are building up the so-called Golgi matrix (Barr and Short, 2003). In this case depletion of PIST would most likely result in a change of Golgi structure, as seen with cells depleted of Golgin160 (Figure 2.14) and other Golgins. However, knockdown of PIST by siRNA had no such effect, as can be seen in Figure 2.15. After 72 hours of PIST siRNA the level of PIST in HeLa cells was clearly reduced, whereas GM130 was equal to control conditions (Figure 2.15 A). Tubulin was probed to show equal protein levels of LaminA control and PIST siRNA samples on the Western blot. Also in immunofluorescence PIST was depleted after 72 hours of siRNA. Under these conditions both Golgi markers GM130 and TGN46 were unaltered as well as the PIST binding partners Rab6 and Golgin160 (Figure 2.15 B). So, PIST depletion has neither an effect on Golgi structure nor on its binding partners Rab6 and Golgin160 which leaves the question about PIST's function in HeLa cells still unanswered.
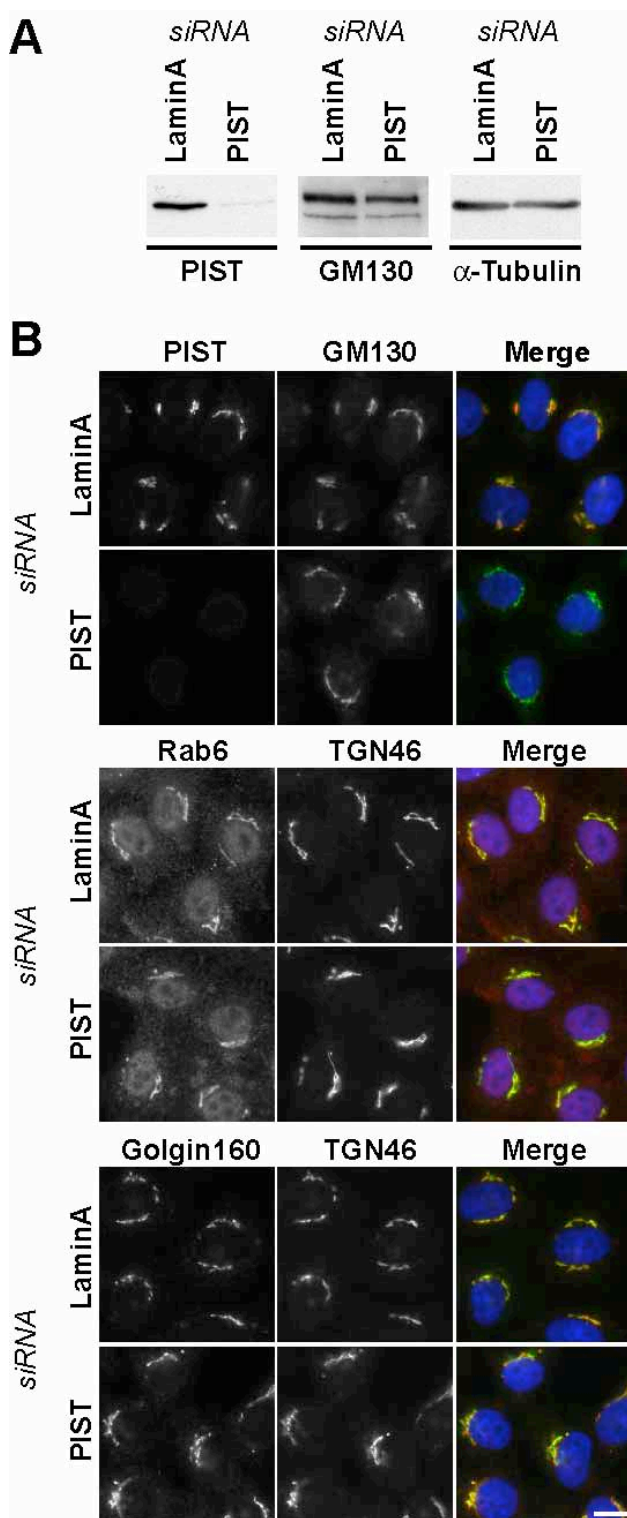
Figure 2.15 Depletion of PIST by siRNA has no effect on Golgi morphology and the localisation of Rab6 and Golgin160. (A) Western blot of LaminA and PIST siRNA cells probed for PIST, GM130 and Tubulin. (B) Immunofluorescence of LaminA and PIST siRNA cells, stained for PIST, Rab6 or Golgin160 (red) and GM130 or TGN46 (green). DNA was visualised with DAPI (blue). Bar indicates 10 μm in all panels.

2.3 Conclusions

In this part of the work the coiled-coil and PDZ domain protein PIST was identified and characterised as a novel Rab6 binding protein. For the characterisation of PIST a polyclonal antibody was generated and validated. Both, the recombinant protein purified from *E. coli* and endogenous PIST from HeLa extract bound Rab6 in a GTP-dependent manner. Yeast two-hybrid analysis as well as direct binding assays showed that the N-terminal coiled-coil region of PIST is necessary for the interaction with Rab6. Within the Rab family of GTPases the interaction of PIST is specific for Rab6. An interaction with the Rho family GTPase TC10, as published by Neudauer et al., 2001, could not be confirmed, either by yeast two-hybrid analysis or by direct binding assays. Additionally, when cloning the TC10 gene, the original database entry turned out to contain errors. According to expressed sequence data and confirmed by cloning of the respective nucleotide sequence from various cDNA libraries, the sequence of the TC10 protein is 8 amino acids shorter from the N-terminus than published by Neudauer et al., 2001.

Immunofluorescent staining of HeLa cells revealed that PIST is a Golgi localised protein. The Golgi targeting region was mapped to the second coiled-coil domain of PIST. Also in cells depleted of endogenous PIST the second coiled-coil was sufficient to localise to Golgi membranes. Thus, Rab6 binding and Golgi localisation are accomplished by two different regions in PIST, namely the first coiled-coil for Rab6 binding and the second coiled-coil region for Golgi localisation. In line with this, alteration of Rab6 levels by over-expression or siRNA had no effect on the Golgi localisation of PIST. Subsequently, the search for PIST binding proteins should clarify the question how PIST is targeted to the Golgi apparatus, where it interacts with Rab6. A member of the golgin family, Golgin160 was identified to co-immunoprecipitate with PIST from cell extract. The interaction between PIST and Golgin160 could be confirmed by yeast two-hybrid analysis, where full-length PIST and a region containing the second coiled-coil plus the sequence before the PDZ domain bound Golgin160. The depletion of Golgin160 using siRNA resulted in a fragmentation of the Golgi into mini stacks, but had no effects on the localisation of PIST to Golgi membranes. Concomitantly, the siRNA-mediated depletion of PIST exhibited no apparent phenotype on Golgi structure and localisation of its binding proteins Golgin160 and Rab6.

In summary, PIST is a high affinity binding partner of Rab6 in vitro and in vivo, but the functional relationship between these proteins remains unclear. The Golgi localised coiled-coil protein Golgin160 is also capable of binding PIST, but not required to target PIST to Golgi membranes.

3 Rab GTPase-activating proteins defining Shiga toxin and epidermal growth factor uptake pathways

3.1 Aim of the work

Activated Rab GTPases regulate membrane trafficking steps by recruiting effector proteins with various functions to a target membrane. The active state of a Rab is switched off by interaction with its specific Rab GTPase-activating protein (GAP), which catalyses the GTP hydrolysis reaction and turns the Rab into the inactive GDP-bound state. It has been shown before in the case of Rab5 that transient expression of a RabGAP can be used to inactivate the endogenous pool of a Rab and in this way interfere with the process this Rab is involved in (Haas et al., 2005). Non-specific effects of RabGAP expression can easily be discriminated from the specific effects of Rab inactivation by use of an inactive point mutant in which the catalytic arginine residue is replaced by alanine (Haas et al., 2005).

The retrograde transport of Shiga toxin from the cell surface to the ER is a multi-step process (Sandvig et al., 2002). Because each membrane trafficking step is thought to be regulated by a discrete set of Rabs (Zerial and McBride, 2001), it is likely that several Rabs are implicated in Shiga toxin trafficking. However, only Rab6 has been shown to be involved in the retrograde transport of Shiga toxin to date (Girod et al., 1999; Mallard et al., 2002; White et al., 1999). In order to better understand the mechanisms of retrograde trafficking, the aim of this part of the work was to identify Rab GAPs that interfere with the transport of Shiga toxin from the cell surface to the Golgi apparatus. First, conditions to follow Shiga toxin within the cell were established and validated using the published Rab6 GAP GAPCenA (Cuif et al., 1999). To find Rab GAPs that act specifically on the retrograde route of Shiga toxin to the Golgi and not on general endocytic pathways, a second functional assay for the uptake of epidermal growth factor (EGF) and its receptor to early endosomes was used. In total, 39 human TBC domain proteins, predicted to act as Rab GAPs, were screened in both Shiga toxin transport and EGF uptake assays. In combination with biochemical analysis, of the 60 Rabs and 39 RabGAPs, respective Rab – RabGAP pairs involved in either pathway were then identified.

3.2 Results

3.2.1 Establishment of the Shiga toxin and EGF retrograde transport assay

One method to study Shiga toxin trafficking is to use of fluorescently labelled B-subunit (STxB) in combination with immunofluorescence microscopy. Toxin B-

subunit can be recombinantly expressed and purified from *E. coli* (see 5.7.1). Cells are then incubated with fluorescently labelled B-subunit and observed over a period of time. Together with intracellular markers, like resident Golgi proteins, the transport of STxB can be followed. This assay can be performed in a high-throughput format and was therefore suitable to screen Rab GAPs for their ability to inhibit retrograde transport of Shiga toxin between the plasma membrane and the Golgi apparatus

To establish the right conditions for uptake and retrograde transport of the Shiga Toxin B-subunit (STxB) to the Golgi apparatus a time course experiment was performed (see Figure 3.1). Fluorescently labelled STxB was bound to HeLa cells on ice for 30 minutes, before starting the uptake of the toxin at 37 °C by quenching with warm growth medium. The cells were fixed with PFA after the indicated times and imaged by immunofluorescence microscopy. Initially (0 min), fluorescently labelled B-subunit was bound to the cell surface of HeLa cells. After 30 minutes at 37 °C STxB was internalised and had partially reached the Golgi, marked by co-staining with the cis-Golgi marker GM130. This Golgi associated pool of STxB was clearly visible in the majority of cells after 60 minutes of uptake.
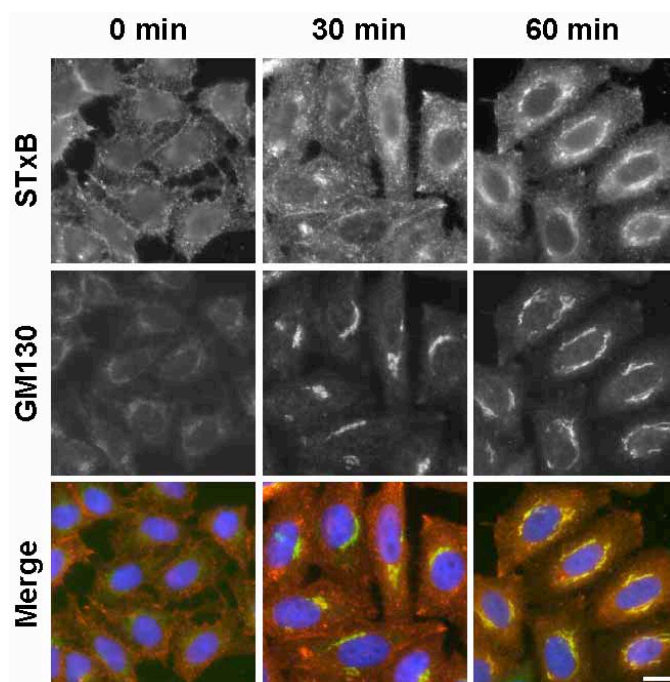
Figure 3.1 Shiga toxin B-subunit (STxB) reaches the Golgi compartment after 60 minutes. Fluorescently labelled STxB (red) was bound to the surface HeLa cells on ice (0 min) and internalised at 37 °C for 30 or 60 minutes. Co-staining with GM130 (green) marked the Golgi apparatus, DNA was visualised with DAPI (blue). Bar indicates 10 μm in all panels.

Earlier steps in STxB endocytosis were visualised by another time course experiment in a co-uptake with fluorescently labelled epidermal growth factor (EGF). It is known from previous experiments that EGF uptake and trafficking to the early endosome takes place within the first 20 to 30 minutes at 37 °C (Haas et al., 2005). Therefore this experiments shows if STxB follows the same route as EGF before being diverted to the Golgi apparatus. Figure 3.2 shows that both ligands bound to the cell surface of HeLa cells efficiently, and became internalised into small punctate structures after 10 to 20 minutes. After this, the two markers separated and STxB accumulated in the perinuclear region from 30 to 60 minutes, shown before to correspond to Golgi stacks (Figure 3.1), while EGF remained in punctate endosomal structures best visible after 30 minutes. Interestingly, while both ligands have been reported to be taken up by clathrin dependent pathways (Nichols et al., 2001; Sandvig et al., 1989) the kinetics of uptake were clearly different. This indicates that there may be some differences in the mechanistic details of the two uptake pathways, such as the requirement for Rab GTPases. For further experiments, it was therefore decided to take 60 minutes uptake of Shiga toxin to measure the efficiency of its transport to the Golgi, and 30 minutes uptake of EGF to measure its uptake into early endosomes.
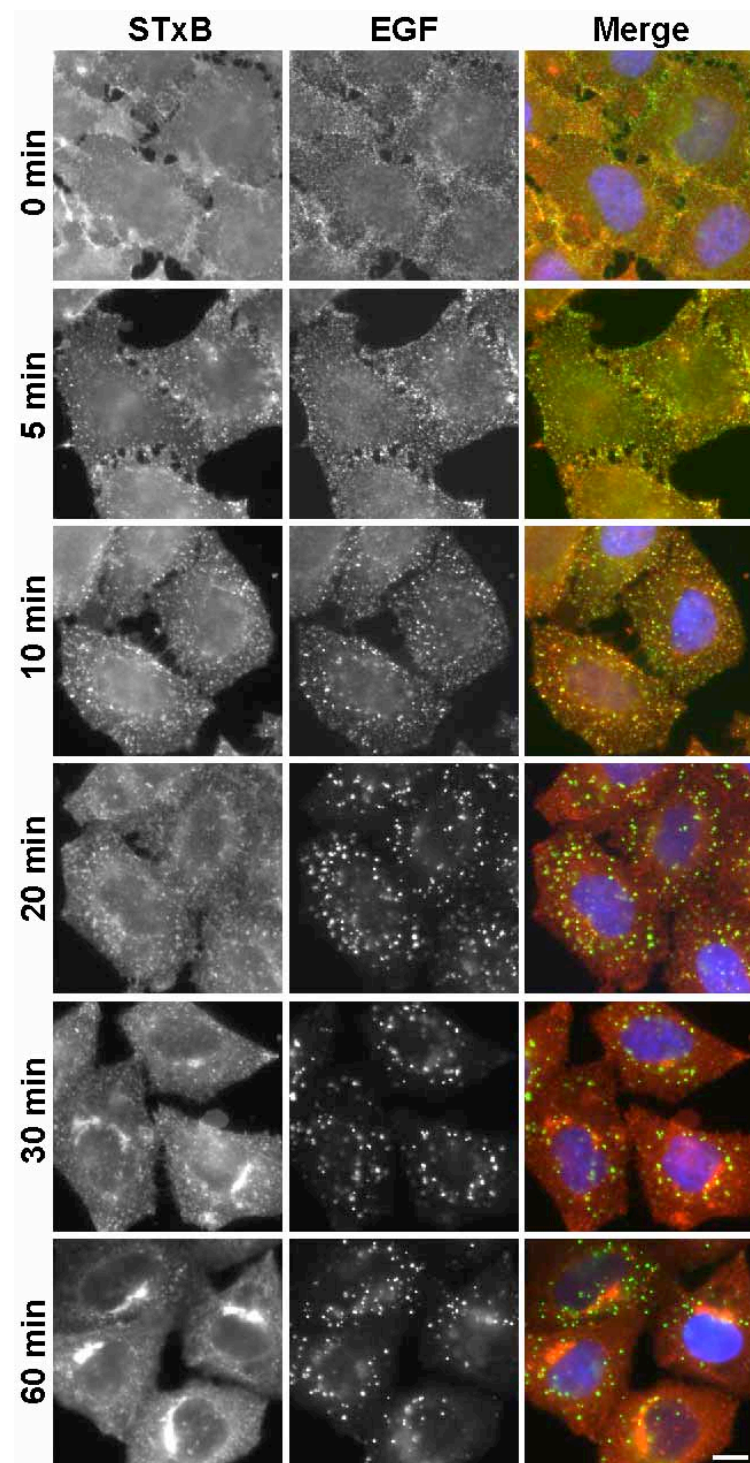
Figure 3.2 Comparison of the Shiga toxin and EGF uptake pathways. Fluorescently labelled STxB (red) and EGF (green) were bound to the surface of HeLa cells (0 min) and internalised at 37 °C for the indicated times. DNA was visualised with DAPI (blue). Bar indicates 10 μm in all panels.

3.2.2 Shiga toxin transport but not EGF uptake is Rab6 dependent

Rab6 has been shown before to be required for Shiga Toxin transport from endosomes to the Golgi apparatus (Mallard et al., 2002; White et al., 1999) while the uptake of EGF should be Rab6 independent. To verify this, the effects of Rab6 depletion were examined (Figure 3.3 and Figure 3.4). Both isoforms of Rab6, Rab6a/a' and Rab6b, were depleted using siRNA and immunostained with antibodies against the trans Golgi marker TGN46, the Rab6 effector protein Bic-D1 and Rab6 itself (shown in Figure 3.3 A). According to the antibody staining Rab6 seemed to be depleted from Rab6 siRNA cells while Golgi structure was like in control cells. Importantly, the Rab6 effector Bic-D1 (Matanis et al., 2002; Short et al., 2002) was redistributed from Golgi membranes to the cytoplasm in Rab6 siRNA cells, which served as a control for the efficient depletion of the active pool of Rab6.

Additionally, cells depleted of Rab6 and control cells were transfected with GFP-tagged versions of either Rab6a or Rab6b for 24 hours and probed on Western blot for GFP signal (Figure 3.3 B). After a total of 72 hours siRNA for Rab6a or Rab6b both GFP-tagged proteins were reduced or completely depleted compared to the expression in control cells. Tubulin was probed as a loading control, the levels of which were equal in Rab6 siRNA and control cells. Because over-expressed Rab6 was depleted by specific single siRNAs it was assumed, that also the endogenous pools of Rab6a/a' and Rab6b were gone in the treatment with both siRNA duplexes mixed 1:1. In further descriptions this treatment will be called simply Rab6 siRNA.
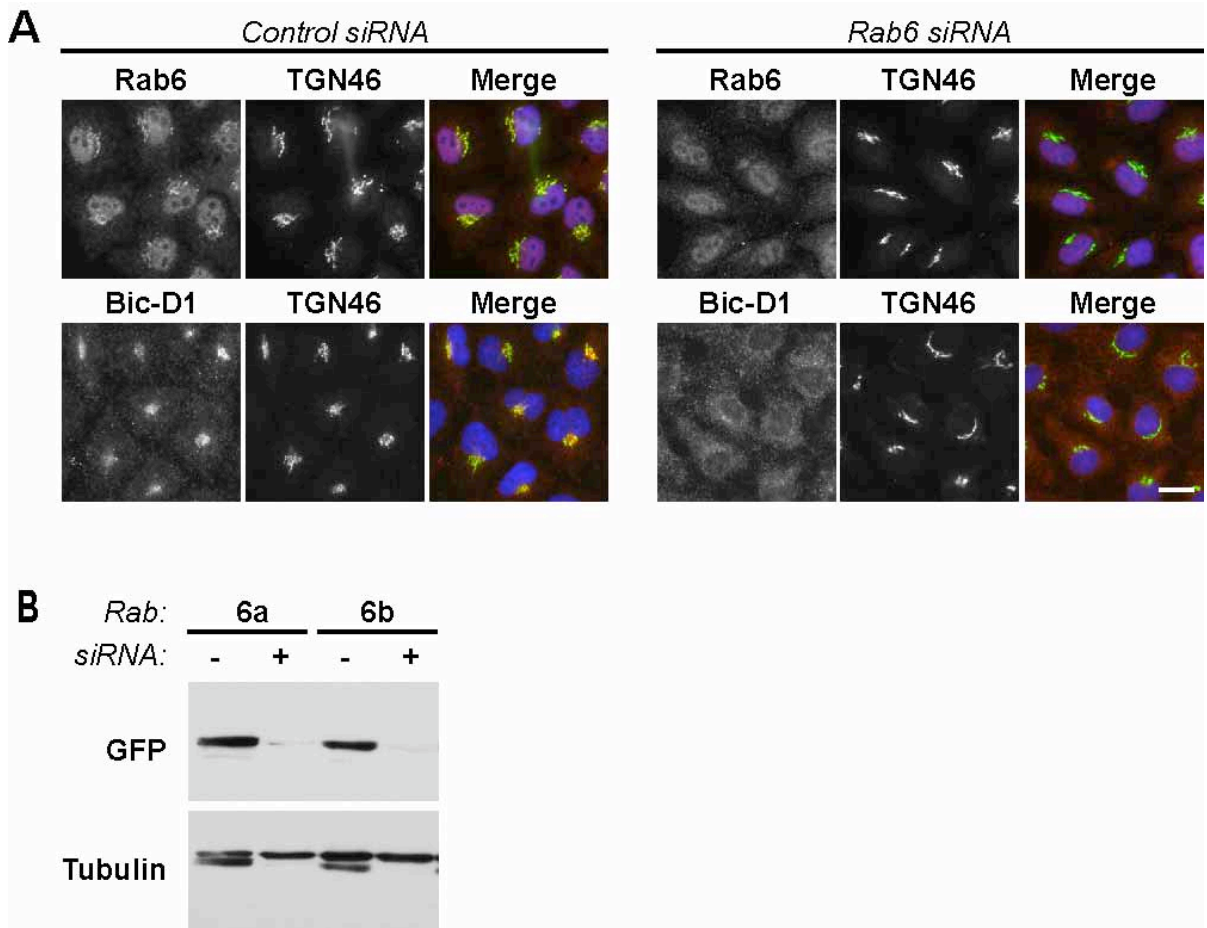
Figure 3.3 Depletion of Rab6a and Rab6b by siRNA. (A) HeLa cells were treated for 72 hours with mixed Rab6a and Rab6b (1:1) siRNA duplexes and stained with antibodies against Rab6 or Bic-D1 (red) and the trans Golgi marker TGN46 (green). DNA was visualised with DAPI (blue). Bar indicates 10 μm in all panels. **(B)** HeLa cells treated for 48 hours with either control (-) or specific (+) siRNA duplexes were transfected for 24 hours with constructs for the corresponding GFP-tagged Rab as indicated in the figure. Cell extracts were western blotted for GFP to detect the expression of the Rabs. Blots were re-probed for tubulin as a loading control.

Subsequently Rab6 depleted HeLa cells were assayed for STxB and EGF uptake. Figure 3.4 depicts the immunofluorescent pictures of this experiment. Whereas in control siRNA cells STxB was transported to the trans Golgi network efficiently, marked by the strong perinuclear signal overlapping with TGN46 staining (60 min), the Golgi localised pool of STxB in Rab6 siRNA was significantly reduced. This reduction was not due to reduced STxB levels in general as initial binding of the toxin B-subunit (0 min) was comparable. However, no complete block of STxB transport to the Golgi could be observed, which might be linked to siRNA efficiency or redundancy of Rab regulated transport pathways.

The partial block of STxB in Rab6 depleted cells seemed to be specific because EGF was taken up normally into early endosomal structures, marked by EEA1, in both control and Rab6 siRNA cells.
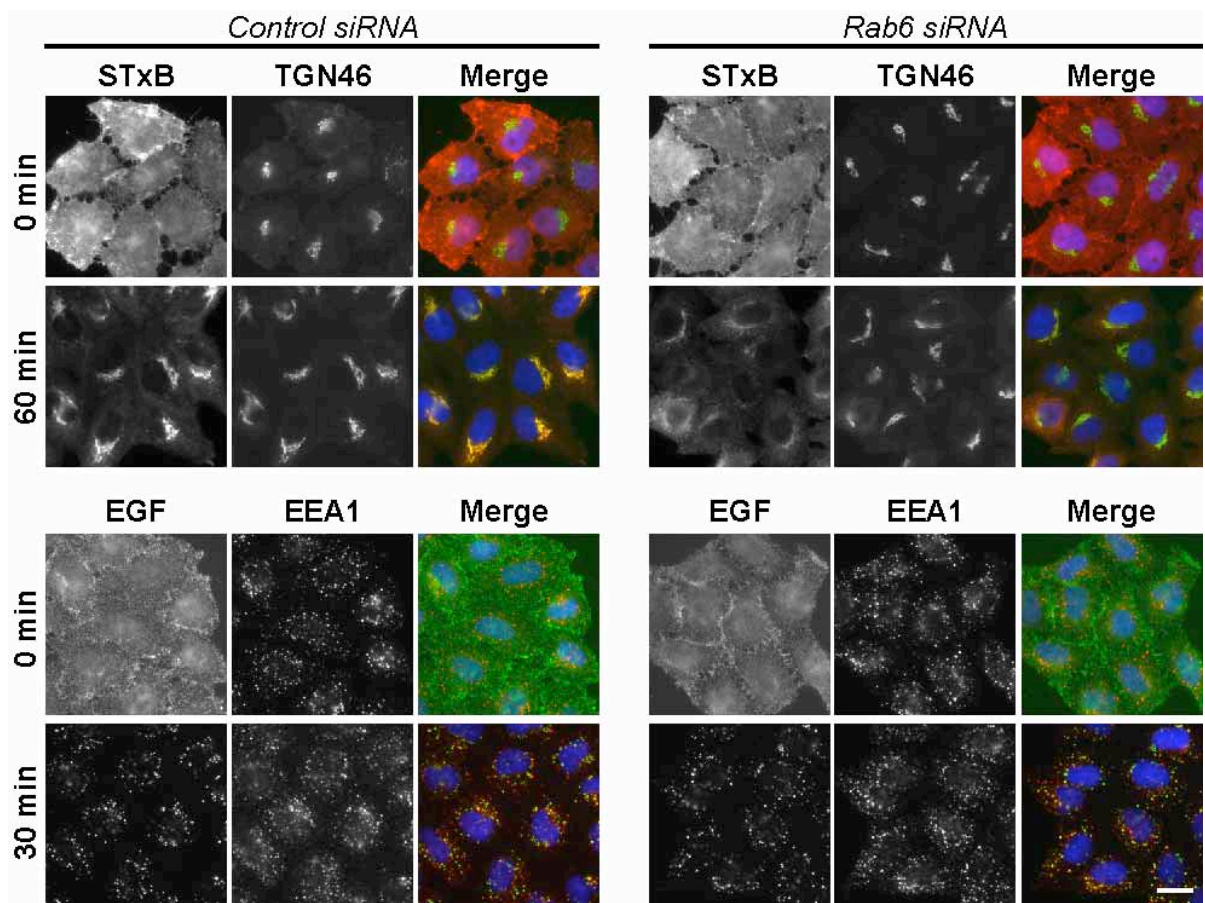
Figure 3.4 Shiga toxin but not EGF uptake is Rab6 dependent. HeLa cells were treated for 72 hours with control or Rab6 siRNA and used for STxB (red) or EGF (green) uptake assays and co-stained for TGN46 (green) or EEA1 (red). DNA was visualised with DAPI (blue). Bar indicates 10 μm in all panels.

For functional studies of a Rab GTPase, shifting the GTPase cycle towards inactive Rab GTPase by over-expression of its specific GTPase activating protein (GAP) can be used as a method instead of depleting the Rab itself by siRNA. This was shown before to work beautifully with Rab5 and its GAP RabGAP-5 (Haas et al., 2005). Since this method overcomes the problem of siRNA efficiency and specificity it should be tested whether the GAP for Rab6 could inhibit Shiga toxin transport to the Golgi equally well or even more efficiently than shown in the Rab6 siRNA experiment.

3.2.3 TBC1D11/GAPCenA acts on Rab4 and does not block Shiga toxin transport

It has previously been reported that TBC1D11/GAPCenA is the GAP for Rab6 (Cuif et al., 1999) and this was therefore tested for its ability to block trafficking of Shiga toxin to the Golgi apparatus (Figure 3.5). Surprisingly the expression of GAPCenA had no obvious effect on the transport of Shiga toxin to the Golgi apparatus (Figure 3.5 A). STxB was bound to the surface evenly (0 min) and had reached the perinuclear compartment after 60 minutes in both, transfected and untransfected cells. Also, the ability of Rab6 or of the Rab6-dependent effector Bic–D1 to target to Golgi membranes was not impaired in GAPCenA expressing cells (Figure 3.5 B).
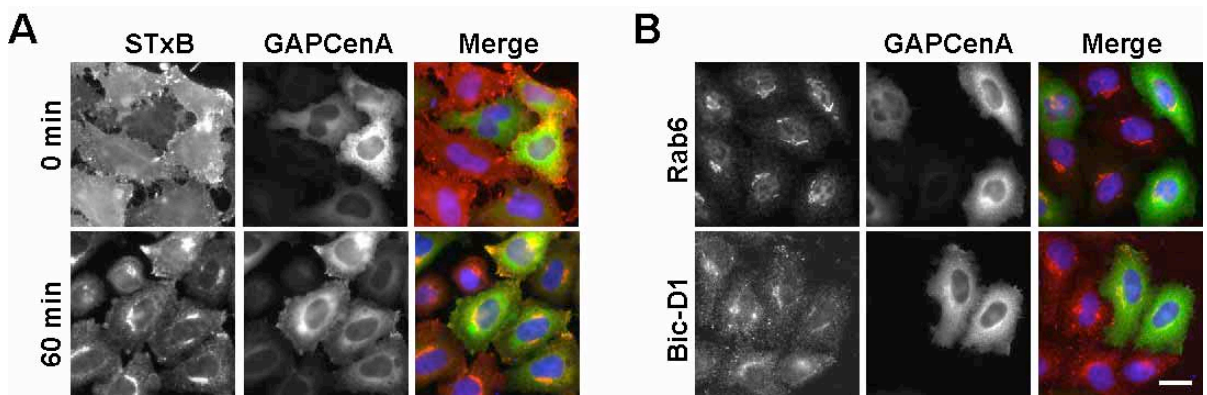
Figure 3.5 TBC1D11/GAPCenA does not block Shiga toxin transport. (A) HeLa cells transfected with GFP-tagged TBC1D11/GAPCenA (green) were used for Shiga toxin uptake assays (red). (B) The ability of Rab6 or Bic-D1 (red) to localise to the Golgi was tested in cells expressing GFP-tagged TBC1D11/GAPCenA (green). DNA was visualised with DAPI. Bar indicates 10 μm in all panels.

GAPCenA was therefore investigated further to find out if it has the biochemical properties expected of a Rab6 GAP. Confirming previous findings (Cuif et al., 1999), a C-terminal fragment of GAPCenA was identified when Rab6 was screened against a yeast-two-hybrid cDNA library. However, this fragment corresponding to a predicted coiled-coil region adjacent to the GAP domain (aa 723-998) does not show specific interaction with Rab6, and binds human Rabs of many different subfamilies when tested against a representative collection of human Rabs (Figure 3.6). When full-length GAPCenA was tested, it showed a strong interaction with Rab4, a weaker interaction with Rab11, and only a very weak interaction with Rab6. A more detailed analysis, where GAPCenA deletion mutants lacking the N-terminal PTB domain (aa 201-998) or the C-terminal coiled-coil region (aa 1-723) were tested, revealed that regions N- and C-terminal to the core TBC domain contribute to the recognition of specific Rabs.
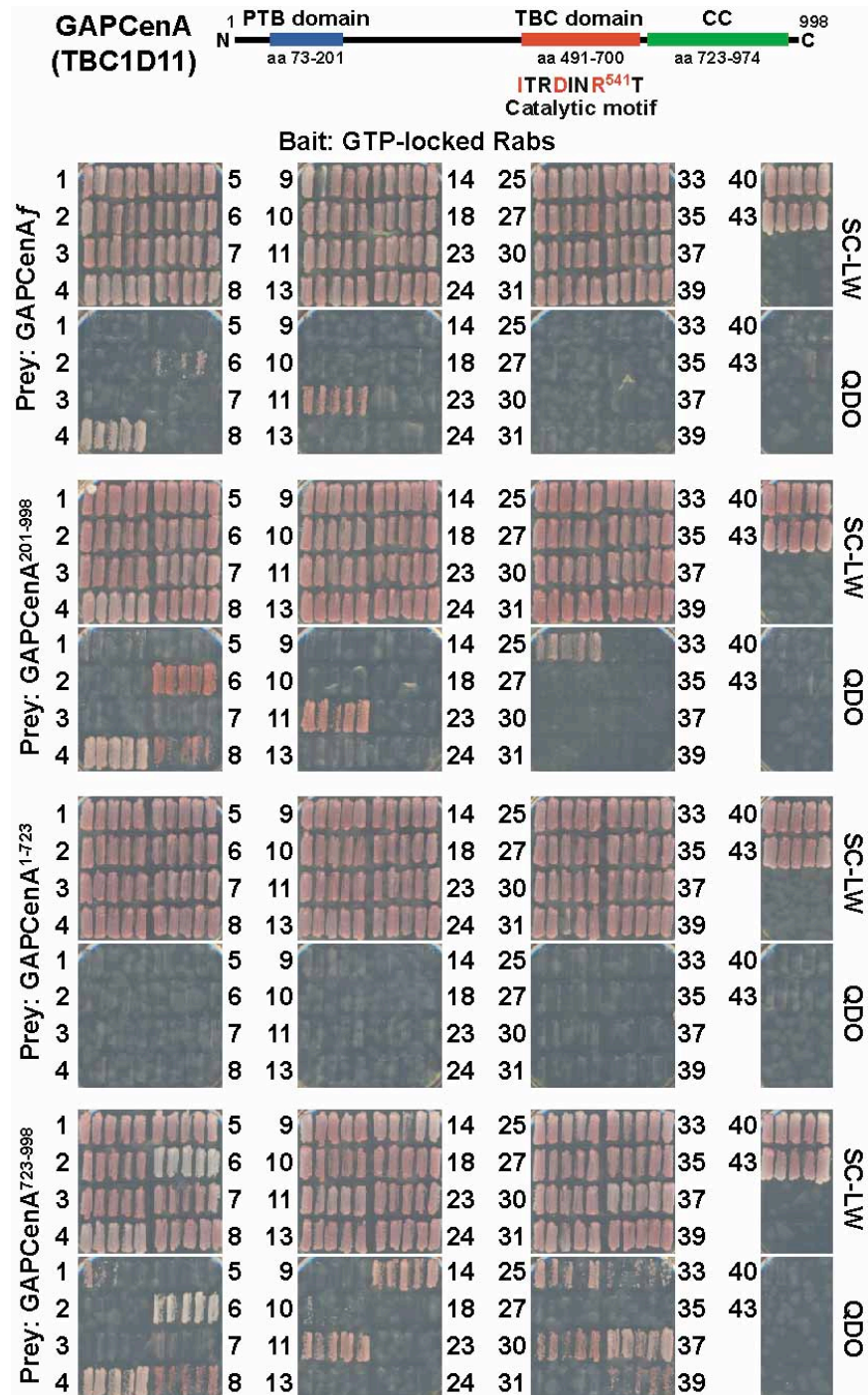
Figure 3.6 Interaction specificity of TBC1D11/GAPCenA with human Rab GTPases involves regions outside the TBC domain. A schematic of TBC1D11/GAPCenA shows the putative phosphotyrosine binding domain (PTB; blue), the TBC domain (red), and a C-terminal coiled-coil region (green). GTP-locked mutants of the Rabs indicated were tested using the yeast two-hybrid assay against full-length TBC1D11/GAPCenA, deletion mutants lacking the N-terminal PTB domain or the C-terminal predicted coiled-coil region, and the C-terminal coiled-coil region only, which was identified by an unbiased yeast two-hybrid library screen. In all cases, five independent colonies were tested on SC-LW and QDO. Growth on QDO indicates an interaction between bait and prey.

These results suggested that Rab6 might not be the target for TBC1D11/GAPCenA after all, and biochemical assays were carried out to test this. For measuring GTP-hydrolysis Rab proteins were first loaded with GTP, which was traced with $[\gamma\text{-}^{32}P]$-GTP, and then incubated together with TBC1D11/GAPCenA (see 5.7.4). In agreement with the yeast two-hybrid data, TBC1D11/GAPCenA had strong GAP activity towards Rab4 and a lesser activity towards Rab11 (Figure 3.7). Only very weak activity was detected towards Rab2 and Rab14, which fall into the same Rab subfamily as Rabs 4 and 11, showing that TBC1D11/GAPCenA can discriminate between closely related Rabs. No significant activity could be detected towards Rab6 or any of the other Rabs tested (Figure 3.7). It was previously suggested that Rab6 has to be prenylated in order to be an efficient substrate for TBC1D11/GAPCenA (Cuif et al., 1999). However, no GAP activity could be seen when prenylated Rab6 purified from insect cells was used (Figure 3.7, Rab6^{Sf9}). It should be also noted that Rab4 was prepared in bacteria, and therefore not prenylated, yet was still an excellent substrate for TBC1D11/GAPCenA. In summary, these data show that TBC1D11/GAPCenA is a GAP for Rab4 but not Rab6, and that it does not alter the trafficking of Shiga toxin to the Golgi apparatus.
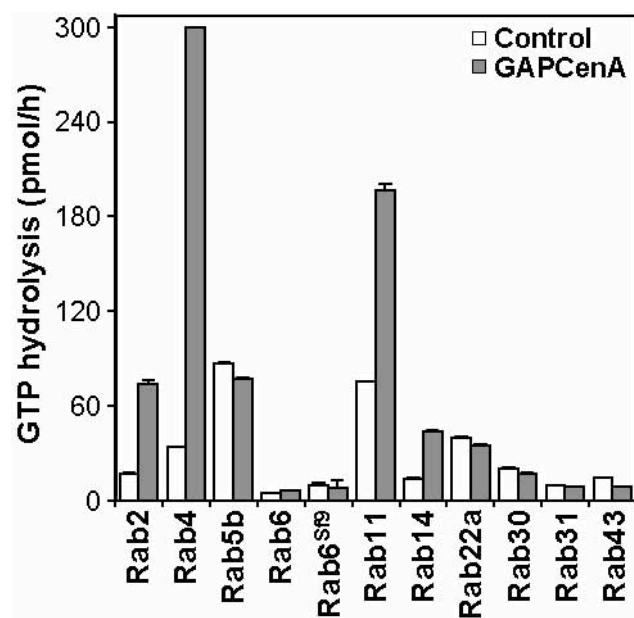
Figure 3.7 TBC1D11/GAPCenA is a GAP for Rab4. GAP assays were performed using 0.5 pmol recombinant TBC1D11/GAPCenA (filled bars) or a buffer control (open bars) and 100 pmol of the Rabs indicated in the figure. Two preparations of Rab6 were used: one from bacteria (Rab6), the other a prenylated preparation produced in insect cells (Rab6^{Sf9}).

3.2.4 A subset of human RabGAPs influences Shiga toxin transport

An unbiased approach was therefore taken to identify which RabGAPs act on the Shiga toxin transport pathway. Cells expressing the various predicted wild type human RabGAPs were tested blindly for their ability to inhibit the transport of Shiga toxin to the Golgi apparatus (Table 3.1 and Figure 3.8). Candidate positives from the first round of screening were then re-tested, comparing the effects of wild type GAP to that of catalytically inactive point mutant. In this screen, 6 of 39 predicted GAPs showed catalytic activity dependent effects on Shiga toxin trafficking to the Golgi apparatus: EVI5, RN-tre, TBC1D10A, TBC1D10B, TBC1D10C and TBC1D17 (Table 3.1, white on dark gray background and Figure 3.8).

Table 3.1 Effects of human TBC-domain containing proteins on Shiga toxin transport. HeLa cells were transfected for 24 h with GFP-tagged wild type or catalytically inactive Rab GAPs. These cells were then used for Shiga toxin B-subunit (STxB) or EGF-uptake assays, and the uptake of STxB and EGF scored at 1 h or 30 minutes, respectively. A 0 minute time point was also taken to verify that both STxB and EGF were bound to the cell surface with equal efficiency for all conditions. The localization of the GFP-tagged Rab GAPs was also scored. Fields with dark gray background show the positive Rab GAP candidates blocking STxB. Empty fields mean "not determined" (nd). Notes: 1) Some highly expressing cells failed to bind EGF at the zero time point, indicating a defect in the trafficking of EGF receptor to the cell surface. However, the majority of cells bound and took up EGF as normal. 2) The RabGAP-5 GAP domain was used for this experiment. 3.) The PARIS-1 longer splice variant gave results indistinguishable from TBC1D2. 4) Expression triggered extensive cell death.

Rab GAP	Wild type TBC domain				Catalytically inactive TBC domain		
	STxB (1h)	GAP localization	EGF (30 min)	Golgi	STxB (1 h)	GAP localization	EGF (30 min)
EVI-5	Golgi and vesicular	Cytosolic	Early endosomes[1]	Intact	Golgi	Tubules, cytosolic	nd
RN-tre	Cell surface	Cell surface	Early endosomes[1]	Fragmented	Golgi	Cell surface	nd
RUTBC1	Golgi	Cytosolic, nuclear	Early endosomes				
RUTBC2	Golgi	Cytosolic	Early endosomes				
RabGAP-5 (RUTBC3)	Golgi	Cytosolic	Cell surface	Intact	Golgi[2]	Cytosolic	Early endosomes
TBC1D1	Golgi	Cytosolic	Early endosomes				
TBC1D2[3]	Golgi	Cytosolic	Early endosomes				
TBC1D3B[4]	Recycling endosomes	Vacuoles	nd				
TBC1D4	Golgi	Cytosolic	Early endosomes				
TBC1D5	Golgi	Cytosolic	Early endosomes				
TBC1D6	nd						
TBC1D7	Golgi	Cytosolic, nuclear	Early endosomes				

| Rab GAP | Wild type TBC domain | | | | Catalytically inactive TBC domain | | |
	STxB (1h)	GAP localization	EGF (30 min)	Golgi	STxB (1 h)	GAP localization	EGF (30 min)
TBC1D8	Golgi	Reticular, cytosolic	Early endosomes				
TBC1D10A	Recycling endosomes	Cell surface	Early endosomes[1]	Intact	Golgi	Cell surface	nd
TBC1D10B	Recycling endosomes	Cell surface	Early endosomes	Intact	Golgi	Cell surface	nd
TBC1D10C	Recycling endosomes	Filopodia, cell surface	Early endosomes	Intact	Golgi	Cell surface	nd
TBC1D11 (GAPCenA)	Golgi	Cytosolic	Early endosomes	Intact	nd	nd	nd
TBC1D12	nd						
TBC1D13	Golgi	Cytosolic, nuclear	nd				
TBC1D14	Recycling endosomes	Recycling endosomes	Early endosomes	Fragmented	Recycling endosomes	Recycling endosomes	nd
TBC1D15	Golgi fragments	Cytosolic, nuclear	Early endosomes[1]	Fragmented			
TBC1D16	Golgi	Cytosolic	nd				
TBC1D17	Vesicular	Cytosolic	Early endosomes	Intact	Golgi	Cytosolic	nd
TBC1D18	Golgi	Cytosolic	nd				
TBC1D19	Golgi	Cytosolic, nuclear	nd				
TBC1D20	Vesicular	ER	Early endosomes1	Fragmented			
TBC1D21	Golgi	Cytosolic	nd				
TBC1D22A	Golgi fragments	Cytosolic, nuclear	Early endosomes	Fragmented	Recycling endosomes	Cytosolic/ nuclear	nd
TBC1D22B	Golgi fragments	Cytosolic, nuclear	Early endosomes	Fragmented	Recycling endosomes	Cytosolic/ nuclear	nd
USP6	Golgi	Cell surface	nd				
AK074305	Golgi	Cytosolic	nd				
KIAA1055	Golgi	Cytosolic	nd				
KIAA0676	Golgi	Cytosolic	nd				
KIAA0882	nd						
NP_060222	nd						
NP_060779	Golgi	Cytosolic, Golgi	nd				
EVI5-like	Golgi	Cytosolic, aggregates	nd				
KIAA0984	Vesicular	Cytosolic, aggregates	Early endosomes[1]	Fragmented	Vesicular	Cytosolic, aggregates	nd
KIAA1171	Golgi	Cell surface	nd				
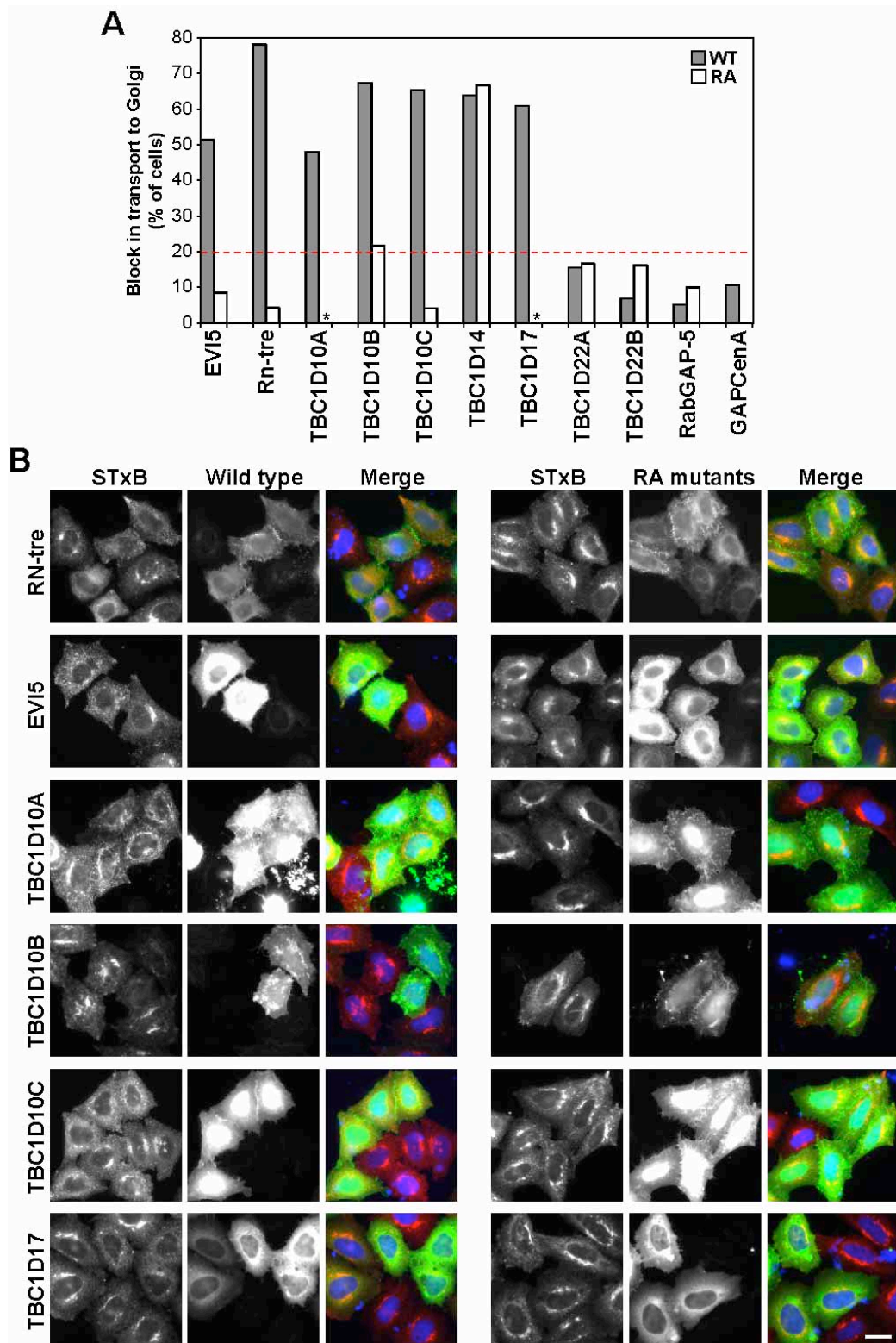
Figure 3.8 A subset of human Rab GAPs influence Shiga toxin transport. Shiga Toxin uptake assays were performed on HeLa cells transfected with a library of wild type human Rab GAPs listed in Table 3.1. Those Rab GAPs showing a block in Shiga toxin uptake were re-tested as catalytically inactive RA mutants. (A) To measure the extent of Shiga toxin uptake, cells were fixed and stained for a Golgi marker. The percentage of untransfected and transfected cells where STxB had not reached the Golgi was counted for each condition, and the specific

reduction in Shiga toxin transport calculated by subtracting these two figures (transfected – untransfected cells). These numbers are plotted on the bar graph. The dotted line indicates the cut-off chosen for consideration as a positive. (B) Images of the Rab GAPs (green) showing a catalytic activity dependent block or reduction in Shiga toxin (red) uptake after 60 minutes are shown. DNA was visualised with DAPI (blue). Bar indicates 10 μm in all panels.

TBC1D14 was excluded from the list of positive candidate GAPs after the second round of screening because the inhibitory effect on Shiga toxin trafficking was also seen with the catalytically inactive mutant of TBC1D14 suggesting that these effects were not due to Rab inactivation but due to another mechanism independent of the GAP activity of TBC1D14.

To confirm that the lack of a Golgi signal for Shiga toxin after 60 minutes of uptake was not simply due to disruption of the Golgi, the integrity of this organelle was tested using markers for the cis- and trans-Golgi compartments (Figure 3.9). This resulted in the elimination of GAPs such as TBC1D22A and TBC1D22B where the Golgi was fragmented and Shiga toxin was found to localise to these fragments. In contrast, RN-tre, although fragmenting the Golgi (Figure 3.9), caused a block of Shiga toxin in more peripheral structures discrete from the Golgi dependent on its catalytic activity and was therefore counted as a positive (Figure 3.8). It should be noted already at this point that RabGAP-5, a Rab5 GAP (Haas et al., 2005), did not show a phenotype in Shiga toxin uptake (see Figure 3.8 A) pointing to the fact that Shiga toxin endocytosis is independent of Rab5.

The question remained whether any of the positive Rab GAPs blocking Shiga toxin transport to the Golgi apparatus acts on Rab6. To answer this, positive Rab GAPs were co-transfected with the Rab6 effector Bic-D1, whose Golgi localisation is dependent on active Rab6 (Figure 3.3). Interestingly, none of the positive GAPs were able to cause release of Bic-D1 from Golgi membranes (Figure 3.10), suggesting that they do not act on Rab6 but rather on other Rab GTPases.
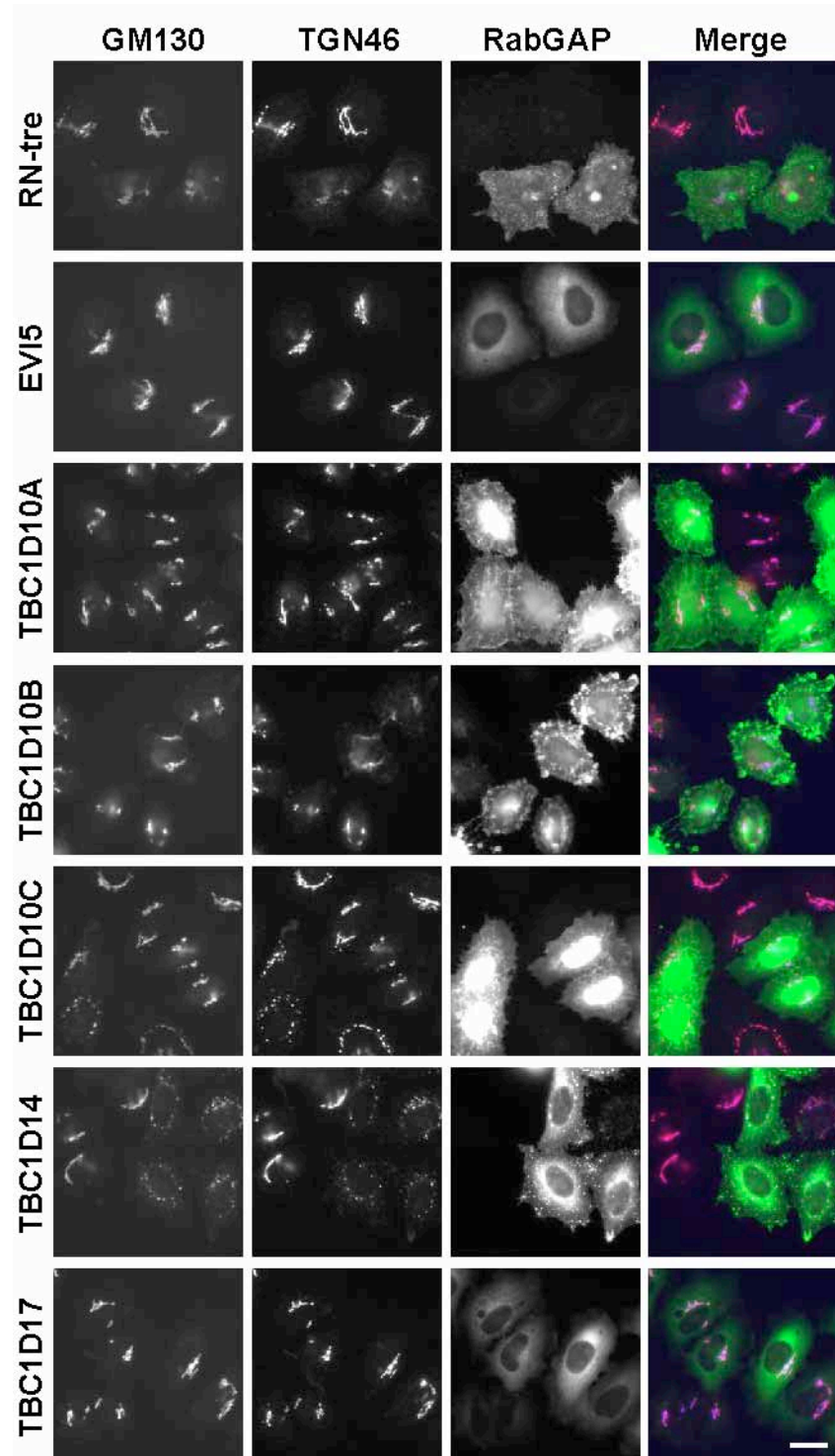
Figure 3.9 Effect of Rab GAPs blocking Shiga toxin uptake on Golgi morphology. HeLa cells transfected for 24 hours with the GFP-tagged Rab GAPs (green) indicated in the figure were fixed and then stained for GM130 (blue) and TGN46 (red). Bar indicates 10 μm in all panels.
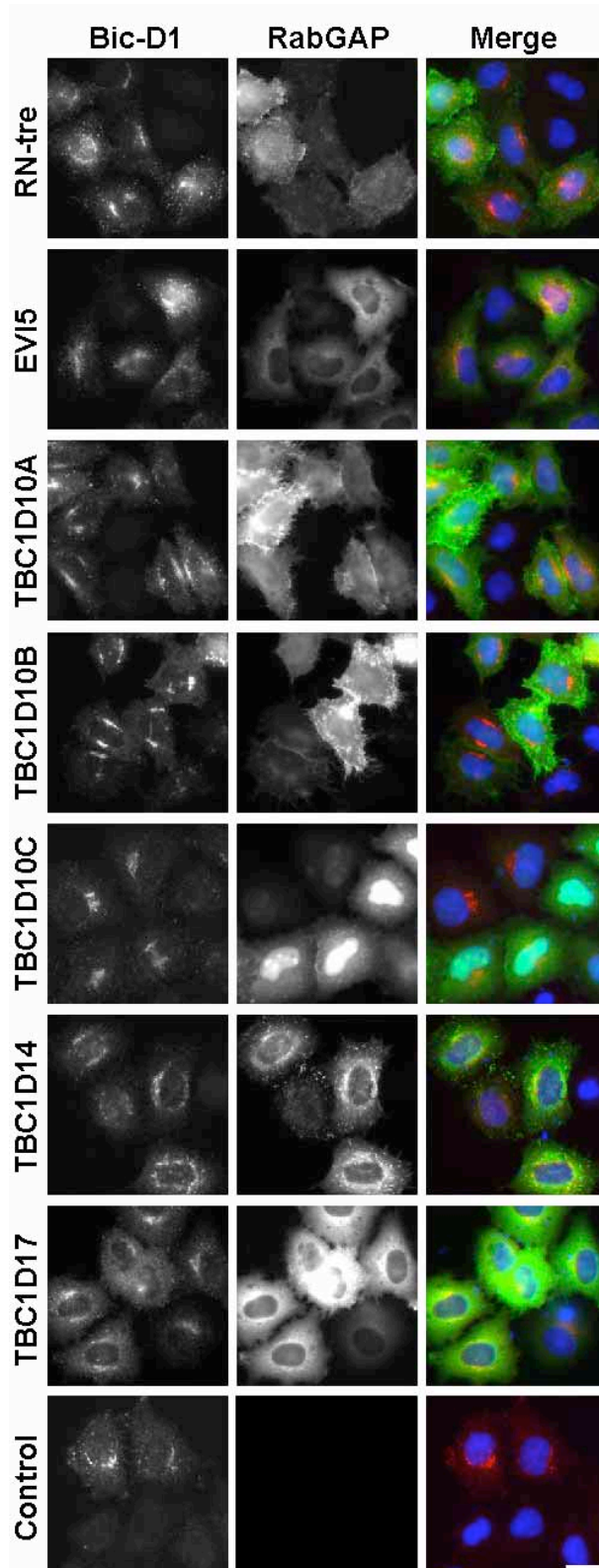
Figure 3.10 Effect of Rab GAPs blocking Shiga toxin uptake on the Rab6 effector Bic-D1. HeLa cells co-transfected for 24 hours with the GFP-tagged Rab GAPs (green) indicated in the figure and Myc-tagged Bic-D1 (red) were fixed and then stained with mouse anti-Myc antibodies and Cy3-conjugated anti-mouse secondaries. DNA was visualised with DAPI (blue). Bar indicates 10 μm in all panels.

To further validate the screening results observed with the fluorescently labelled B-subunit of Shiga toxin, screen positives were tested for their ability to protect cells against the cytotoxic effects of fully active Shiga-like toxin 1 (Figure 3.11). This assay measures protein synthesis, which is inhibited if Shiga toxin can reach the ER and enter the cytoplasm and is therefore a more stringent measure of Shiga toxin trafficking than fluorescent assays (Spooner et al., 2004). Figure 3.11 shows that EVI5, RN-tre and TBC1D17 indeed protected cells against Shiga-like toxin 1. The IC_{50} values in wild-type GAP expressing cells were significantly higher than in RA mutant GAP expressing cells, and the protection was between 1.87- and 3.35 fold. The TBC1D10 family of GAPs showed variable extents of protection, it is therefore unclear if these represent specific positives with this assay. Importantly, RabGAP-5, with a fold protection of 1.07, did not exhibit a protective effect, and this is in perfect consistency with the fluorescent data (Figure 3.8).
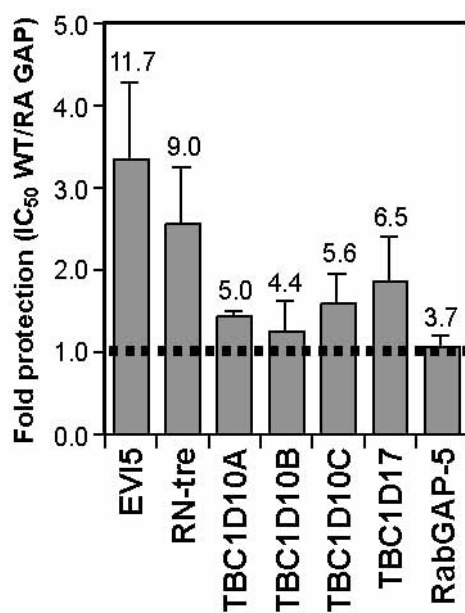
Figure 3.11 A subset of human Rab GAPs protects cells against fully active Shiga-like toxin 1. Cytotoxicity assays were performed using the Rab GAPs listed in the figure. The IC_{50} of Shiga-like toxin 1 was measured in HeLa cells expressing either the wild type (WT) or the catalytically inactive (RA) mutant GAPs. These values were then corrected for transfection efficiency averaging 13.9 - 18.7 %. An increase in the IC_{50} for WT compared with RA GAPs indicates reduced cytotoxicity, which is plotted in the graph as the fold protection, with 1 (dotted line) corresponding to no protection (n ≥ 3). The corrected IC_{50} values for each condition are shown above each column, and the IC_{50} of empty vector-transfected control cells was 3.5 ng/ml. Error bars represent SD.

In summary, this means that the trafficking pathway of Shiga toxin from the cell surface to the Golgi is defined by the Rab GAPs EVI5, RN-tre and TBC1D17, and possibly the TBC1D10 family.

3.2.5 Only RabGAP-5 is able to block EGF uptake

Next it should be determined whether the inhibitory effect of this set of Rab GAPs is specific for the Shiga toxin pathway or whether they also give a block in endocytosis of epidermal growth factor (EGF). In order to address this question in an unbiased way the full set of human Rab GAP candidates (Table 3.1) was tested blindly in EGF uptake assays (Figure 3.12). Since EGF was not bound to all cells equally, both the percentage of transfected cells not binding EGF at 0 minutes and of cells showing a block of EGF endocytosis at 30 minutes were counted and compared in Figure 3.12 A. The result clearly shows that only one Rab GAP, that is RabGAP-5, was able to block EGF transport to early endosomes, whereas the Shiga toxin blocking Rab GAPs had no effect on endocytosis of EGF (Figure 3.12 B).
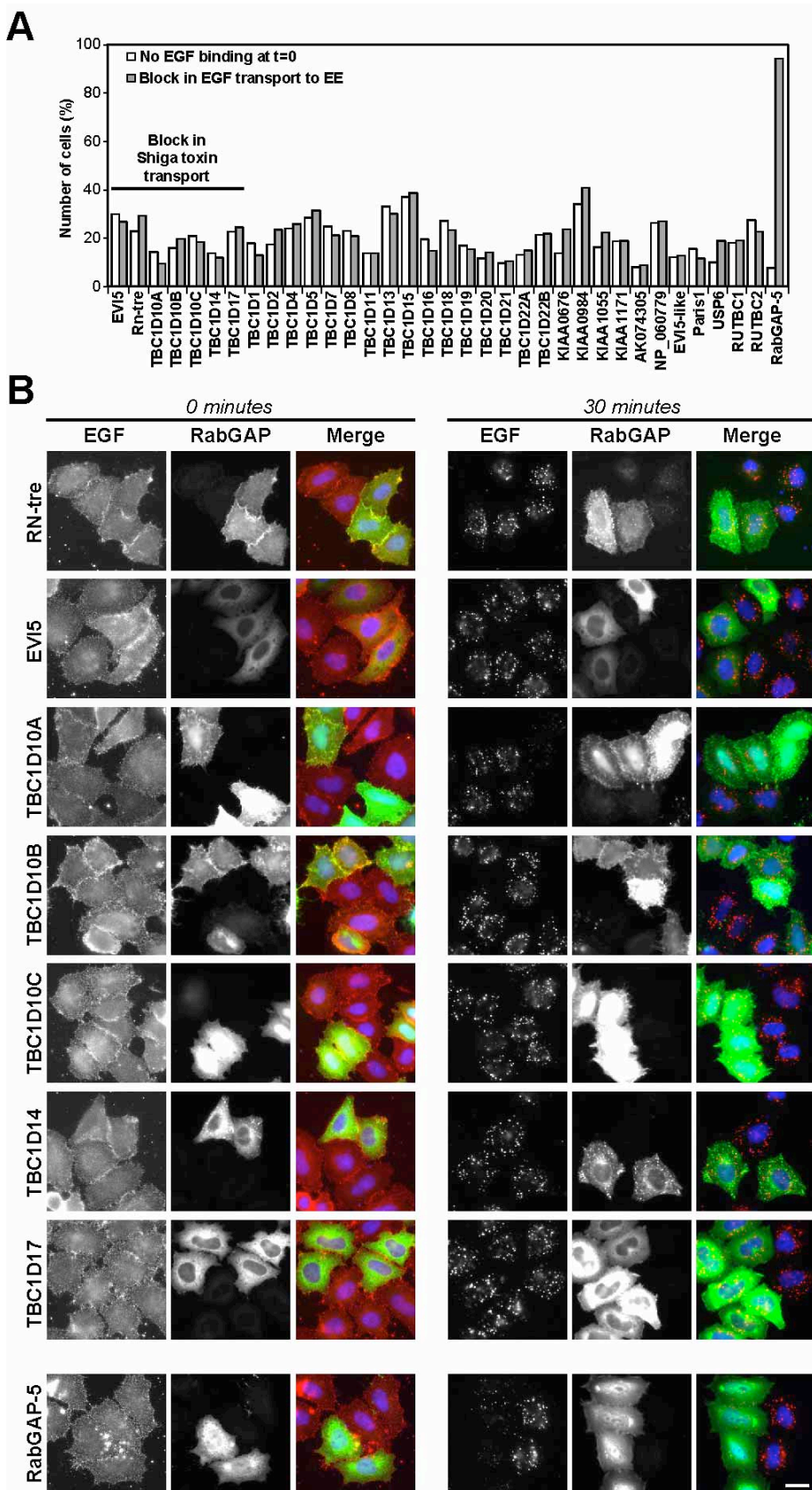
Figure 3.12 Rab GAPs altering Shiga toxin transport do not prevent EGF uptake. (A) EGF uptake assays were performed on HeLa cells transfected with a library of wild type human

Rab GAPs listed in Table 3.1. The number of cells binding and then taking up EGF was counted. The graph shows cells either failing to bind (open bars) or take up (filled bars) EGF. (B) The initial bound EGF at 0 minutes of transport, and extent of EGF transport at 30 minutes are shown for GAPs that had an effect on Shiga toxin transport, as indicated in the figure. EGF is in red, transfected Rab GAPs in green and DNA is stained in blue. Bar indicates 10 μm in all panels.

3.2.6 Different RabGAPs define Shiga toxin and EGF uptake pathways

Although RN-tre was initially suggested to act on Rab5 and hence the EGF uptake pathway (Lanzetti et al., 2000), more recently another GAP, RabGAP-5 has also been proposed to fulfil this function (Haas et al., 2005). To clarify this point, the effects of RN-tre and RabGAP-5 on the uptake of EGF and Shiga toxin were directly compared (Figure 3.13 and Figure 3.14). RabGAP-5 was able to block the uptake of EGF (Figure 3.13 A), and to displace the Rab5-dependent effector molecule EEA1 from endosomes (Figure 3.13 B) which is consistent with its function of inactivating Rab5. RN-tre or the catalytically inactive point mutant of RabGAP-5 did not show these effects on EGF uptake. Also, the localisation of EEA1 on endosomes is normal in RN-tre or RabGAP-5^{R165A} expressing cells.

In contrast, RN-tre was able to block the transport of Shiga toxin to the Golgi apparatus (Figure 3.14 A) and caused partial fragmentation of the Golgi apparatus (Figure 3.14 B), consistent with previous observations that its target, Rab43*, is localised to this organelle (Haas et al., 2005). RabGAP-5 or the catalytically inactive point mutant of RN-tre^{R150A} did not show these effects on Shiga toxin transport and Golgi structure.

In some cells expressing very high levels of RN-tre EGF uptake was indeed blocked. However, further investigation revealed that these cells lack detectable EGF receptor on the cell surface, and therefore the apparent uptake block is due to lack of EGF binding, and not a defect in endocytosis of the receptor-ligand complex. One explanation for the reduced level of EGF receptor at the cell surface could be the disrupted Golgi apparatus seen in RN-tre expressing cells (Figure 3.14 B). So, any effects of RN-tre on EGF receptor uptake would appear to be indirect.

---

* Note that Rab43 was previously referred to as Rab41 (Haas2005), which is consistent with the naming in mice. However, the gene nomenclature has been clarified, so that this gene is now called Rab43 in human and mouse.
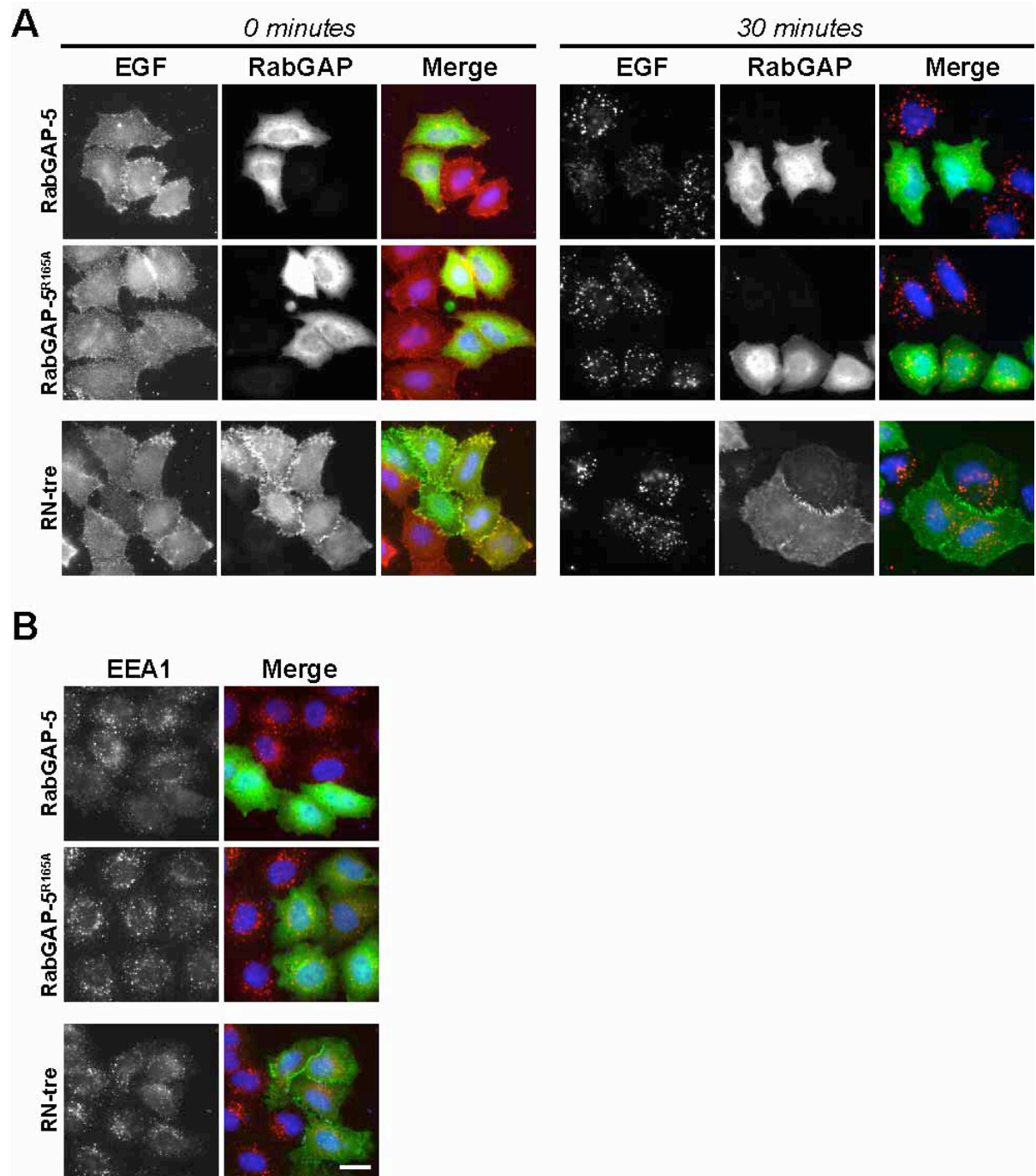
Figure 3.13 RabGAP-5 but not RN-tre defines the EGF uptake pathway. (A and B) HeLa cells were transfected for 24 hours with RabGAP-5, the catalytically inactive mutant RabGAP-5^{R165A}, or RN-tre. (A) EGF uptake assays were performed, and the initial bound EGF at 0 minutes of transport, and the extent of EGF transport at 30 minutes are shown in the figure. EGF is in red, transfected Rab GAPs in green and DNA is stained in blue. (B) The cells were stained for the transfected Rab GAPs (green) and EEA1 (red). DNA was visualised with DAPI (blue). Bar indicates 10 μm in all panels.
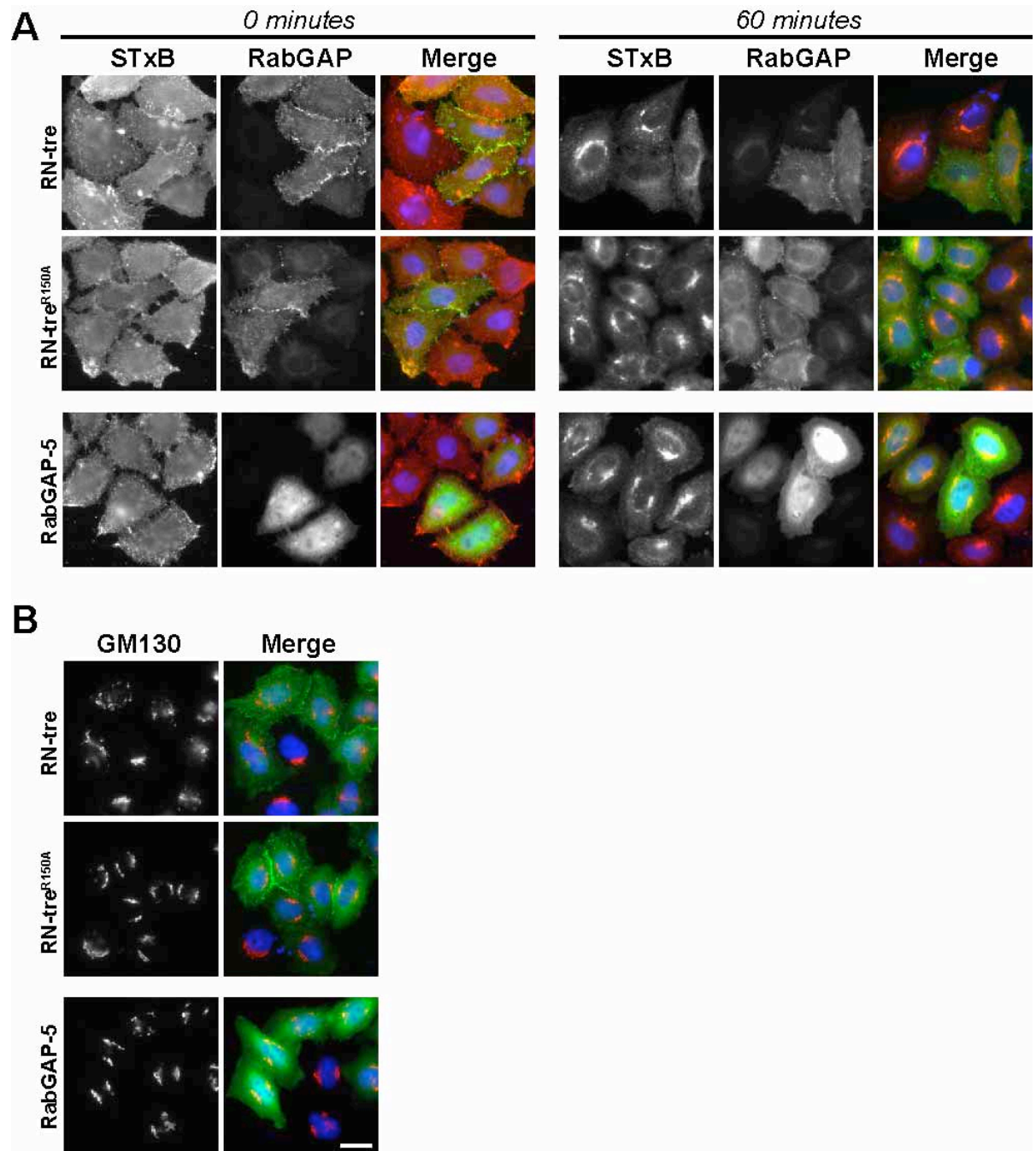
Figure 3.14 RN-tre but not RabGAP-5 defines the Shiga toxin transport pathway. (A and B) HeLa cells were transfected for 24 hours with RN-tre, the catalytically inactive mutant RN-tre^{R150A}, or RabGAP-5. (A) Shiga toxin uptake assays were performed, and the initial bound STxB at 0 minutes of transport, and the extent of STxB transport at 60 minutes are shown in the figure. STxB is in red, transfected Rab GAPs in green and DNA is stained in blue. (B) The cells were stained for the transfected Rab GAPs (green) and GM130 (red). DNA was visualised with DAPI (blue). Bar indicates 10 μm in all panels.

3.2.7 Biochemical identification of target Rabs

It was shown before that six out of 39 human Rab GAPs could block the transport of Shiga toxin to the Golgi apparatus (Figure 3.8 and Figure 3.11), and only RabGAP-5 the endocytosis of EGF (Figure 3.12). For a better understanding of the molecular details of Shiga toxin and EGF trafficking it would be necessary to know the target Rabs of the positive Rab GAPs. Therefore these GAPs were tested for their ability to accelerate GTP hydrolysis by a specific Rab in biochemical assays with a representative set of human Rabs (Figure 3.15). At least one member of every Rab subfamily was tested. For every Rab GAP all the indicated Rabs were analysed in the very same experiment, so that GTP-hydrolysis rates could be compared directly within the set of Rabs. These data clearly show that of the Rabs tested, the Rab5a-c subfamily are substrates for RabGAP-5, while RN-tre acts on Rab43. EVI5 showed strong and specific activity towards Rab35, with over 1200 pmoles GTP hydrolysed per hour, however, Rab35 was found to be weakly (6-fold less) activated with a number of the GAPs tested here, suggesting that this may be a false positive hit. The substrate of TBC1D10B and TBC1D17 could not be identified with certainty from the data obtained. Careful analysis of the pattern of GTP hydrolysis, suggests that TBC1D10B might act on Rab22a/ Rab31, which fall into the same branch of the Rab5 subfamily, while TBC1D17 might be a GAP for Rab21 (Figure 3.15).
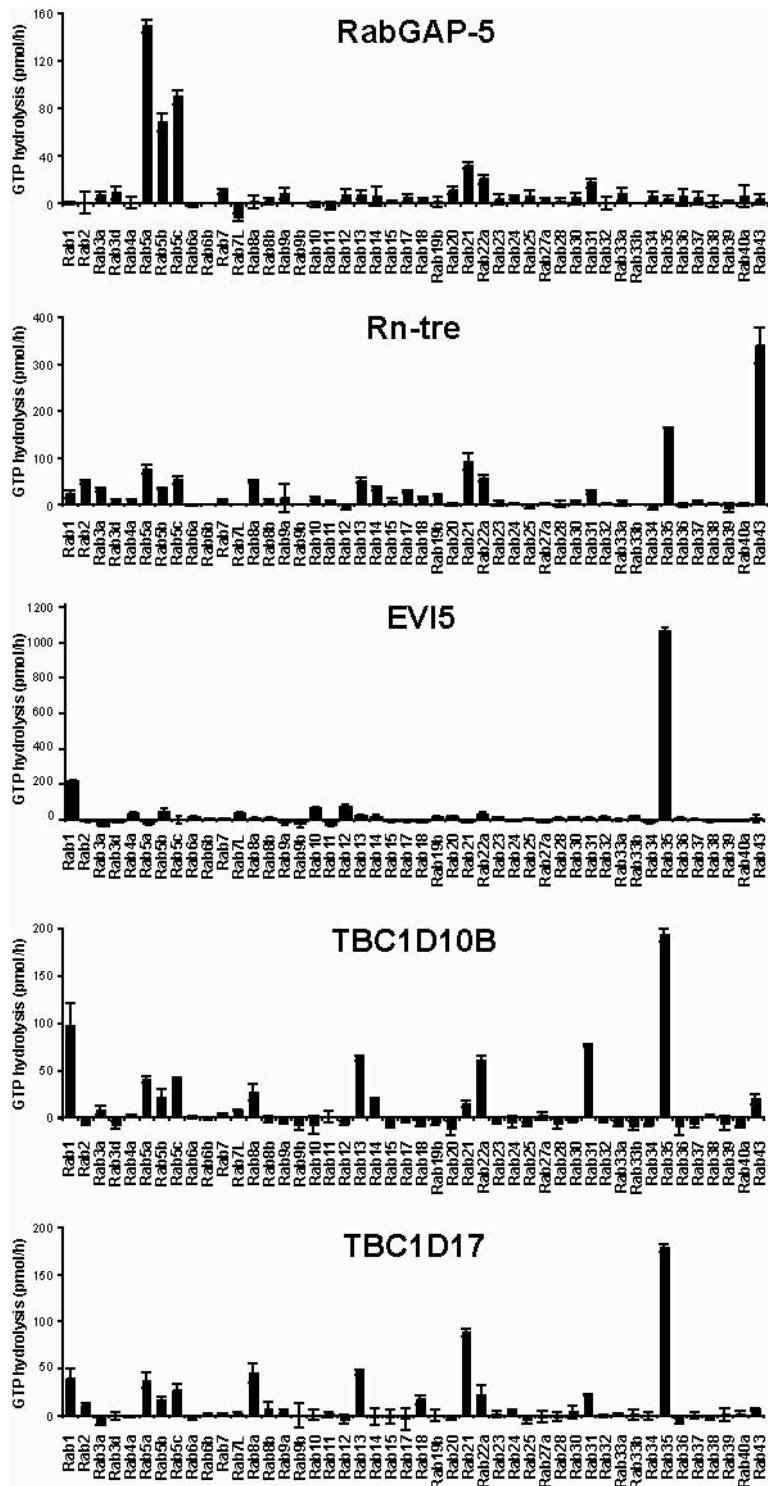
Figure 3.15 Biochemical screening for the target Rabs of specific TBC-domain proteins. Biochemical assays for GTP-hydrolysis were performed with the Rabs and GAPs indicated, using the procedure described in the methods. All reactions were carried out for 60 minutes. To determine the specific activity towards a range of GTPases, 0.5 pmoles RN-tre, RabGAP-5, EVI5, TBC1D10B, and TBC1D17 were tested against 100 pmoles of the Rab GTPase indicated. The basal GTP hydrolysis seen with a buffer control was substracted for each GTPase.

3.2.8 Functional verification of target Rabs for RN-tre and RabGAP-5

If the effects of RabGAP-5 on EGF uptake are mediated through Rab5, and those of RN-tre on Shiga toxin transport are mediated through Rab43, then cells depleted of these Rabs should display a similar defect like that seen on over-expressing the respective GAP, since both conditions reduce the pool of active Rab on target membranes. This was tested by siRNA experiments depleting either the Rab5a-c subfamily or Rab43 from HeLa cells (Figure 3.16 F) and testing these cells in EGF and Shiga toxin uptake assays (Figure 3.16 A-D).

In line with the prediction, EEA1 failed to localise to endosomes and there was a strong reduction in EGF uptake in cells depleted of Rab5 (Figure 3.16 A). These cells were still able to transport Shiga toxin to the Golgi apparatus similar to the control cells (Figure 3.16 B). In contrast the Golgi was disorganised and there was a strong reduction in the transport of Shiga toxin to the Golgi in cells depleted of Rab43 (Figure 3.16 C). However, these cells were still able to take up EGF similar to the control cells (Figure 3.16 D). Consistent with a role for RN-tre and Rab43 in the transport of Shiga toxin to the Golgi apparatus, Rab43 localised to this organelle and showed a staining pattern most similar to the trans-Golgi marker TGN46 (Figure 3.16 E). Rab43 showed no overlap with the early endosome marker EEA1 (Figure 3.16 E), suggesting it does not function at early endosomes.

To control the efficiency of siRNA mediated knockdown, cells depleted of Rabs 5a-c or 43 and control cells were transfected with GFP-tagged versions of either Rab5a, 5b, 5c or Rab43 for 24 hours and probed on Western blot for GFP signal (Figure 3.16 F). After a total of 72 hours siRNA for Rab5a-c or Rab43 each GFP-tagged protein was reduced or completely depleted compared to the expression in control cells. Tubulin was probed as a loading control, the levels of which were equal in Rab5a-c or Rab43 siRNA and control cells. Because over-expressed Rabs were depleted by specific siRNAs it was assumed, that also the endogenous pools of the respective Rabs were depleted from cells.

Depletion of Rab21, Rab22a, Rab31 and Rab35 by RNA interference had no clear effects on either Shiga toxin or EGF uptake (data not shown) and it is therefore unclear if these Rabs are the targets of the TBC1D10 family of GAPs, TBC1D17, and EVI5. Thus, it will require further investigation to find and validate the targets of these GAPs.
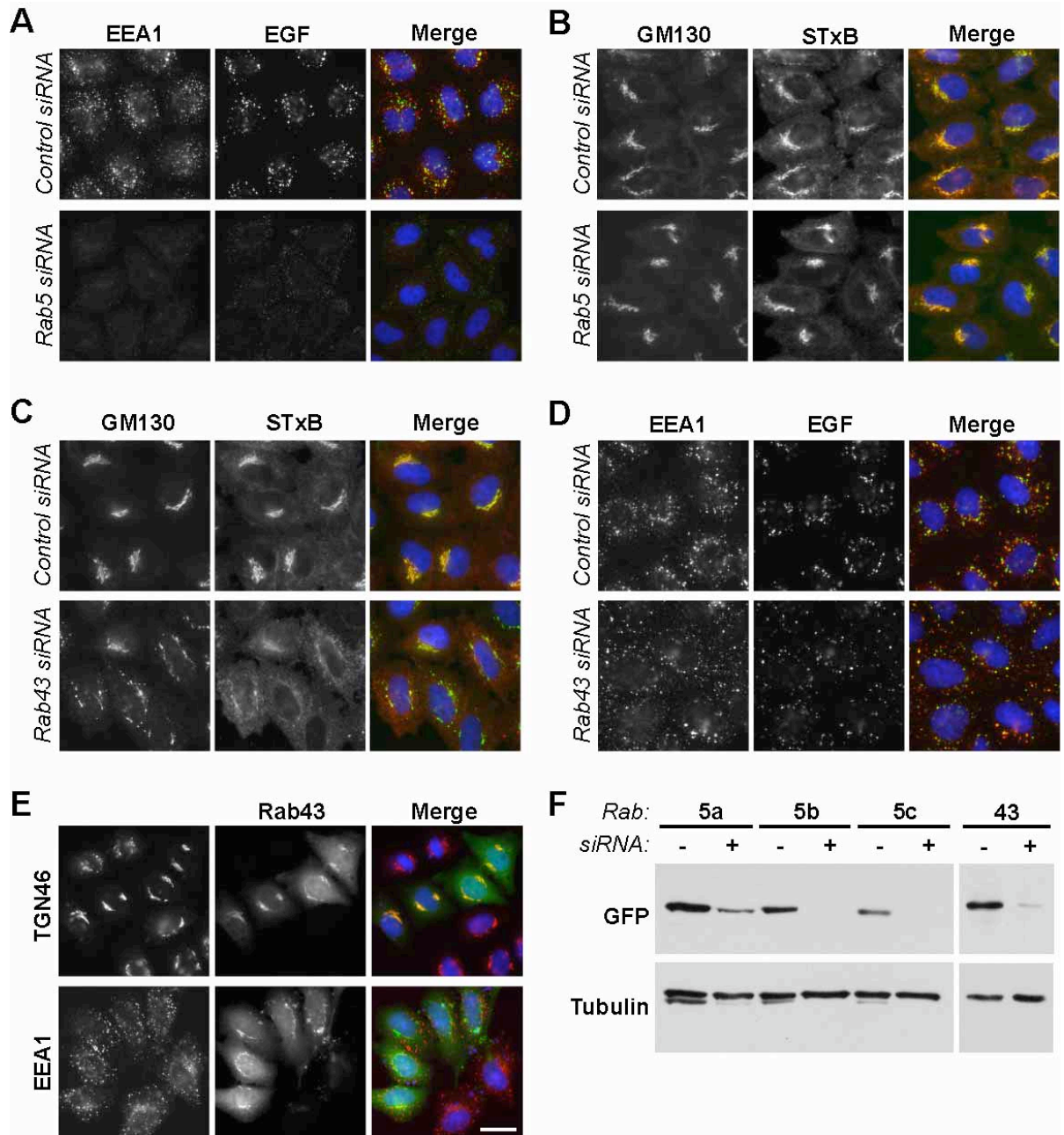
Figure 3.16 Functional verification of the targets of RN-tre and RabGAP-5. HeLa cells were transfected with siRNA duplexes to deplete (A and B) all three isoforms of Rab5, or (C and D) Rab43. (A and D) EGF uptake assays were performed, and the extent of EGF transport at 30 minutes is shown in the figure. EGF is in green, and EEA1 is in red. (B and C) Shiga toxin uptake experiments were performed, and the extent of STxB transport to the Golgi at 60 minutes is shown in the figure. STxB is in red and GM130 is in green. (E) HeLa cells transfected with GFP-tagged Rab43 (green) for 24 hours were stained with antibodies to the Golgi marker TGN46 or the early-endosome marker EEA1 (red). DNA is stained blue in all panels. Bar indicates 10 μm in all panels. (F) HeLa cells treated for 48 hours with either control (-) or specific (+) siRNA duplexes were transfected for 24 hours with constructs for the corresponding GFP-tagged Rab as indicated in the figure. Cell extracts were western blotted for GFP to detect the expression of the Rabs. Blots were re-probed for tubulin as a loading control.

In summary, these observations support two important conclusions. Firstly, that RN-tre specifically blocks Rab43 dependent trafficking of Shiga toxin to the trans-Golgi apparatus, and that EGF does not follow this pathway. Secondly, that RabGAP-5 specifically blocks the Rab5 dependent trafficking of EGF through early endosomes, and that Shiga toxin does not follow this pathway. These two Rab GAPs and their target Rabs therefore define specific trafficking routes for Shiga toxin and EGF.

3.3 Conclusion

In this part of the work, 39 human TBC domain proteins and putative RabGAPs were tested for their ability to block the transport of STxB to the Golgi apparatus or the uptake of EGF into early endosomes.

Before, the optimal conditions for both functional assays were established and validated. The two ligands showed different kinetics of early endocytic steps. Whereas EGF uptake was very rapid and the bulk of the ligand had reached the early endosome after 30 minutes, transport of STxB was slower and STxB was best visisble at the Golgi apparatus after 60 minutes at 37 °C. Consistent with published data (Mallard et al., 2002; White et al., 1999), the depletion of Rab6a/a' and Rab6b by siRNA resulted in a partial block of STxB transport to the Golgi. However, the published Rab6 GAP TBC1D11/GAPCenA (Cuif et al., 1999) did not show any effect on the trafficking of STxB and could therefore not be confirmed as a GAP for Rab6. In contrast, TBC1D11/GAPCenA turned out to act as a GAP for Rab4 both, in extensive yeast-2-hybrid analysis and in biochemical assays.

The screen for RabGAPs blocking the transport of STxB to the Golgi apparatus produced 6 positive candidates: EVI-5, RN-tre, TBC1D10A, TBC1D10B, TBC1D10C and TBC1D17. None of these proteins could redistribute the Rab6 effector protein Bic-D1 from Golgi membranes, which hints to the fact that none acts on Rab6. In a side-by-side screen for TBC domain proteins blocking the endocytosis of EGF only RabGAP-5 proved positive. Interestingly, RabGAP-5 was specific for the EGF uptake route and had no effect on STxB trafficking. To further strengthen the results of the screenings with fluorescent STxB, all screen positives were tested in a cytotoxicity assay measuring the arrival of fully active Shiga-like 1 holotoxin in the ER and cytoplasm, where the toxin inhibits proteins synthesis of the host cell. In agreement with the fluorescent data, EVI-5, RN-tre and TBC1D17 were able to protect the cell significantly against intoxication by Shiga-like toxin 1, whereas RabGAP-5 could not. The effect of the TBC1D10 family was less clear. Biochemical analysis measuring the GAP activity of the screen positives with a representative set of human Rabs confirmed RabGAP-5 as a specific GAP for the Rab5 family (a-c)

and RN-tre as a specific GAP for the Golgi localised Rab43. In direct comparison, RabGAP-5 expression as well as Rab5 depletion by siRNA resulted in a block of EGF but not of STxB, whereas RN-tre expression as well as Rab43 depletion by siRNA blocked STxB transport but not EGF uptake. These two RabGAPs and their target Rabs therefore define specific trafficking routes for Shiga toxin and EGF. In summary, EGF trafficking through early endosomes is a Rab5 dependent pathway, which is not followed by Shiga toxin. Instead, the transport of Shiga toxin to the Golgi apparatus is dependent on Rab43.

4 Discussion

4.1 The novel Rab6 binding protein PIST

The Golgi localised GTPase Rab6 regulates the minus-end-directed transport of vesicles along microtubules. This is accomplished through the interaction of Rab6 with the dynein-dynactin motor complex, either directly through the p150[glued] subunit of dynactin or indirectly through the coiled-coil proteins Bic-D1 and Bic-D2 (Matanis et al., 2002; Short et al., 2002). However, the nature of these Rab6 regulated transport vesicles and the exact mechanism of minus-end-directed movement is unclear. In order to achieve a better understanding of the molecular mechanisms underlying Rab6 function a screen for novel Rab6 effector proteins was carried out. This led to the identification of the coiled-coil and PDZ domain protein PIST as a Rab6 binding protein.

4.1.1 PIST binds Rab6 with high affinity and specificity

When tested against a representative set of Rab family members in their active state (QL mutants) in yeast two-hybrid PIST showed an interaction with Rab6 (a and b isoforms) only. This suggests that, within the family of Rab GTPases, PIST is a specific binding partner for Rab6. The use of Rab mutants, where the conserved glutamine of the G-domain (DxxG$\underline{Q}$) is replaced with leucine (QL mutant) is thought to lock the Rab in its active state where GTP cannot be hydrolysed (Martinez et al., 1994). As Rab effector proteins bind specifically to the active conformation of a Rab, Rab QL mutants are used to stabilise the Rab effector interaction. In a yeast two-hybrid assay a stable interaction of the two fusion proteins (GAL4AD- and GAL4BD-fusion) is essential for promoter activation and growth of the transformed yeast on quadruple drop-out medium (QDO). Short-lived interactions, such as enzyme-substrate reactions are therefore likely to be difficult to detect with the yeast two-hybrid system. Assuming that all QL mutants of the Rab GTPases used are efficiently locked in their active state and exhibit a similar behaviour towards effector protein binding in yeast two-hybrid, PIST interacts specifically with Rab6.

The PIST-Rab6 interaction is dependent on the active GTP-bound state of Rab6 as shown in GST–pulldown and –binding assays with recombinant Rab6. For both experiments bacterially expressed GST-tagged Rab6 was loaded either with GTP (wild-type and QL mutant) or GDP (TN mutant). Because Rab6 possesses a very low intrinsic rate of GTP-hydrolysis (Bergbrede et al., 2005), wild-type Rab6 is stable in its active GTP-bound state for the period of several days at 4 °C (Tim

Bergbrede, personal communication). Both, endogenous PIST from HeLa extract and recombinant full-length PIST bound Rab6 in its active state (wild-type and QL mutant) but not in its inactive conformation mimicked by the TN mutant. The fact that purified recombinant PIST binds Rab6 suggests that the interaction is direct and not mediated by an additional factor.

Known Rab6 effectors like Bic-D1 and p150^{glued} were used as controls for the efficiency of the pulldown reaction from HeLa cell extract and showed the same band pattern like PIST, namely binding of wild-type Rab6 and the QL mutant but not the TN mutant of Rab6. The signal for bound dynactin subunit p150^{glued} appears to be very weak. This can be explained by the fact that the dynein-dynactin motor complex fulfils various functions within the cell (Habermann et al., 2001; Vaughan et al., 2002; Watson et al., 2005; Watson and Stephens, 2006) and only a small fraction of the complex interacts with Rab6 at the Golgi. Also the Bic-D1 signal in complex with wild-type Rab6 was not as strong as expected from a real effector protein. The affinity of the rabbit polyclonal Bic-D1 antibody (generated by Johannes Egerer, this laboratory) is obviously not sufficient for efficient detection of the antigen. The detection of unspecific, wrong sized bands in the pulldown reaction with Rab6^{T27N} suggests that the Bic-D1 antibody cross-reacts with impurities in the protein preparation of Rab6^{T27N}.

Long coiled-coil proteins tend to aggregate in vitro, which lead to unspecific signals in binding assays. As a control for the specificity of PIST in Rab6 binding the Rab1 effector and coiled-coil protein p115 was probed together with PIST in the very same pulldown experiment. The lack of p115 binding, although present in the HeLa extract, provides evidence that the interaction of Rab6 with PIST is not based on general stickiness of coiled-coil proteins but is specific for PIST.

4.1.2 PIST does not bind the Rho GTPase TC10

PIST was originally identified as PDZ domain protein interacting specifically with TC10 (Neudauer et al., 2001). However, an interaction of PIST with the Rho family GTPase TC10 could not be observed in the course of this work, neither by yeast two-hybrid nor by direct binding assays with recombinant PIST. One reason for this discrepancy with published results could be the presence of an error in the TC10 cDNA sequence used by Neudauer et al., 2001. When cloning the TC10 gene from a human cDNA library for this work, the original database entry turned out to contain an error. According to the expressed sequence tag database and the isolated clones, the TC10 mRNA encodes a protein 8 amino acids shorter at the N-terminus than published by Neudauer et al., 2001. The authors stated that PIST bound TC10

in yeast two-hybrid and with low affinity in in vitro binding assays, but that the two proteins could not be co-immunoprecipitated from cell extract. One caveat important when considering the work of Neudauer et al., 2001 is their use of a PIST fragment (amino acids 155-320) instead of the full-length protein. Based on the knowledge that proteins fragments can alter the behaviour towards interaction partners, the use of fragments without comparing to the full-length protein can be misleading. In this work full-length PIST showed no interaction with TC10 in yeast two-hybrid and in vitro binding assays. Due to the strong and specific interaction with Rab6, full-length PIST is regarded correctly folded both in yeast and purified from *E. coli*. Unfortunately there was no interaction partner of TC10 available to prove the activity of TC10 in both assays. However, since TC10 was expressed and purified in the same way as Rab6 and other GTPases successfully characterised in the laboratory, it is expected to behave in a similar manner and be a suitable substrate for in vitro binding assays.

4.1.3   How is PIST localised to Golgi membranes?

Immunofluorescence staining of HeLa cells with specific antibodies showed that PIST is a Golgi localised protein. The fact that PIST exhibits no structural features for direct membrane insertion or anchoring such as transmembrane helices or lipid modifications raises the question of how PIST is targeted to Golgi membranes. By the use of various deletion constructs of PIST the Golgi targeting region was mapped to the second coiled-coil domain of PIST. Because PIST was shown previously to form homodimers via the second coiled-coil domain (Neudauer et al., 2001), the Golgi targeting of PIST fragments was examined in a PIST siRNA background where endogenous PIST was depleted from HeLa cells prior to trans-fection with GFP-constructs. Importantly, also in cells depleted of endogenous PIST the second coiled-coil was sufficient to localise to Golgi membranes (PIST$^{142-255}$). Yet, the Golgi signal was much stronger in cells expressing a fragment of PIST with both coiled-coil stretches (PIST$^{1-255}$). This suggests that the Golgi localisation of PIST is dependent on the interaction of the second coiled-coil with Golgi resident proteins or lipids and that this interaction is stabilised by the N-terminal coiled-coil of the protein.

Interestingly, there is good evidence that the interaction with Rab6 is dispensable for the Golgi localisation of PIST. First, yeast two-hybrid analysis as well as direct binding assays showed that the N-terminal coiled-coil region of PIST (PIST$^{1-141}$) mediates the interaction with Rab6, whereas the fragment containing the second coiled-coil domain plus PDZ domain (PIST$^{142-454}$) did not bind Rab6.

Unfortunately, the PIST deletion mutant containing the second coiled-coil alone (PIST$^{142-255}$) was slightly toxic in yeast and could not be purified from *E. coli*, which makes a direct comparison of both coiled-coil domains in yeast two-hybrid and direct binding assays impossible. Nevertheless, further evidence for the Rab6 independent localisation of PIST is provided by the fact that neither elevated nor decreased Rab6 levels affect the targeting of the endogenous PIST to the Golgi. While depletion of Rab6 by siRNA resulted in the loss of its effector protein Bic-D1 from Golgi membranes, the localisation of PIST was unaltered in Rab6 depleted cells. One drawback of the Rab6 siRNA experiment is the poor quality of the Rab6 polyclonal antibody. Rab6 cannot be detected efficiently on Western blot with this antibody and Rab6 protein levels might be decreased but not completely depleted. Furthermore, in this part of this work siRNA oligos targeting only Rab6a but not Rab6b were used. So, different effector proteins, like Bic-D1 and PIST, might exhibit different sensitivity to Rab6 isoforms and levels. Rab6b is reported to be expressed predominantly in brain (Opdam et al., 2000), but this might be a simplification as the nucleotide sequence encoding the Rab6b protein was cloned recently from a HeLa cell cDNA library (Shin-ichiro Yoshimura, unpublished results). All binding and pulldown reactions were performed using the Rab6a isoform, but PIST might bind stronger to Rab6b and be unaffected by altered Rab6a levels. The same problem accounts for the overexpression studies with Rab6a. PIST levels at the Golgi were unaltered irrespective which Rab6a mutant was expressed. One expects a Rab effector interaction to be titrated out by the overexpression of the inactive Rab TN mutant. Overexpression of Rab6^{T27N} had no effect on PIST, but neither on Bic-D1. Therefore, this experiment was counted insignificant. Most likely, endogenous Rab6 acts in a dominant active manner over the expression of the mutants and holds effector proteins like Bic-D1 in place. Taken together, these results suggest that Rab6 is not required for the localisation of its binding protein PIST.

In search for other putative targeting factors for PIST at the Golgi the coiled-coil protein Golgin160 was identified and could be confirmed as a binding partner for PIST by co-immunoprecipitation of endogenous proteins from cell extract and by yeast two-hybrid analysis. The Golgin160 binding region was mapped by yeast two-hybrid to a region within PIST containing the second coiled-coil plus the sequence in front of the PDZ domain. The second coiled-coil alone (PIST$^{142-255}$), which is sufficient for Golgi localisation of PIST, and the PDZ domain alone (PIST$^{256-454}$) did not give a signal when tested against Golgin160 in the yeast-2-hybrid assay. Additionally, depletion of Golgin160 by siRNA resulted in fragmentation of the Golgi into mini stacks, but had no effects on the localisation of PIST to Golgi membranes.

These data suggest that Golgin160 is not the Golgi targeting factor for PIST. During the course of this work the interaction of PIST with Golgin160 was published by the Machamer lab (Hicks and Machamer, 2005). The authors found PIST in a yeast two-hybrid screen with the N-terminal non-coiled-coil head domain of Golgin160, which is important for targeting of Golgin160 to the cytoplasmic face of the Golgi apparatus (Hicks and Machamer, 2002). In agreement to the data presented in this work they mapped the Golgin160 binding region within PIST to the second coiled-coil domain plus the sequence before the PDZ domain (Hicks and Machamer, 2005). In addition, Hicks and Machamer, 2005 also showed that PIST can be co-immunoprecipitated with Golgin160 from cell extract. Together, these independent but congruent data suggest that PIST is a binding partner of Golgin160 at the Golgi but is not dependent on Golgin160 for its localisation.

Another hint for the mechanism of Golgi localisation of PIST can be found in Charest et al., 2001. The authors show biochemical data on the interaction of PIST with the SNARE protein syntaxin 6. Syntaxin 6 was reported to be involved in vesicle fusion at multiple points in the endocytic and exocytic pathways between the TGN and the plasma membrane (Murray et al., 2005; Perera et al., 2003; Wendler and Tooze, 2001) and was suggested to regulate the plasma membrane delivery of protein and lipid components required for caveolar endocytosis (Choudhury et al., 2005). Although the interaction of PIST with syntaxin 6 in GST-binding assays and immunoprecipitation was shown (Charest et al., 2001), data on the localisation of PIST and on the functional relationship between both proteins are missing. Unfortunately, no further studies dealing with PIST in relationship with syntaxin 6 were published, and the issue of both, the Golgi localisation and the function of PIST remains elusive.

4.1.4 What is the function of PIST in complex with Rab6?

PIST is a ubiquitously expressed protein with two coiled-coil stretches and a PDZ domain (Neudauer et al., 2001), but its function is still unclear. The siRNA-mediated depletion of PIST from HeLa cells did not result in any apparent phenotype on Golgi structure or the localisation of its binding partners Rab6 and Golgin160 to Golgi membranes, which most likely excludes a major structural role for PIST at the Golgi. In comparison, other Golgi localised coiled-coil proteins such as Golgin84 are important for the maintenance of the stacked ribbon structure of the Golgi apparatus and upon their depletion the Golgi stack falls apart into single Golgi fragments (Barr and Short, 2003; Diao et al., 2003). Such a Golgi fragmentation phenotype is clearly not the case for the depletion of PIST from HeLa cells and neither for the

investigated tissue cells of PIST knock-out mice (Ito et al., 2004; Yao et al., 2002). PIST$^{-/-}$ mice are viable and show no obvious abnormalities except that male mice are infertile due to a defect in acrosome formation. The acrosome covers the anterior one third of the sperm head and contains hydrolytic enzymes needed for the binding of the sperm to the zona pellucida of the oocyte during fertilisation. In PIST$^{-/-}$ mice acrosome formation during spermiogenesis is blocked because Golgi-derived proacrosomal vesicles fail to fuse with each other (Ito et al., 2004; Yao et al., 2002). Thus, PIST most likely plays a role in Golgi to plasma membrane transport of proacrosomal vesicles and therfore in acrosome formation. As the acrosome is a unique organelle in spermatids the question arises which role PIST plays in other cell types.

In addition to its coiled-coil stretches PIST also contains a PDZ domain in the very C-terminus. PDZ domain proteins are known to fulfil the role as scaffold proteins in multisubunit protein complexes and to be essential players for various cell signalling processes such as cell polarisation (Harris and Lim, 2001; Nourry et al., 2003; Roh and Margolis, 2003). Several proteins have been identified as binding partners of the PIST PDZ domain (Cheng et al., 2002; Hassel et al., 2003; Ito et al., 2006; Yao et al., 2001). Intriguingly, a number of these are transmembrane proteins including the plasma membrane chloride channel CFTR (Cheng et al., 2002). The plasma membrane expression of CFTR in COS-7 cells seems to be decreased by elevated PIST levels and the authors suggest that PIST down-regulates total and cell surface CFTR by targeting CFTR for degradation in the lysosome (Cheng et al., 2002; Cheng et al., 2004; Cheng et al., 2005). This would mean that PIST acts as a specialised cargo receptor at the Golgi and directs Golgi-derived vesicles to the endocytic system or to the plasma membrane. The interaction of PIST with the SNARE syntaxin 6 (see above) would fit into this model. But how would Rab6 be involved? PIST is suggested to bind transmembrane cargo proteins via its PDZ domain. It localises to the Golgi via its C-terminal coiled-coil domain, possibly by interaction with syntaxin 6 or any other Golgi resident protein and binds Rab6 via its N-terminal coiled-coil domain. Rab6 has been implicated in microtubule-dependent transport by interaction with the dynein-dynactin motor complex (Matanis et al., 2002; Short et al., 2002). Fitting all data together, one could speculate that Rab6 regulates the transport of PIST-cargo loaded vesicles along microtubules. The fact that neither PIST nor Rab6 depletion in HeLa cells show any obvious effect on cell morphology or viability indicates a role of both proteins in specialised secretion or transport of certain molecules, or a role in transport to destinations within polarised cells such as apical and basolateral membrane that cannot be distinguished in the

HeLa cell model system. Another reason for the lack of phenotype after PIST depletion in HeLa cells could be the existence of functional redundant proteins in cell types other than spermatids.

4.2 Rab GTPase activating proteins defining Shiga toxin and epidermal growth factor uptake

Rab GTPases act as molecular switches and regulate membrane trafficking events. In their active GTP-bound state they recruit specific functional proteins, so called effectors, to target membranes. The active state of a Rab is terminated by interaction with its specific Rab GTPase-activating protein (GAP), which catalyses the GTP hydrolysis reaction and turns the Rab into the inactive GDP-bound state. There are over 60 Rab family GTPases encoded by the human genome, and at least 39 TBC-domain containing Rab GAPs. However, little is known about the function of the majority of these proteins. This is partly due to the enormous complexity of membrane trafficking systems, and the lack of suitable cell biological models for Rabs with functions in specific tissues.

As a first step in unravelling this complex network, a cell biological screen for Rab GAPs that can influence the trafficking of Shiga toxin to the Golgi apparatus, or of EGF to early endosomes was performed. Furthermore, the target Rabs for some of these GAPs were identified using biochemical assays. The results suggest that while the trafficking of Shiga toxin from the cell surface to the Golgi is a multi-step process dependent on at least 6 different Rabs and Rab GAPs, EGF trafficking depends only on the action of Rab5 and RabGAP-5.

4.2.1 A subset of human Rab GAPs influences Shiga toxin transport

The retrograde transport of Shiga toxin from the cell surface via the Golgi to the ER is a multi-step process (Sandvig et al., 2002). Because each membrane trafficking step is regulated by a discrete set of Rabs (Zerial and McBride, 2001), it is likely that several Rabs are implicated in Shiga toxin trafficking. Yet, to date only Rab6 has been implicated in the retrograde transport of Shiga toxin (Girod et al., 1999; Mallard et al., 2002; White et al., 1999). To achieve a better understanding of the molecular mechanisms of retrograde trafficking pathways Rab GAPs were screened for their ability to interfere with the transport of Shiga toxin from the cell surface to the Golgi apparatus.

Transient expression of a Rab GAP can be used to inactivate the endogenous pool of a Rab and in this way interfere with the process this Rab is involved in (Haas et al., 2005). Therefore, each of the 39 predicted human Rab

GAPs was expressed in HeLa cells and the transport of fluorescently labelled Shiga toxin B-subunit (STxB) was followed in theses cells. The time points chosen for fixation and immunofluorescent staining of the samples were 0 and 60 minutes. In control cells STxB had accumulated in the perinuclear Golgi region after 60 minutes at 37 °C. A lack of Golgi signal at this time point was counted as a "transport block" phenotype. It is extremely important to control the surface binding of STxB at t0 on ice before the uptake reaction is started by addition of warm growth medium. Otherwise, no conclusion can be drawn from cells without STxB signal at the Golgi after 60 minutes. The binding of STxB to HeLa cells of the stock used in the laboratory of Francis Barr was very reliable, that means a high percentage of cells expressed the Shiga toxin receptor Gb3 and this was stable over a high number of passages in cell culture. There are reports from other laboratories working with Shiga toxin that HeLa cells express Gb3 only sporadically in a certain percentage of cells and drift in sensitivity towards Shiga toxin by passage number (Robert Spooner, personal communication). This could be due to diversity between HeLa stocks, which has evolved over the many years of culturing this cell line, or due to different culture conditions such as the quality of the serum used.

In the first round of screening, TBC domain proteins in their wild-type form were tested blindly according to their plasmid number, without any bias towards known Rab GAPs, for the signal of STxB in the perinuclear region after 60 minutes. Out of 39 GAPs 9 candidates impaired the capability of STxB to reach the perinuclear region. In order to assure that the "transport block" phenotype on Shiga toxin trafficking was mediated by the catalytic activity of a Rab GAP on its target Rab and not by any other mechanism, positive candidates from the first round were re-tested as inactive point mutants. It was shown before that non-specific effects of RabGAP expression can easily be discriminated from the specific effects of Rab inactivation by use of an inactive point mutant in which the catalytic arginine residue is replaced by alanine (RA mutant) (Haas et al., 2005). During this second screening round only one GAP, TBC1D14 showed the same effect on STxB transport regardless of its wild-type or RA mutant state, and was therefore excluded from the list of positives.

In the initial screen the blue channel was used for DAPI staining of the nuclei and relied on the detection of STxB in the perinuclear region, assuming it accumulated in Golgi membranes. This allowed a quick assessment of the general (nuclear) status of the cell and a rapid exclusion of non-phenotype GAPs. However, cells without a typical perinuclear Golgi structure such as dispersed Golgi fragments could be classed as false-positives in this way. Therefore, screen positives were tested again in Shiga toxin transport assays, this time with the Golgi matrix protein

GM130 stained in blue to check for Golgi morphology in GAP expressing cells. Co-staining with GM130 revealed that in cells expressing TBC1D22A and TBC1D22B the Golgi stack was fragmented but STxB accumulated exactly in these Golgi fragments. This result suggests that TBC1D22A and TBC1D22B act on Rabs that play a role in maintaining Golgi structure but not in Shiga toxin transport. In contrast, in RN-tre expressing cells normal Golgi structure was disrupted as well but STxB had clearly not accumulated in these Golgi fragments. Taken together, after checking for catalytic activity dependence and Golgi morphology, 6 GAP candidates were counted positive in their ability to block the transport of STxB: RN-tre, EVI5, TBC1D10A-C and TBC1D17.

To further validate the results obtained with the fluorescently labelled B-subunit, the candidates were tested in another approach, measuring their ability to protect cells against the cytotoxic effects of fully active Shiga-like toxin 1. Once Shiga toxin reaches the ER, it gets translocated to the cytosol where it inhibits protein synthesis at the ribosome. Therefore, measuring protein synthesis is an indirect but very sensitive tool to measure the uptake and transport of the toxin within the cell (Spooner et al., 2004). Rab GAP expressing cells were incubated with various amounts of Shiga-like toxin 1 before the incorporation of [^{35}S]-methionine was measured. The IC$_{50}$ values of wild-type and RA mutant GAP expressing cells were used to calculate the fold protection shown by a wild-type GAP against Shiga-like toxin 1. In agreement with the data obtained with fluorescently labelled STxB, RN-tre, EVI5 and TBC1D17 were able to protect cells against Shiga toxin between. The effect of the TBC1D10 family is not so clear as fold protection varies. One major caveat of the method is the transient expression of GAPs. The background of untransfected cells might artificially decrease the protective effect of a GAP. Although the transfection efficiency for each GAP was counted and used to correct the raw data obtained in the cytotoxicity assay, the exact ratio and behaviour of untransfected versus transfected cells in each single experiment remains unknown. Another issue is the nature of the block of Shiga toxin. In fluorescent analysis the detection threshold is relatively high, whereas cytotoxicity can be measured even with very low amounts of Shiga toxin reaching the cytoplasm. This means, a block in Shiga toxin transport would have to be 100 % in order to yield high protective values. Most likely, Shiga toxin is blocked from reaching the Golgi by the list of screen positive GAPs as observed by immunofluorescence studies, but not completely at molecular level as measured in the cytotoxicity assay. In combination, the issues of transfection efficiency and degree of block might decrease the real protective effect to the level of measured protection. However, multiple repetitions of

the experiment showed a clear trend towards RN-tre, EVI5 and TBC1D17 protecting cells against Shiga-like toxin 1. Importantly, RabGAP5, a GAP for Rab5 (Haas et al., 2005) did not influence the transport of Shiga toxin, neither in fluorescent assays nor in cytotoxicity measurements. This suggests that endocytosis and retrograde transport of Shiga toxin is independent of Rab5.

4.2.2 The role of Rab6 in the Shiga toxin trafficking pathway

In previous studies, Rab6 has been implicated in Shiga toxin transport (Girod et al., 1999; Mallard et al., 2002; White et al., 1999). This could be confirmed in this work using Rab6 siRNA. Shiga toxin transport to the Golgi was partially blocked in cells depleted of Rab6a and Rab6b. STxB was still detectable in the perinuclear region but compared to control cells greatly reduced. One reason for the incomplete block could be an inefficient depletion of Rab6 by siRNA. As the Rab6 antibody does not work in Western blotting endogenous protein levels could not be judged. Although the Rab6 effector Bic-D1 was lost from the Golgi in Rab6 depleted cells, low levels of either Rab6 isoform might be sufficient for the transport of Shiga toxin. Another theory could be an indirect role of Rab6 in Shiga toxin trafficking such as the delivery of cell surface components needed for efficient endocytosis of the toxin. In Rab6 depleted cells these components would inevitably be titrated out more or less rapidly according to their half-life. The issue of time span in different experimental setups could be essential for the effect on Shiga toxin trafficking. While a transiently expressed Rab GAP can act very rapidly in cells (within hours), the functional knock-down of a Rab by siRNA can take days. Furthermore, the expression of Rab GAPs is dominant whereas siRNA mediated depletion cannot be controlled for remaining functional pools of Rab below the detection threshold. Therefore, the identification of a Rab6 GAP could clarify the role of Rab6 in Shiga toxin trafficking. However, none of the Rab GAPs capable of blocking Shiga toxin transport was able to cause release of Bic-D1 from the Golgi to the cytoplasm. This indicates that they do not act on Rab6, because the Golgi localisation of Bic-D1 is Rab6 dependent. Furthermore, none of the tested GAPs was able to stimulate GTP-hydrolysis by Rab6 in biochemical assays. Why the Rab6 GAP was not found in the screen is unclear. There is evidence that some TBC-domain proteins form hetero-dimeric complexes (Pereira et al., 2001), and that this is necessary for their activity. If this is the case for the Rab6 GAP then it could have been missed in the current screen.

What is clear is that TBC1D11/GAPCenA, previously suggested to act on Rab6 (Cuif et al., 1999), is unlikely to be the GAP for Rab6. It displays robust biochemical activity towards Rab4 but not Rab6, and has none of the cell biological

properties expected for a Rab6 GAP. It cannot block Shiga toxin trafficking, or cause release of the Rab6 effector Bicaudal-D1 from the Golgi. Investigation of the interaction between TBC1D11/GAPCenA and the full set of Rabs in yeast two-hybrid showed that regions outside of the minimal predicted catalytic-domain are required for specific Rab-binding. Strikingly, deletion of these regions relaxes the interaction specificity of the protein. Many previous studies have used truncated GAP domains rather than full-length proteins (Albert and Gallwitz, 1999; Pan et al., 2006), and in the light of the data presented in this work this may be problematic since these proteins may have relaxed specificity and thus be able to accelerate GTP-hydrolysis on a broader spectrum of Rabs.

Thus, it is clearly important to study the full-length proteins and not only truncated fragments corresponding to predicted domains. At the present time the identity of the Rab6 GAP remains mysterious and requires further investigation.

4.2.3 Only RabGAP5 is able to block EGF uptake

The TBC domain proteins RN-tre, EVI5, TBC1D10A-C and TBC1D17 were shown to influence the intracellular trafficking of Shiga toxin. The question remained whether these GAPs act specifically on the retrograde route of Shiga toxin to the Golgi apparatus or on general endocytic pathways such as receptor mediated endocytosis. Therefore, a second functional assay for the uptake of epidermal growth factor (EGF) and its receptor to early endosomes was used. Again, the full set of 39 human TBC domain proteins was screened blindly according to the plasmid number. The uptake of fluorescently labelled EGF was followed and time points for fixation and immunofluorescence analysis were chosen to be 0 and 30 minutes. After 30 minutes EGF had reached the early endosomal compartment, marked by the early endosomal antigen 1 (EEA1) in control cells. The binding of EGF to the surface of HeLa cells was not as reliable as the binding of STxB. Dependent on the Rab GAP expressed the fraction of cells without bound EGF at t0 was in the range of 5 to 40 %. Therefore, the number of cells without bound EGF at t0 and the number of cells with a block in endocytosis of EGF to early endosomes after 30 minutes were counted and compared side-by-side. From this direct comparison it became clear that only RabGAP-5 was able to block EGF uptake into early endosomes. In contrast, the GAPs inhibiting Shiga toxin trafficking to the Golgi did not affect the endocytosis of EGF and are therefore considered specific for the Shiga toxin route.

There has been some controversy in the literature concerning the relative importance of RN-tre and RabGAP-5 as regulators for Rab5 and their involvement

in the uptake of endocytosed ligands (Haas et al., 2005; Lanzetti et al., 2000). However, the results presented in this work clearly show that although both these GAPs are involved in the trafficking of endocytosed ligands, they act on discrete trafficking pathways. One explanation for the differential sensitivity of EGF receptor trafficking to RN-tre could relate to the conditions and cell lines used. With low doses of EGF, the EGF receptor is almost entirely transported via the clathrin dependent pathway, while at higher or saturating doses it spills over into the clathrin independent pathway (Sigismund et al., 2005). Thus, with saturating amounts of EGF, RN-tre would be able to prevent transport of the pool of EGF receptor entering via the clathrin-independent pathway, however the data in this work on RN-tre and its target Rab suggest that this would be a Rab5-independent and Rab43-dependent pathway.

4.2.4 What are the target Rabs for the GAPs blocking Shiga toxin transport or EGF endocytosis?

It has been suggested that Rab GAPs are not particularly specific towards their target Rab (Albert and Gallwitz, 1999; Pan et al., 2006). However, this is somewhat counter-intuitive since Rabs are argued to be important components acting at specific membrane trafficking steps and for specification of organelle identity (Munro, 2002; Pfeffer, 2001). Therefore one would expect their regulators to be equally specific. The data presented in this work support the idea that GAPs are likely to be specific towards particular target Rabs, or Rab subfamilies. First, Rab GAPs have highly specific effects on discrete membrane-trafficking pathways, consistent with the idea they act on specific Rabs in vivo. While RabGAP-5 is able to block the uptake of EGF into early endosomes, RN-tre, EVI5, TBC1D10A-C and TBC1D17 have been identified to play a role in the multi-step pathway of Shiga toxin. Furthermore, GAPs such as RabGAP-5, and RN-tre are highly active towards specific Rabs in biochemical assays, and depletion of the respective Rabs leads to the same effect observed with the expression of the GAP.

RN-tre, EVI5, TBC1D10B, TBC1D17 and RabGAP-5 were tested in biochemical assays for their ability to accelerate GTP hydrolysis by a specific Rab. A single Rab GAP was analysed at the same time together with a representative set of human Rabs, where each Rab subfamily was represented with at least one member. In this way experimental conditions and the activity state of the GAP were the same and GTP-hydrolysis rates could be compared directly within the set of Rabs. Only in the context with the full set of Rabs a single signal of hydrolysed GTP becomes meaningful. The results clearly show that RabGAP-5 acts specifically on

the Rab5a-c isoforms. This confirms previous data that RabGAP-5 is a GAP for Rab5 (Haas et al., 2005) and underlines the strong specificity of this GAP. Even very closely related Rabs such as Rab22a and Rab22b were not recognised by RabGAP-5 as a substrate. The Shiga toxin blocking GAP RN-tre showed specific activity towards Rab43. One might argue that also Rab35 is activated by RN-tre because its hydrolysis rate is approximately half of Rab43. However, Rab35 was found to be weakly activated by a number of GAPs tested. This suggests that Rab35 might be a false positive hit and also questions the significance of the very high hydrolysis rate of Rab35 by the GAP EVI5. Similarly, substrates for TBC1D10B and TBC1D17 could not be identified with certainty. The reason why the biochemical GTP-hydrolysis assay gave ambiguous results for EVI5, TBC1D10B and TBC1D17 could be linked to the activity of the recombinant GAP proteins.

What is clear is that RabGAP-5 acts on Rab5a-c and RN-tre on Rab43 with high specificity. In order to validate the target Rabs for both GAPs in vivo Rab5 and Rab43 were tested in the functional assays STxB transport and EGF uptake. Consistent with the results observed with RabGAP-5 cells depleted of all three isoforms of Rab5 were not able to take up EGF into early endosomes but transported Shiga toxin to the Golgi apparatus. Cells depleted of Rab43 showed an inhibition of Shiga toxin transport, whereas endocytosis of EGF was normal.

Taken together, these results suggest that RabGAP-5 is a specific GAP for Rab5 and controls the endocytosis of EGF, whereas RN-tre is a GAP for Rab43 and regulates the trafficking of Shiga toxin from the plasma membrane to the Golgi apparatus. Thus, different sets of Rab GAPs and their target Rabs control specific endocytic trafficking pathways. The approach used in this work, combining functional in vivo data with biochemical assays for target Rab identification should be useful for the study of other trafficking events, for trafficking between the ER and Golgi apparatus, or a wide variety of different regulated secretory events.

5 Material and Methods

5.1 Material

5.1.1 Reagents

Reagents were obtained from Sigma-Aldrich (Seelze, Germany) or VWR (Darmstadt, Germany) unless stated in the text.

5.1.2 Equipment

A list of commonly used equipment and its suppliers is given in the table below.

Equipment	Description and manufacturer
Benchtop centrifuge	Eppendorf Centrifuge 5417C
Benchtop refrigerated centrifuge	Eppendorf Centrifuge 5417R
Blotting machine	BioRad Trans-blot SD
Cell Culture Incubators	Heraeus HeraCell
Cell Culture Safety Hoods	Heraeus HeraSafe
Centrifuge	Heraeus Multifuge 3 L-R
Electroporation system	BioRad MicroPulser
Film Developer	Kodak X-OMAT 2000 Processor
Gel system	BioRad Mini-PROTEAN
Heating block/ mixer	Eppendorf Thermomix Compact
Incubators	Heraeus Function Line
Magentic stirrer	IKA RET basic IKAMAG
PCR machine	Perkin Elmer Gene Amp 2400
pH meter	Beckman ϕ340pH/Temp meter
Power pack	BioRad Power Pack 200 and 300
Scintillation counter	Packard Tri-carb 2900TR
Scintillation counter (96-well)	Perkin Elmer Wallac Microbeta Trilux
Shakers for bacterial and yeast culture	Infors AG Multitron Grant Boekel BFR25
Sonicator	Bandelin Sonopuls
SW28 rotor	Beckman
SW40 rotor	Beckman
Transilluminators	UVP 2UV Transilluminator UVP Gel Documentation System Fujifilm LAS3000
Ultracentrifuge	Beckman Optima LE-80K
UV/Visible Spectrophotometer	Amersham-Pharmacia Ultrospec 300pro
Vortex shaker	IKA MS3 basic
Waterbath	Haake DC10

5.1.3 Solutions

The composition of standard solutions not described in the respective methods chapter is given in the table below. Unless otherwise stated the solvent is water.

Solution	Composition
DNA loading dye (6x)	0.25% (w/v) bromophenol blue 40% (w/v) sucrose in TE
L-Broth (LB)	10 g/l Bacto-tryptone 5 g/l Bacto-yeast extract 10 g/l NaCl
LB-Agar	LB plus 15 g/l Bacto-agar
Milk-PBS (blocking buffer)	4% milk powder in PBS plus 0.2% (w/v) Tween-20
PBS	8 g/l NaCl 0.2 g/l KCl 1.44 g/l Na_2HPO_4 0.24 g/l KH_2PO_4 (pH 7.4)
Ponceau stain	0.2% Ponceau red in 1% acetic acid
RIPA buffer	10 mM Tris-HCl pH 7.5 150 mM NaCl 1% (w/v) Triton-X 100 0.1% (w/v) SDS 1% (w/v) sodium deoxycholate
SDS-PAGE lower buffer (4x)	181.72 g/l Tris base 4 g/l SDS
SDS-PAGE running buffer (10x)	30.2 g/l Tris base 188 g/l glycine 10 g/l SDS
SDS-PAGE sample buffer (3x)	For 100 ml: 2.3 g Tris base 9.0 g SDS 30 ml glycerol Adjust pH to 6.8 with HCl, then adjust volume to 90 ml with dH_2O 50 mg bromophenol blue Add 10% ß-mercaptoethanol prior to use
SDS-PAGE transfer buffer	1x SDS-PAGE running buffer 10% methanol
SDS-PAGE upper buffer (4x)	60.6 g/l Tris base 4 g/l SDS
TAE (50x)	For 1 l: 242.4 g Tris base 57.2 ml glacial acetic acid 50 mM EDTA pH 8.0
TE	10 mM Tris-HCl pH 8.0 1 mM EDTA

Solution	Composition
TNTE	10 mM Tris-HCl pH 7.5
	150 mM NaCl
	0.3% (w/v) Triton-X 100
	5 mM EDTA

5.1.4 Plasmids

The plasmids used in this thesis are listed in the table below and carry the pFB numbers of the plasmid stock in the Barr laboratory.

Number	Name	Vector	Insert and Notes
pFB0789	pGBT9.Golgin160	pGBT9	Mouse Golgin160 fl, derived from pFB180
pFB1162	pEGFP.C2.HumanTBC1D22a	pEGFPC2	Human TBC1D22a fl, BamHI-SalI, derived from pBS412
pFB1468	pGBT9.Rab6aWT	pGBT9	Human Rab6a, derived from pBS477
pFB1469	pGBT9.Rab6aQ72L	pGBT9	Human Rab6a Q72L GTP-restricted mutant, derived from pBS478
pFB1470	pGBT9.Rab6aT27N	pGBT9	Human Rab6a T27N GDP-restricted mutant, derived from pBS479
pFB1471	pFAT2.Rab6aWT	pFAT2	Human Rab6a, derived from pBS477
pFB1471	pFAT2.Rab6aWT	pFAT2	Human Rab6a, BamHI-SalI, derived from pBS477
pFB1472	pFAT2.Rab6aQ72L	pFAT2	Human Rab6a Q72L GTP-restricted mutant, derived from pBS478
pFB1473	pFAT2.Rab6aT27N	pFAT2	Human Rab6a T27N GDP-restricted mutant, derived from pBS479
pFB1474	pEGFP.C2.Rab6aWT	pEGFPC2	Human Rab6a, derived from pBS477
pFB1476	pEGFP.C2.Rab6aT27N	pEGFPC2	Human Rab6a T27N GDP-restricted mutant, derived from pBS479
pFB1706	pQE32.PIST	pQE32	Human PIST fl, derived from pBS592
pFB1709	pACT2.PIST	pACT2	Human PIST fl, derived from pBS592
pFB1710	pEGFP.C2.PIST	pEGFPC2	Human PIST fl, derived from pBS592
pFB1724	pFAT2.Rab33bwt	pFAT2	Mouse Rab33b wt, BamHI-SalI, plus STOP codon, derived from pBS609
pFB1779	pFBT9.Rab33bQ92L	pFBT9.	Mouse Rab33b Q92L active mutant Gal4BD fusion from pFB1719
pFB1799	pAct2.PIST1-255	pAct2	Human PIST aa 1-255, derived from pFB1794, 1st + 2nd CC
pFB1800	pAct2 PIST142-454	pAct2	Human PIST aa 142-454, derived from pFB1795, 2nd CC + PDZ

Number	Name	Vector	Insert and Notes
pFB1801	pAct2 PIST1-141	pAct2	Human PIST aa 1-141, derived from pFB1796, 1st CC
pFB1802	pAct2 PIST142-255	pAct2	Human PIST aa 142-255, derived from pFB1797, 2nd CC
pFB1803	pAct2 PIST256-454	pAct2	Human PIST aa 256-454, derived from pFB1798, PDZ
pFB1809	pEGFP PIST1-255	pEGFPC2	Human PIST aa 1-255, derived from pFB1794, 1st + 2nd CC
pFB1810	pEGFP PIST142-454	pEGFPC2	Human PIST aa 142-454, derived from pFB1795, 2nd CC + PDZ
pFB1811	pEGFP PIST1-141	pEGFPC2	Human PIST aa 1-141, derived from pFB1796, 1st CC
pFB1812	pEGFP PIST142-255	pEGFPC2	Human PIST aa 142-255, derived from pFB1797, 2nd CC
pFB1813	pEGFP PIST256-454	pEGFPC2	Human PIST aa 256-454, derived from pFB1798, PDZ
PFB1824	pHIS PIST1-255	pQE32	Human PIST aa 1-255, derived from pFB1794, 1st + 2nd CC
PFB1825	pHIS PIST142-454	pQE32	Human PIST aa 142-454, derived from pFB1795, 2nd CC + PDZ
PFB1826	pHIS PIST1-141	pQE32	Human PIST aa 1-141, derived from pFB1796, 1st CC
PFB1827	pHIS PIST142-255	pQE32	Human PIST aa 142-255, derived from pFB1797, 2nd CC
PFB1828	pHIS PIST256-454	pQE32	Human PIST aa 256-454, derived from pFB1798, PDZ
pFB1842	pFBT9 Rab2 Q65L	pFBT9.	Human Rab2a Q65L GTP mutant, BamHI-SalI, derived from pFB1830
pFB2116	pFAT2 Rab7likewt	pFAT2	Human Rab7like, derived from pFB2000, BamHI, XhoI
pFB2118	pFAT2 Rab8wt	pFAT2	Human Rab8, derived from pFB1986, BamHI, XhoI
pFB2120	pFAT2 Rab10wt	pFAT2	Human Rab10, derived from pFB1987, BamHI, XhoI
pFB2122	pFAT2 Rab30wt	pFAT2	Human Rab30, derived from pFB1993, BamHI, XhoI
pFB2298	pEGFPC2.TBC1D20	pEGFPC2	Human TBC1D20, BglII SalI, derived from pFB2264
pFB2420	pFAT2.TC10	pFAT2	Human TC10, derived from pFB2411
pFB2422	pFBT9.TC10	pFBT9	Human TC10, derived from pFB2411
pFB2424	pFBT9.Rab1 Q70L	pFBT9	Mouse Rab1 GTP restricted, derived from pBS574
pFB2428	pFAT2.TC10Q67L	pFAT2	Human TC10Q67L, GTP-restricted, derived from pFB2426
pFB2429	pFAT2.TC10S23N	pFAT2	Human TC10S23N, GDP-restricted, derived from pFB2427
pFB2430	pFBT9.TC10Q67L	pFBT9	Human TC10Q67L, GTP-restricted, derived from pFB2426

Number	Name	Vector	Insert and Notes
pFB2431	pFBT9.TC10S23N	pFBT9	Human TC10S23N, GDP-restricted, derived from pFB2427
pFB2434	pMalT.PISTfl	pMalTEV	Human PISTfl
pFB2476	pACT2.TBC1D11/TBC1D11/GAPCenA	pACT2	Human TBC1D11/TBC1D11/GAPCenA fl
pFB2506	pEGFPC2.TBC1D13	pEGFP-C2	Human TBC1D13 fl
pFB2508	pEGFPC2.TBC1D4	pEGFP-C2	Human TBC1D4 fl
pFB2509	pEGFPC2.TBC1D20 R105A	pEGFP-C2	Human TBC1D20 R105A
pFB2512	pEGFPC2.TBC1D2	pEGFP-C2	Human TBC1D2 fl
pFB2515	pEGFPC2.TBC1D3B/PRC 17	pEGFP-C2	Human TBC1D3B/PRC17 fl
pFB2516	pEGFPC2.TBC1D22B	pEGFP-C2	Human TBC1D22B fl
pFB2521	pEGFPC2.TBC1D5	pEGFP-C2	Human TBC1D5 fl
pFB2600	pFBT9.Rab1bQ67L	pFBT9	Human Rab1bQ67L, GTP mutant, derived from pFB2366
pFB2601	pFBT9.Rab2bQ65L	pFBT9	Human Rab2bQ65L, GTP mutant, derived from pFB2368
pFB2602	pFBT9.Rab3bQ81L	pFBT9	Human Rab3bQ81L, GTP mutant, derived from pFB2369
pFB2603	pFBT9.Rab4aQ72L	pFBT9	Human Rab4aQ72L, GTP mutant, derived from pFB2582
pFB2604	pFBT9.Rab5bQ79L	pFBT9	Human Rab5bQ79L, GTP mutant, derived from pFB2370
pFB2605	pFBT9.Rab6aQ72L	pFBT9	Human Rab6aQ72L, GTP mutant, derived from pFB2371
pFB2606	pFBT9.Rab8aQ67L	pFBT9	Human Rab8aQ67L, GTP mutant, derived from pFB2372
pFB2608	pFBT9.Rab9bQ66L	pFBT9	Human Rab9bQ66L, GTP mutant, derived from pFB2374
pFB2609	pFBT9.Rab10Q68L	pFBT9	Human Rab10Q68L, GTP mutant, derived from pFB2375
pFB2610	pFBT9.Rab11aQ70L	pFBT9	Human Rab11aQ70L, GTP mutant, derived from pFB2376
pFB2611	pFBT9.Rab13Q67L	pFBT9	Human Rab13Q67L, GTP mutant, derived from pFB2377
pFB2612	pFBT9.Rab14Q70L	pFBT9	Human Rab14Q70L, GTP mutant, derived from pFB2378
pFB2613	pFBT9.Rab18Q67L	pFBT9	Human Rab18Q67L, GTP mutant, derived from pFB2591
pFB2614	pFBT9.Rab23Q68L	pFBT9	Human Rab23Q68L, GTP mutant, derived from pFB2380
pFB2615	pFBT9.Rab27aQ78L	pFBT9	Human Rab27aQ78L, GTP mutant, derived from pFB2383
pFB2616	pFBT9.Rab27bQ78L	pFBT9	Human Rab27bQ78L, GTP mutant, derived from pFB2384
pFB2617	pFBT9.Rab30Q68L	pFBT9	Human Rab30Q68L, GTP mutant, derived from pFB2595
pFB2618	pFBT9.Rab31Q65L	pFBT9	Human Rab31Q65L, GTP mutant, derived from pFB2386
pFB2619	pFBT9.Rab35Q67L	pFBT9	Human Rab35Q67L, GTP mutant, derived from pFB2388
pFB2620	pFBT9.Rab40cQ73L	pFBT9	Human Rab40cQ73L, GTP mutant, derived from pFB2599
pFB2761	pFAT2.Human Rab4awt	pFAT2	Human Rab4a wt, derived from pFB2305

Number	Name	Vector	Insert and Notes
pFB2762	pFAT2.Human Rab5bwt	pFAT2	Human Rab5b wt, derived from pFB 2307
pFB2773	pEGFP.C2.TBC1D11/GAPCenA	pEGFP.C2	Human TBC1D11/GAPCenA fl
pFB2780	pFBT9.Human Rab3aQ81L	pFBT9	Human Rab3aQ81L, derived from pFB2753
pFB2781	pFBT9.Human Rab33aQ95L	pFBT9	Human Rab33aQ95L, derived from pFB2754
pFB2782	pFBT9.Human Rab37Q82L	pFBT9	Human Rab37Q82L, derived from pFB2755
pFB2783	pFBT9.Human Rab39Q72L	pFBT9	Human Rab39Q72L, derived from pFB2756
pFB2824	pEGFP.C2.Rab6Q72L	pEGFPC2	Human Rab6Q72L, GTP-restricted, derived from Roberts Rabome clone 6.2
pFB2861	pFBT9.Rab9aQ66L	pFBT9	Human Rab9aQ66L, GTP-locked, derived from pFB2585
pFB2866	pEGFP.C2.RabGAP-5	pEGFP.C2	Human RabGAP-5 fl
pFB2867	pCDN3.1mycA. RabGAP-5	pcDNA3.1mycA	Human RabGAP-5 fl
pFB2887	pMALTEVHis. RabGAP-5	pMALTEV-His	Human RabGAP-5 fl wt
pFB2911	pFBT9.Human Rab43Q77L	pFBT9	Human Rab43Q77L, derived from pFB2767
pFB2951	pCDNA3.1mycA.RabGAP-5 R165A	pcDNA3.1mycA	Human RabGAP-5 fl R165A mutant
pFB2952	pACT2.TBC1D11/GAPCenA.aa1.723	pACT2	Human TBC1D11/GAPCenA aa1-723, without coiled-coil
pFB2953	pACT2.TBC1D11/GAPCenA.aa724.998	pACT2	Human TBC1D11/GAPCenA aa724-998, Coiled-coil at C-terminus
pFB2954	pACT2.TBC1D11/GAPCenA.aa201.998	pACT2	Human TBC1D11/GAPCenA.aa 201-998, without PTB Domain
pFB2968	pFAT2.Rab31.Wt	pFAT2	Human Rab31 WT
pFB3009	pFBT9.Human Rab20Q61L	pFBT9	Human Rab20 GTP mutant, derived from pFB2928
pFB3016	pFAT2.Human Rab22awt	pFAT2	Human Rab22a wt, GST+His-tagged, derived from pFB2935
pFB3026	pFAT2.Human Rab1bwt	pFAT2	Human Rab1b wt, GST+His-tagged, derived from pFB2301
pFB3041	pCDNA3.1mycA.RN-tre.R150A	pcDNA3.1mycA	Human RN-tre FL R150A, derived from pFB3039
pFB3042	pEGFPC2.RN-tre.R150A	pEGFP-C2	Human RN-tre FL R150A, derived from pFB3039
pFB3059	pCDNA3.1mycA.RN-tre.FL.WT	pCDNA3.1mycA	Human RN-tre WT FL from Testis
pFB3056	pMALTEV.His.RN-tre.FL	pMALTEV-His	Human RN-tre WT FL
pFB3060	pEGFPC2.RN-tre.FL.WT	pEGFPC2	Human RN-tre WT FL from Testis
pFB3086	pFAT2.Human Rab25wt	pFAT2	Human Rab25wt, derived from pFB2319
pFB3090	pFAT2.Rab5A.WT	pFAT2	Human Rab5A derived from pFB2306
pFB3093	pFAT2.Rab43.WT	pFAT2	Human Rab43 WT
pFB3116	pFBT9.Rab5A.QL	pFBT9	Human Rab5A derived from pFB3112, GTP-lock
pFB3123	pFBT9.Rab32.QL	pFBT9	Human Rab32 derived from pFB2936, GTP-lock

Number	Name	Vector	Insert and Notes
pFB3176	pFAT2.Human Rab2bwt	pFAT2	Human Rab2b wt, derived from pFB2303
pFB3177	pFAT2.Human Rab3awt	pFAT2	Human Rab3a wt, derived from pFB2686
pFB3179	pFAT2.Human Rab9awt	pFAT2	Human Rab9a wt, derived from pFB2310
pFB3180	pFAT2.Human Rab9bwt	pFAT2	Human Rab9b wt, derived from pFB2311
pFB3181	pFAT2.Human Rab14wt	pFAT2	Human Rab14 wt, derived from pFB2315
pFB3182	pFAT2.Human Rab18wt	pFAT2	Human Rab18 wt, derived from pFB2316
pFB3183	pFAT2.Human Rab20wt	pFAT2	Human Rab20 wt, derived from pFB2788
pFB3184	pFAT2.Human Rab23wt	pFAT2	Human Rab23 wt, derived from pFB2364
pFB3185	pFAT2.Human Rab24wt	pFAT2	Human Rab24 wt, derived from pFB2318
pFB3186	pFAT2.Human Rab27awt	pFAT2	Human Rab27a wt, derived from pFB2320
pFB3188	pFAT2.Human Rab33awt	pFAT2	Human Rab33a wt, derived from pFB2689
pFB3189	pFAT2.Human Rab34wt	pFAT2	Human Rab34 wt, derived from pFB2973
pFB3190	pFAT2.Human Rab37wt	pFAT2	Human Rab37 wt, derived from pFB2676
pFB3191	pFAT2.Human Rab39wt	pFAT2	Human Rab39 wt, derived from pFB2677
pFB3195	pFAT2.Rab35.wt	pFAT2	Human Rab35 wt
pFB3196	pFAT2.Human Rab13.wt	pFAT2	Human Rab13 wt
pFB3204	pFBT9.Rab22a.QL	pFBT9	Human Rab22a GTP Lock, derived from pFB2935
pFB3209	pFAT2.Rab5C.WT	pFAT2	Human Rab5C, from U2Os cDNA, WT
pFB3246	pFBT9.Rab5C.QL	pFBT9	Human Rab5C, from U2Os cDNA, Q80L GTP-Lock
pFB3321	pFAT2.Human Rab21wt	pFAT2	Human Rab21 wt, N-terminal His+GST-tag, derived from pFB3029
pFB3325	pFAT2.Human Rab19bwt	pFAT2	Human Rab19b wt, N-terminal His+GST-tag, derived from pFB 3319
pFB3346	pFBT9.Human Rab19bQ79L	pFBT9	Human Rab19b Q79L, GTP mutant, derived from pFB3343
pFB3389	pFAT2.Rab6QL	pFAT2	Human Rab6Q72L, GTP-restricted, derived from pFB2583
pFB3489	pEGFPC2.TBC1D14.fl.RA	PEGFPC2.	Human TBC1D14 fl R472A, BamHI BamHI, derived from pFB3487
pFB3513	pFBT9.Rab34.Q111L	pFBT9	Human Rab34 Q111L, derived from pFB3512
pFB3514	pFBT9.Rab21.Q78L	pFBT9.	Human Rab21 Q78L, derived from pFB3513
pFB3523	pFBT9.Rab28.Q72L	pFBT9	Human Rab28 Q72L
pFB3527	pFBT9.Rab38.Q69L	pFBT9	Human Rab38 Q69L

Number	Name	Vector	Insert and Notes
pFB3554	pEGFPC2.AK074305	PEGFPC2.	Human AK074305 FL WT derived from pFB3551
pFB3558	pFAT2.Human Rab7wt	pFAT2	Human Rab7 wt, derived from pFB3557
pFB3590	pFAT2.Human Rab3d	pFAT2	Human Rab3d wt, derived from pFB3563
pFB3687	pEGFPC2.TBC1D1	pEGFPC2	Human TBC1D1, derived form pFB3678
pFB3706	pEGFPC2.TBC1D4	pEGFPC2	Human TBC1D4, derived frompFB3691
pFB3732	pEGFPC2.EVI5	pEGFPC2	Human EVI5 derived from pFB3724
pFB3733	pEGFPC2.EVI5RA	pEGFPC2	Human EVI5RA derived from pFB3725
pFB3812	pEGFPC2.EVI5-like.FL.WT	pEGFPC2.	Human EVI5-like FL, WT, derived from pFB3811
pFB3820	pEGFPC2.USP6.FL.WT	pEGFPC2.	Human USP6 FL, WT, derived from pFB3819
pFB3832	pEGFPC2.TBC1D10c.FL.WT	pEGFPC2.	Human TBC1D10c FL, WT, derived from pFB3831
pFB3836	pEGFPC2.TBC1D10c.FL.RA	pEGFPC2.	Human TBC1D10c FL, R141A, derived from pFB3835
pFB3840	pEGFPC2.TBC1D21.FL.WT	pEGFPC2.	Human TBC1D21 FL, WT, derived from pFB3839
pFB3848	pEGFPC2.RUTBC1.FL.WT	pEGFPC2.	Human RUTBC1 FL, WT, derived from pFB3847
pFB3856	pEGFPC2.RUTBC2.FL.WT	pEGFPC2.	Human RUTBC2 FL, WT, derived from pFB3855
pFB4034	pEGFP.C2.Human Rab5bQ79A	pEGFP-C2	Human Rab5b Q79A, N-terminal GFP-tag, derived from pFB3948
pFB4095	pEGFPC2.Paris1.FL.WT	pEGFPC2.	Human Paris1 FL WT, derived from pFB4094
pFB4104	pEGFPC2.KIAA1171.FL.WT	pEGFPC2.	Human KIAA1171 FL WT, derived from pFB4103
pFB4131	pEGFPC2.NP_060779.FL.WT	pEGFPC2.	Human NP_060779 FL WT, derived from pFB4130
pFB4136	pEGFPC2.TBC1D18.FL.WT	pEGFPC2.	Human TBC1D18 FL, WT BclI SalI, derived from pFB2891
pFB4141	pEGFPC2.TBC1D22b.FL.RA	pEGFPC2.	Human TBC1D22b FL R274A BamHI, SalI, derived from pFB3532
pFB4143	pEGFPC2.TBC1D22a.FL.RA	pEGFPC2.	Human TBC1D22a FL R286A derived from pFB3530
pFB4149	pEGFPC2.KIAA1055.FL.WT	pEGFPC2.	Human KIAA1055 FL WT, BglII BglII derived from pFB3541
pFB4154	pEGFPC2.TBC1D10B.FL.WT	pEGFPC2.	Human TBC1D10B FL WT, derived from pFB4153
pFB4333	GSTHis.Rab11bwt	pFAT2	Human Rab11bwt
pFB4362	pEGFPC2.RabGAP-5.FL.RA	pEGFPC2	Human RabGAP-5 R165A inactive mutant, fl
pFB4407	pFAT2.Rab6b wt	pFAT2	Human Rab6b wt derived from pFB3565
pFB4408	pEGFPC2.TBC1D7	pEGFPC2	Human TBC1D7 wt derived from pFB4309
pFB4411	pEGFPC2.TBC1D8	pEGFPC2	Human TBC1D8 wt derived

Number	Name	Vector	Insert and Notes
			from pFB3718
pFB4412	pEGFPC2.TBC1D17	pEGFPC2	Human TBC1D17 wt derived from pFB3288
pFB4414	pEGFPC2.TBC1D19	pEGFPC2	Human TBC1D19 wt derived from pFB3289
pFB4417	pEGFPC2.TBC1D16	pEGFPC2	Human TBC1D16 wt derived from pFB3287
pFB4420	pEGFPC2.KIAA0984	pEGFPC2	KIAA0984 wt BamHI-XhoI; derived from pFB3721
pFB4423	pEGFPC2.TBC1D15	pEGFPC2	Human TBC1D15 wt derived from pFB3286
pFB4427	pEGFPC2.KIAA0676	pEGFPC2	Human KIAA0676 wt derived from pFB3290
pFB4430	pEGFP.C2.TBC1D10A fl wt	pEGFPC2	Human TBC1D10A wt
pFB4431	pEGFP.C2.TBC1D10A fl RA	pEGFPC2	Human TBC1D10A RA
pFB4433	pEGFP.C2.TBC1D17 fl RA	pEGFPC2	Human TBC1D17 RA
pFB4434	pEGFP.C2.KIAA0984 RA	pEGFPC2	Human KIAA0984
pFB4441	pMAL.TEV_His TBC1D17wt	pMALTEV-His	Human TBC1D17 wt FL
pFB4555	pEGFPC2.TBC1D10b.Fl.RA	pEGFPC2.	Human TBC1D10b RA , derived from pFB4158.
pFB4619	pFAT2.Human Rab12wt	pFAT2	Human Rab12 wt, N-terminal GST+His6 tag, derived from pFB3583
pFB4620	pFAT2.Human Rab15wt	pFAT2	Human Rab15 wt, N-terminal GST+His6 tag, derived from pFB3569
pFB4621	pFAT2.Human Rab17wt	pFAT2	Human Rab17 wt, N-terminal GST+His6 tag, derived from pFB3498
pFB4622	pFAT2.Human Rab20wt	pFAT2	Human Rab20 wt, N-terminal GST+His6 tag, derived from pFB3760
pFB4623	pFAT2.Human Rab28wt	pFAT2	Human Rab28 wt, N-terminal GST+His6 tag, derived from pFB3520
pFB4624	pFAT2.Human Rab32wt	pFAT2	Human Rab32 wt, N-terminal GST+His6 tag, derived from pFB2936
pFB4625	pFAT2.Human Rab36wt	pFAT2	Human Rab36 wt, N-terminal GST+His6 tag, derived from pFB3573
pFB4626	pFAT2.Human Rab38wt	pFAT2	Human Rab38 wt, N-terminal GST+His6 tag, derived from pFB3524
pFB4627	pFAT2.Human Rab40awt	pFAT2	Human Rab40a wt, N-terminal GST+His6 tag, derived from pFB3571

5.1.5 siRNA oligonucleotides

siRNA oligonucleotides for siRNA-mediated depletion of specific mRNAs were generally designed to a target sequence of NN(N19)dTdT using the si*DESIGN* Center on the Dharmacon homepage (www.dharmacon.com) (Elbashir et al., 2002; Reynolds et al., 2004). The RNA oligonucleotides used in the course of this work are listed in the table below.

Target Gene	Target Sequence
GL2 (Control)	CGUACGCGGAAUACUUCGAUU
LaminA (Control)	CTGGACTTCCAGAAGAACATC
Rab6A 3'UTR	GCUCACUGCUUUGGCCCCCUU
PIST	CCCUGGUGCUAGUUGCAAAUU
Golgin-160	GCAGCCUUCAUGCAGAUUCUU
Rab5A	#1, GCAAGCAAGUCCUAACAUUUU
	#2, UGACACUACAGUAAAGUUUUU
	#3, GGAAGAGGAGUAGACCUUAUU
	#4, AGAGUCCGCUGUUGGCAAAUU
Rab5B	#1, GGAGCGAUAUCACAGCUUAUU
	#2, GAAAGUCAAGCCUGGUAUUUU
	#3, CAACAAACGUAUGGUGGAGUU
	#4, AAGCUGCAAUCGUGGUUUAUU
Rab5C	#1, UCAUUGCACUCGCGGGUAAUU
	#2, GAACAAGAUCUGUCAAUUUUU
	#3, GCAAUGAACGUGAACGAAAUU
	#4, GCUAAGAAGCUUCCCAAGAUU
Rab6A	#1, GUGGAUUGAUGAUGUCAGAUU
	#2, CCAAAGAGCUGAAUGUUAUUU
	#3, GAGCAAAGCGUUGGAAAGAUU
	#4, GAAAGAGGAAGUGAUGUUAUU
Rab6B	#1, GCUGAUAAGAGGCAGAUAAUU
	#2, CAACAGACCUCUAAGUGGAUU
	#3, GAGUUAAGGUUCCAUAAUAUU
	#4, UCAGGAAAGUUGAGUGUAAUU
Rab43	#1, GCGUCGACUUCACCAUGAAUU
	#2, GGAUUGAGGAUGUGAGGAAUU

5.1.6 Antibodies

The antibodies used in the course of this work are listed in the tables below, along with their typical dilutions used for western blotting and immunofluorescence.

5.1.6.1 Primary antibodies

Name	Species	Antigen	Dilution for WB	Dilution for IF	Source
9E10	Mouse	c-myc	1:1000	1:1000	Cancer Research UK
α–Bic-D1	Rabbit	Human Bic-D1 C-terminal fragment	1:100	1:50	Barr laboratory
α–EEA1	Mouse	Human EEA1	1:50	1:50	BD Biosciences
α–GFP	Sheep	His-GFP	1:2000	1:2000	Barr laboratory
α–GM130	Mouse	Human GM130	1:2000	1:2000	BD Biosciences
α–GM130	Sheep	His-rat GM130	1:1000	1:1000	Barr laboratory
α–Golgin-97	Mouse	Human golgin-97	nd	1:100	Molecular Probes
α–Golgin-97	Sheep	Human golgin-97 aa 589-769	1:500	1:500	Barr laboratory
α–Golgin-160	Rabbit	Human golgin-160	1:1000	1:1000	Barr laboratory

Name	Species	Antigen	Dilution for WB	Dilution for IF	Source
α−Histidine	Mouse	Hexahistidine epitope tag	1:1000	-	Dianova
α−p115	Sheep	Rat p115 aa 772-959	1:2000	1:2000	Barr laboratory
α−p150^{glued}	Mouse	Rat p150^{glued}	1:100	1:100	BD Biosciences
α−PIST	Rabbit	Human PIST full-length	1:1000	1:1000	Raised and purified during this work
α−Rab6 (C-19)	Rabbit	Human Rab6 C-terminal peptide	not working	1:100	Santa Cruz Biotech
α−TGN46	Sheep	Human TGN46	1:2000	1:2000	Serotech
α−Tubulin	Mouse	Tubulin	1:1000	1:1000	Sigma-Aldrich

5.1.6.2 Secondary antibodies

Name	Species	Antigen	Dilution for WB	Dilution for IF	Source
AMCA-α-mouse	Donkey	Mouse IgG	-	1:250	Jackson Laboratories
Cy2-α-mouse	Donkey	Mouse IgG	-	1:1000	Jackson Laboratories
Cy3-α-mouse	Donkey	Mouse IgG	-	1:1000	Jackson Laboratories
HRP-α-mouse	Sheep	Mouse IgG	1:2000	-	Amersham-Pharmacia
AMCA-α-mouse	Donkey	Mouse IgG	-	1:250	Jackson Laboratories
Cy2-α-rabbit	Donkey	Rabbit IgG	-	1:1000	Jackson Laboratories
Cy3-α-rabbit	Donkey	Rabbit IgG	-	1:1000	Jackson Laboratories
HRP-α-rabbit	Donkey	Rabbit IgG	1:2000	-	Jackson Laboratories
Cy2-α-sheep	Donkey	Sheep IgG	-	1:1000	Jackson Laboratories
Cy3-α-sheep	Donkey	Sheep IgG	-	1:1000	Jackson Laboratories
HRP-α-sheep	Donkey	Sheep IgG	1:10000	-	Jackson Laboratories

5.2 Bacterial Methods

5.2.1 Growth and maintenance of *E. coli*

Bacteria were grown at 37 °C in LB medium containing an appropriate antibiotic for selection (typically either 100 μg/ml ampicillin, 50 μg/ml kanamycin, or 34 μg/ml chloramphenicol). Short-term storage was on LB-agar plates plus antibiotic at 4 °C.

5.2.2 Bacterial strains

The following *E. coli* strains were used in the course of this work.

Strain	Genotype	Use
XL1-blue	F'::Tn*10* *proA*$^+$*B*$^+$ *lacI*^{q} Δ*(lacZ)M15/ recA1 endA1 gyrA96 (Nal*^{r}*) thi hsdR17 (r*$_K$$^-$ *m*$_K$$^+$*) glnV44 relA1 lac*	General cloning applications
GM2163	F$^-$ *ara-14 leuB6 fhuA31 lacY1 tsx78 glnV44 galK2 galT22 mcrA dcm-6 hisG4 rfbD1 rpsL136 dam13::*Tn*9 xylA5 mtl-1 thi-1 mcrB1 hsdR2*	Cloning of non-methylated DNA for digestion with Dam or Dcm-sensitive restriction enzymes
BL21(DE3)*	F$^-$ *ompT gal [dcm] [lon] hsdS*$_B$ *r*$_B$$^-$ *m*$_B$$^-$; an *E. coli* B strain with DE3, a λ prophage carrying the T7 RNA polymerase gene	Recombinant protein expression
JM109*	F' *traD36 proA*$^+$*B*$^+$ *lacI*^{q} Δ*(lacZ)M15/* Δ*(lac-proAB) glnV44 e14*$^-$ *gyrA96 recA1 relA1 endA1 thi hsdR17*	Recombinant protein expression
TOP10	F$^-$ *mcrA* Δ*(mrr-hsdRMS-mcrBC)* Φ*80lacZ*Δ*M15* Δ*lacX74 recA1 deoR araD139* Δ*(ara-leu)7697 galU galK rpsL (Str*^{R}*) endA1 nupG*	TA-cloning of PCR products

*In most cases, BL21(DE3) and JM109 strains carrying the pRIL plasmid (Stratagene) were used for recombinant protein expression. This plasmid encodes the tRNA genes for rare arginine, isoleucine, and leucine codons and conveys chloramphenicol resistance.

5.2.3 Preparation and transformation of chemically competent bacteria

To prepare chemically competent *E. coli*, a single colony was picked from a fresh plate and used to inoculate 50 ml of LB (with selection, if necessary) and grown overnight at 37 °C with shaking. 1 ml of overnight culture was then used to inoculate 100 ml of fresh LB and the cells were grown at 37 °C until an OD_{600} of 0.5. The culture was then chilled on ice for 15 minutes before being transferred to a sterile centrifuge tube and centrifuged at approximately 3000 x g for 10 minutes at 4 °C. The supernatant was discarded and the cell pellet resuspended in 0.4 total culture volume of TfbI (30 mM KOAc, 100 mM $RbCl_2$, 10 mM $CaCl_2$, 50 mM $MnCl_2$, 15% (v/v) glycerol, pH adjusted to 5.8 with dilute acetic acid). The cells were incubated on ice for 15 minutes and then pelleted as before. The cell pellet was then resuspended in 0.04 volume TfbII (10 mM MOPS, 75 mM $CaCl_2$, 10 mM $RbCl_2$, 15 % (v/v) glycerol, pH adjusted to 6.5 with dilute NaOH). After storing on ice for 15 minutes, the cells were aliquoted into 50 μl aliquots in sterile Eppendorfs, frozen in liquid nitrogen, and stored at – 80 °C until needed.

For transformation, aliquots were thawed on ice before adding the DNA. In general, 5 μl of a ligation reaction was used for transformation of 50 μl competent

bacteria, or 1 µl of plasmid DNA (approx. 200 ng). Cells and DNA were mixed and left on ice for 15 minutes before being heat-shocked in a 42 °C water bath for 45 – 90 seconds. Cells were placed back on ice for 1 minute before the addition of either 250 µl (ligation transformation) or 1000 µl (plasmid transformation) LB. The cells were then allowed to recover for 30 – 60 minutes at 37 °C with shaking before being plated on LB-agar plates containing an appropriate selection antibiotic. All of a ligation transformation was plated while only 100 µl of a plasmid transformation was plated. Plates were then incubated overnight at 37 °C.

5.2.4 Preparation and transformation of electrocompetent bacteria

To prepare electrocompetent *E. coli*, a single colony was picked from a fresh plate and used to inoculate 5 ml of LB and grown overnight at 37 °C with shaking. 2.5 ml of the overnight culture was then used to inoculate 500 ml of fresh LB and grown at 37 °C until an OD_{600} of between 0.5 and 0.6. The culture was then chilled on ice for 15 minutes before being transferred to a sterile centrifuge tube and centrifuged at approximately 3000 x g for 10 minutes at 4 °C. The supernatant was removed and the cells resuspended in 10 ml sterile, ice-cold water. Centrifuge tubes were then filled with 500 ml ice-cold water and centrifuged as before. The supernatant was removed and the volume adjusted to 50 ml with ice-cold 10 % (v/v) glycerol before centrifuging as above. The cell pellet was resuspended in an equal volume of ice-cold 10 % (v/v) glycerol and the cells were aliquoted into 40 µl aliquots in sterile Eppendorf tubes, frozen in liquid nitrogen, and stored at – 80 °C until needed.

For electroporation, sterile 2 mm electroporation cuvettes were placed on ice to chill while cells were thawed on ice. 1-2 µl of yeast miniprep DNA or 1-10 ng plasmid DNA was added to the cuvette followed by 40 µl of electrocompetent cells. The cuvette was flicked to mix the DNA and cells and left on ice for 5 minutes. The electroporator was set to 2.5 kV, 25 µFarads. Cuvettes were dried with a tissue wipe and placed into the chamber and the cells electroporated (ideally, with a time constant of 4.7). 250 µl of LB medium was added to the cuvette immediately and the cells were transferred to a sterile Eppendorf tube and incubated at 37 °C for 1 hour before being plated on LB-agar plates containing an appropriate selective antibiotic and grown at 37 °C.

5.2.5 Plasmid DNA preparation from bacteria

Plasmid DNA was prepared using either miniprep or maxiprep kits (Qiagen, Hilden, Germany) according to the manufacturers instructions. Typically, minipreps were prepared from 1,5 ml, maxipreps from 150 ml of overnight cultures grown in LB containing selective antibiotic at 37 °C.

5.2.6 Purification of 6xHis- and 6xHisGST-tagged proteins from bacteria

A single colony was picked from a fresh plate of transformed *E. coli* and used to inoculate 25 ml of LB plus selective antibiotics and grown overnight at 37 °C with shaking. 10 ml of the overnight culture was then used to inoculate 1 l of fresh LB plus antibiotics and grown at 37 °C until an OD_{600} of 0.5 – 0.6 was reached. Depending upon the protein being expressed, cultures were shifted to 18 °C for 30 minutes before being induced with 0.5 mM Isopropyl β-D-thiogalactoside (IPTG) from a 1 M stock or induced immediately at 37 °C. Cultures were then left for either

3 hours (37 °C) or overnight (18 °C). Bacteria were then harvested by centrifugation at 3000 x g for 15 minutes at 4 °C and cell pellets were frozen on dry ice for 20 minutes.

For protein purification, cell pellets were thawed by the addition of 20 ml lysis buffer per litre of original culture. Lysis buffer consisted of 0.5 mg/ml lysozyme and protease inhibitors added to IMAC5-TX (20 mM Tris-HCl pH 8.0, 300 mM NaCl, 5 mM imidazole, 0.1 % TX100). The cell pellet was resuspended and incubated at 37 °C for 5 minutes or until the lysate became extremely viscous. The lysate was sonicated on ice using a Bandelin Sonopuls sonicator (Bandelin, Berlin, Germany) until the DNA was sheared and the lysate became much less viscous. The lysate was then centrifuged at 28000 rpm for 30 minutes at 4 °C in an SW28 rotor in a Beckman Optima LE-80K Ultracentrifuge (Beckman, USA) to pellet the cell debris. The cleared lysate supernatant was transferred into a clean falcon tube. 0.5 ml of Ni-NTA agarose (Qiagen) per litre of original culture, washed in IMAC5-TX, was added to the cleared lysate and the tube was rotated for 2 hours at 4 °C to allow protein binding to occur. The resin was then pelleted by centrifugation at 1000 x g for 5 minutes at 4 °C and washed in 2 x 30 ml of IMAC20-TX (20 mM Tris-HCl pH 8.0, 300 mM NaCl, 20 mM imidazole, 0.1 % TX100). The resin was then washed in a further 30 ml of IMAC20 without TX100 and bound protein was eluted by the addition of IMAC200 (20 mM Tris-HCl pH 8.0, 300 mM NaCl, 200 mM imidazole). The eluate was collected in 0.5 ml fractions. After SDS-PAGE analysis of 10 µl of these fractions, peak fractions containing recombinant protein were pooled and dialysed overnight at 4 °C into a suitable buffer (usually PBS). Protein concentration was then determined, before aliquoting and storage.

5.2.7 Purification of MBP-tagged proteins from bacteria

For purification of MBP-tagged proteins bacteria were grown as described in 5.2.6 except that glucose was added to a final concentration of 0.2 % in order to prevent the up-regulation of amylase enzymes. After induction with 0.5 mM IPTG cultures were left shaking for 3 hours at 37 °C. Bacteria were then harvested by centrifugation at 3000 x g for 15 minutes at 4 °C and cell pellets were frozen on dry ice for 20 minutes.

For protein purification, cell pellets were thawed by the addition of 20 ml lysis buffer per litre of original culture. Lysis buffer consisted of 0.5 mg/ml lysozyme added to TBS-TX (50 mM Tris-HCl pH7.5, 150 mM NaCl, 0.1 % TX100). The cell pellet was resuspended and incubated at 37 °C for 5 minutes or until the lysate became extremely viscous. The lysate was sonicated on ice using a Bandelin Sonopuls sonicator (Bandelin, Berlin, Germany) until the DNA was sheared and the lysate became much less viscous. The lysate was then centrifuged at 28000 rpm for 30 minutes at 4 °C in an SW28 rotor in a Beckman Optima LE-80K Ultracentrifuge (Beckman, USA) to pellet the cell debris. The cleared lysate supernatant was transferred into a clean falcon tube. 1 ml of amylose resin (New England Biolabs, USA) per litre of original culture, washed in TBS-TX, was added to the cleared lysate and the tube was rotated for 4 hours at 4 °C to allow protein binding to occur. The resin was then pelleted by centrifugation at 1000 x g for 5 minutes at 4 °C and washed in 2 x 30 ml of TBS-TX and 1 x 30 ml TBS without TX100 (50 mM Tris-HCl pH7.5, 150 mM NaCl). Bound protein was then eluted by the addition of 20 mM free maltose in TBS. The eluate was collected in 1 ml fractions. After SDS-PAGE

analysis of 10 µl of these fractions, peak fractions containing recombinant protein were pooled and dialysed overnight at 4 °C into TBS containing 2 mM DTT. Protein concentration was then determined, before aliquoting and storage.

5.3 DNA methods

Standard DNA manipulations were performed essentially as described (Sambrook and Russel, 2001). Enzymes for DNA modification were obtained from New England Biolabs (Ipswich, MA, USA), Promega (Madison, WI, USA), or Invitrogen (Carlsbad, CA, USA) and used according to the suppliers instructions.

5.3.1 "Shortway" cloning strategy

As far as possible, a standard cloning strategy, referred to as the "Shortway" system, was used when generating constructs, in order to make all inserts compatible with a wide range of different vectors. This involved generating inserts with a *BamHI*, *BglII*, or *BclI* site at the 5' end and a *SalI* or *XhoI* site at the 3' end. The ATC of the *BamHI/ BglII/ BclI* site was designed to be in frame with the start codon of the insert i.e.

      GGG ATC CCC *ATG* (*BamHI)*
      GAG ATC TCC *ATG* (*BglII*)
      GTG ATC ACC *ATG* (*BclI*, *dam* sensitive)

where the restriction site is underlined and the start codon is in italics.

These restriction sites were added by PCR and the insert was TA-TOPO cloned into the vector pCRIITOPO (Invitrogen). Constructs were sequenced from pCRIITOPO and then subcloned into the following vectors:

Yeast 2-hybrid bait vector pFBT9 (modified pGBT9 carrying a Kan resistance gene)
Yeast 2-hybrid prey vector pFBT9 (pACT2)
N-terminal 6xHis-tagging vectors (pQE32)
N-terminal MBP-tagging vector (pMalTev6xHis)
N-terminal 6xHisGST-tagging vector (pFAT2)
N-terminal GFP-tagging vector (pEGFP-C2)
C-terminal GFP-tagging vectors (pEGFP-N1, 2, or 3)
N-terminal tagged mammalian expression vectors (pcDNA3.1/MycA or /Flag)

If a sequence of interest was not clonable using this approach, alternative restriction sites were added to the 5' and 3' ends.

5.3.2 Restriction digests and agarose gel electrophoresis of DNA

Analytical restriction digests were carried out in a total volume of 20 µl using 0.5 µl of each enzyme in an appropriate buffer to digest approximately 500 ng of DNA. Digests were carried out for 2 hours at an appropriate temperature before being mixed with DNA loading buffer and loaded for electrophoresis onto a 1 % agarose gel (1 % (w/v) agarose dissolved in 1 x TAE containing 0.8 µg/ml ethidium bromide). The gel was run in 1 x TAE at a constant voltage of 80 V for approximately 50 minutes and DNA was visualized on a UV transilluminator.

      Preparative restriction digests were performed similarly except that 2-3 µg DNA was used. Vector DNA was usually treated with alkaline phosphatase by the

addition of 1 µl enzyme to the digestion mix for 15 minutes immediately prior to loading on the gel. Following electrophoresis, appropriate bands were excised using a clean scalpel blade and purified using a gel extraction kit (Qiagen) according to the manufacturers instructions.

5.3.3 Cloning digested DNA fragments

Ligations were performed in a total volume of 20 µl using 1 µl of T4 DNA ligase (NEB) in 1x ligase buffer (NEB). 100 ng of vector DNA was used along with enough insert DNA to make a 3:1 molar ratio of insert:vector DNA. Ligations were incubated for 2 hours at room temperature before transformation of bacteria with 5 µl ligation product.

5.3.4 mRNA isolation and cDNA synthesis

Total RNA from HeLa cells was isolated using TRIZOL reagent (Invitrogen), which is a solution of phenol and guanidine isothiocyanate. Per 3.5 cm diameter dish of cells grown in a monolayer, 1 ml of TRIZOL reagent was added and pipetted up and down several times to homogenise the sample. After 5 minutes incubation at room temperature 200 µl of chloroform were added. The sample was mixed vigorously by hand for 15 seconds and incubated for 3 minutes at room temperature. Centrifugation at 10000 x g at 4 °C separated the sample into a lower organic phase and into an upper aqueous phase containing the RNA. This upper phase was transferred carefully to a new tube and mixed with 500 µl of isopropyl alcohol to precipitate the RNA. After an incubation of 10 minutes at room temperature, the RNA precipitate was pelleted by centrifugation at 10000 x g at 4 °C, the pellet was washed once with 75 % ethanol and centrifuged again at 7500 x g for 5 minutes at 4 °C. Then, the RNA was briefly air-dried, redissolved in RNase-free water and quantified by UV-spectroscopy measuring A_{260} and A_{280}.

cDNA was generated by reverse transcription using the Advantage RT-for-PCR kit from BD Clontech (Franklin Lakes, NJ, USA). For this, 1 µg of total RNA was diluted to 12.5 µl in RNase-free water and, together with 1 µl of the oligo(dT)$_{18}$ primer (20 pmol/µl), heated for 2 minutes at 70 °C. After rapid cooling on ice the following components were added to the mixture: 4 µl of 5 x reaction buffer (250 mM Tris-HCl pH 8.3, 375 mM KCl, 15 mM MgCl$_2$), 1 µl of dNTP mix (10 mM), 0.5 µl of RNase inhibitor and 1 µl of MMLV reverse transcriptase. The reaction was incubated for 1 hour at 42 °C, then heated for 5 minutes at 94 °C to stop the reaction and to destroy DNase activity and diluted with RNase-free water to 100 µl total volume.

5.3.5 PCR and cloning of PCR products

Oligonucleotides for PCR reactions were obtained from Metabion (Martinsried, Germany), or Qiagen (Hilden, Germany) and dissolved to 100 µM stocks in TE buffer.

For all PCR reactions a GeneAmp PCR System 2400 thermocycler (Perkin-Elmer, Waltham, MA, USA) was used. Reactions were carried out in a total volume of 50 µl and contained 1 x polymerase reaction buffer, 1.25 µM forward and reverse primers, 0.25 mM dNTPs, and 1 µl (2.5 U) *Pfu* turbo polymerase (Stratagene, La Jolla, CA, USA) or 1 µl (1 U) KOD hot start polymerase (Novagen, Madison, WI,

USA). As a template, either 10 ng plasmid DNA or 5 µl marathon-ready cDNA library (Clontech, Palo Alto, CA, USA) or HeLa cDNA library (see 5.3.4) was used. Typically, 25 cycles of denaturation at 94 °C for 15 seconds, annealing at 55 °C for 30 seconds, and extension at 68 °C for 2 minutes per kb to be amplified, were used with an initial denaturation step of 2 minutes and a final extension step of 2 minutes per kb. PCR products were then analysed by agarose gel electrophoresis and, if required, bands were excised, gel extracted, and used for cloning. In the case of PCR cloning from cDNA libraries, a nested approach was generally used. A first round of PCR was performed as described above. The PCR product was then directly purified using a PCR nucleotide removal kit (Qiagen) according to the manufacturers instructions. 5 µl of the purified PCR product was then used in a second round of PCR using a set of primers designed internally to the primers used in the first round. This PCR product was then purified by agarose gel electrophoresis and used for cloning.

Following gel extraction of PCR products, cloning was performed into the pCRIITOPO vector using the TA-TOPO cloning system (Invitrogen). Adenosine overhangs were added to the 3' ends of the PCR product by incubation of the product with 1 µl *Taq* polymerase (Promega) at 72 °C for 30 minutes in the presence of polymerase buffer and 0.25 mM dNTPs in a total volume of 50 µl. 2 µl of this mix was then added to a sterile Eppendorf along with 0.5 µl TA-TOPO cloning mix and incubated for 5 minutes at room temperature. This mix was then used for transformation of TOP10 bacteria.

5.3.6 Site-directed mutagenesis

Point mutagenesis was carried out using the Quickchange method. Forward and reverse mutagenic primers were designed to be 33 bases long with the codon to be altered in the middle, with 15 unchanged bases on either side. The quickchange reaction was then set up in a total volume of 50 µl with 1 x *pfu* polymerase buffer, 1.25 µM forward and reverse primers, 0.25 µM dNTPs, 25 ng DNA template, and 1 µl (2.5 U) *pfu* turbo polymerase. The following cycling parameters were then used: 95 °C for 30 seconds followed by 18 cycles of 95 °C for 30 seconds, 53-55 °C for 30 seconds, and 68 °C for 2 minutes per kb of plasmid. After cooling to 4 °C, 1 µl of the restriction enzyme *DpnI* was added to the reaction mix for 1 hour at 37 °C to digest methylated (parental) DNA. 5 µl of the reaction mix was used to transform XL1-blue bacteria.

5.3.7 DNA sequencing

All insert DNAs generated by PCR or mutagenesis, were sequenced commercially by Medigenomix (Martinsried, Germany), or in house at the Core Facility of the Max-Planck-Institute.

5.4 Protein methods

5.4.1 SDS-PAGE and Coomassie staining

Small (8 x 6.5 x 0.075 cm) SDS polyacrylamide gels were prepared as described (Sambrook and Russel, 2001). Samples were prepared in SDS-PAGE sample buffer

and boiled for 5 minutes. Gels were run in a BioRad Mini-PROTEAN 3 gel chamber (BioRad, Munich, Germany) in SDS-PAGE running buffer at 200 V, 30 mA.

Protein gels were Coomassie stained by immersion in 0.01 % Coomassie Brilliant Blue R-250 in 50 % methanol, 10 % acetic acid for 20 minutes, with shaking. Gels were then destained in 20 % isopropanol, 20 % acetic acid.

5.4.2 Tryptic digest for mass-spectrometry

Sample preparation and analysis was carried out according to a protocol adapted from (Shevchenko et al., 1996). Coomassie stained bands from protein gels were excised with a clean scalpel, transferred to a Eppendorf Biopure tube and cut into 1 mm cubes. The gel pieces were washed with 100 µl 50 mM NH_4HCO_3 for 10 minutes at 22 °C, then shrunk in 100 µl acetonitrile for 10 minutes at 22 °C, all steps with shaking at 1000 rpm in an Eppendorf Thermomixer. This was repeated twice. Gel pieces were then dried in a vacuum centrifuge for 5 minutes at 35 °C. 10-15 µl of 10 mM DTT in 50 mM NH_4HCO_3 was added to the dried gel pieces and the mixture was incubated at 56 °C for 45 minutes. The gel pieces were returned to room temperature and overlaid with 10-15 µl 55 mM iodoacetamide in 50 mM NH_4HCO_3. The reaction was left for 30 minutes at room temperature in the dark. The supernatant was removed and replaced with 100 µl 50 mM NH_4HCO_3 and washed as above. The gel pieces were dried again for 5 minutes. 10-15 µl trypsin solution (12.5 ng/µl trypsin in 50 mM NH_4HCO_3; Sequencing-grade modified trypsin, Promega) was added to the dried gel cubes and left on ice for 30 minutes. Additional 50 mM NH_4HCO_3 (5-15 µl) was added to the mixture and the digest reaction was performed for 16 hours at 37°C.

After that 2 µl 10% TFA were added to the digest. 1 µl of acidified sample was spotted onto the sample matrix (1-Cyano-4-hydroxycinnamic acid, Bruker Daltonik GmbH, Germany). The spot was washed once with 0.2% TFA. Mass spectrometry of the samples was performed by Dr. Roman Körner (MPI of Biochemistry, Department of Cell Biology, Martinsried, Germany) on a ReflexIII instrument (Bruker) MALDI TOF mass spectrometer, equipped with a Scout 384 Ion source. The spectra were processed with Xmass 5.1.1 software (Bruker). Proteins were identified using the database programs MASCOT (http://www.matrixscience.com) and ProFound (http://129.85.19.192/profound_bin/ WebProFound.exe).

5.4.3 Western blotting

Proteins run on SDS-gels were transferred to 45 µm Hybond-C Extra Nitrocellulose (Amersham-Pharmacia, UK) by semi-dry blotting in transfer buffer (1x SDS-PAGE running buffer plus 10 % methanol) using a Trans-Blot SD Transfer Cell (BioRad, Germany) at 15 V, 300 mA, for 45 minutes. Blots were then blocked in milk solution (4 % milk powder in PBS, plus 0.1 % Tween-20) for 1 hour before addition of the primary antibody.

Blots were usually incubated with the primary antibody in milk solution for 1 hour at room temperature before being washed 3 x 10 minutes in milk solution. Secondary antibodies linked to horseradish peroxidase were then also incubated with the blot for 1 hour before the blots were washed for a further 3 x 10 minutes in milk. Bound antibodies were then detected by chemiluminescence using ECL Western blot detection reagents (Amersham) according to the manufacturers

instructions, exposed to Kodak X-Omat XAR-5 film for an appropriate length of time and developed in a Kodak X-OMAT 2000 Processor.

5.4.4 Determination of protein concentration

Protein concentrations were determined using the BioRad Protein Assay kit, a modified version of the Bradford Assay. The dye reagent was diluted 1:5 in water and 1 ml 1x reagent was used per assay point. Different concentrations of bovine serum albumin (BSA) were used to construct a standard curve by addition to 1 ml aliquots of the dye reagent, mixing, and transfer to disposable cuvettes for measurement of the OD_{595} in an Ultrospec 3000 Pro spectrophotometer (Amersham-Pharmacia). Protein samples were measured in the same way and their concentration was calculated using the BSA standard curve.

5.4.5 Protein precipitation with TCA

When necessary proteins were precipitated using trichloroacetic acid (TCA) for loading on SDS-PAGE gels. Typically, protein samples were adjusted to 1 ml with water. Sodium deoxycholate was then added to a final concentration of 0.02 % and the sample vortexed. Next TCA was added to a final concentration of 12 %, the sample vortexed, and left on ice for 45 minutes. Precipitated proteins were then recovered by centrifugation at 20000 x g for 20 minutes at 4 °C. The supernatant was discarded and the pellet washed two times with ice-cold acetone before being centrifuged for a further 10 minutes. The supernatant was discarded and the pellet resuspended in an appropriate amount of 1.5x SDS-PAGE sample buffer with a small amount of 1 M Tris-HCl pH 8.0 added, as necessary, to adjust the pH of the sample.

5.4.6 GST-Rab binding and pulldown assays

For big scale pulldown assays from cell extract 500 μg GST-tagged Rab was bound to 50 μl glutathione sepharose 4B (Amersham) in a total volume of 1 ml in buffer NE100 (20 mM HEPES-NaOH pH 7.5, 100 mM NaCl, 10 mM EDTA, 0.1 % TX100) on a roller for 60 minutes at 4 °C. The beads were pelleted by centrifugation at 600 g for 1 minute at 4 °C and washed three times with 1 ml buffer NE100 to remove bound nucleotide from the Rab. For the incubation with extract the loaded beads were resuspended in buffer NL100 (20 mM HEPES-NaOH pH 7.5, 100 mM NaCl, 5 mM $MgCl_2$, 0.1 % TX100) and transferred to a 15 ml tube.

In a total volume of 6 ml NL100 the beads were incubated for 60 minutes on a roller at 4 °C with 40 mg protein from RIPA lysed HeLa L cells or from rat liver cytosol. (Rat liver cytosol was prepared (Hino et al., 1978; Leelavathi, 1970) and provided by Ben Short.) To load the Rab with nucleotide GTP (for Rab6wt and Rab6^{Q72L}) or GDP (for Rab6^{T27N}) (both 100 mM frozen stock in NL100) was added to a final concentration of 5 mM. The beads were pelleted by centrifugation and washed three times with 1 ml NL100. Bound proteins were eluted in 500 μl buffer NE200 (20 mM HEPES-NaOH pH 7.5, 200 mM NaCl, 20 mM EDTA, 0.1 % TX100), rotating at 4 °C for 5 minutes. Eluted proteins were TCA precipitated (see 5.4.5) before being loaded on a SDS-gel.

For small scale binding assays the same procedure was followed, except that only 4 μg GST-Rab was bound to 15 μl glutathione sepharose 4B (Amersham) and 10 μg

His-tagged protein was added to a total volume of 400 μl buffer NL100. Bound protein was eluted directly in 1.5x SDS sample buffer and analysed on a 7.5 % SDS-gel.

5.4.7   Antibody generation and purification

A polyclonal α-PIST antibody was generated by immunisation of two rabbits with 6xHis-tagged recombinant full-length PIST in collaboration with Charles River Laboratories, L'Arbresle Cedex, France. Rabbits were immunised initially subcutaneously with 250 μg antigen mixed with Freund's complete adjuvant followed by four intramuscular boosts with 250 μg antigen mixed with Freund's incomplete adjuvant. All test bleed and the final bleed out samples were tested on Western Blot for their ability to recognise recombinant antigen and endogenous PIST in cell extracts. PIST specific antibodies were purified from the bleed out of one rabbit via affinity chromatography.

In order to exclude antibodies against the 6xHis-tag of the original antigen, MBP-tagged PIST full-length was coupled to Affigel-15 (BioRad). 4 ml of Affigel-15 beads were washed once with water to remove the isopropanol storage solution and added to 4 ml protein solution of 1 mg/ml recombinant PIST in PBS. After 2 hours of incubation with rolling at 4 °C, the gel was pelleted for 2 minutes at 1000 x g and washed three times with 15 ml PBS, once with 15 ml of 0.2 M glycine pH 2.8 and again three times with 15 ml PBS. This removed any uncoupled protein and mimicked the conditions used to elute the antibody. For purification of the antibody 15 ml serum was filtered to remove debris and was incubated with 1 ml of the affinity matrix (coupled to approx. 1 mg antigen) rolling for 90 minutes at 4 °C. After three washes with 15 ml PBS, bound antibodies were eluted using 0.2 M glycine pH 2.8 and collecting 1 ml fractions into Eppendorf tubes containing 200 ml 1M Tris-HCl pH 8.0. Samples were immediately mixed to neutralise and stored on ice. After SDS-PAGE analysis antibody peak fractions were pooled, dialysed overnight against PBS, aliquoted and stored at – 80 °C or kept at 4 °C for immediate use.

5.5   Yeast methods

5.5.1   Strains, media and growth

The *S.cerevisiae* strain PJ69-4A (James et al., 1996) was used for all two-hybrid experiments, the genotype of which is:
*MAT*a, *trp1-901, leu2-3, 112, ura3-52, his3-200, gal4Δ, gal80Δ, LYS2::GAL1$_{UAS}$-GAL1$_{TATA}$-HIS3, GAL2$_{UAS}$-GAL2$_{TATA}$-ADE2, MEL1 met2::GAL7-lacZ*
Yeast were grown in either YPDA or SC dropout media selecting for appropriate plasmids at 30 °C. Short-term storage was on agar plates at 4 °C.

YPDA medium consisted of 20 g/l peptone (Difco/Becton-Dickinson), 10 g/l yeast extract (Difco), and 20 g/l glucose (plus 20 g/l Bacto-agar for YPDA-agar). The medium was then sterilised in an autoclave and, after cooling to approximately 55 °C, 6 ml 0.2 % sterile filtered adenine hemisulphate was added.

Synthetic complete (SC) dropout medium was prepared as follows: Amino acid base (-His/-Trp/-Leu/-Ura) was prepared by mixing 20 g alanine, arginine, asparagine, aspartic acid, cysteine, glutamine, glutamic acid, glycine, inositol, isoleucine, lysine, methionine, phenylalanine, proline, serine, threonine, tyrosine,

and valine with 5 g adenine and 2 g para-aminobenzoic acid. To prepare dropout mixes, 36.7 g of amino acid base was mixed with either 2 g histidine, 4 g leucine, 2 g tryptophan, or 2 g uracil, as appropriate to form the correct dropout mix. SC dropout medium consisted of 6.7 g/l nitrogen base (without amino acids, Difco), 2 g/l appropriate dropout mix, 20 g/l glucose and pH adjusted to 7.5 (Hepes-NaOH) (plus 20 g/l Bacto-agar for SC dropout agar). After autoclaving and cooling to approximately 55 °C, 6 ml 0.2 % sterile filtered adenine hemisulphate was added, unless dropout medium was also to be without adenine.

5.5.2 Yeast transformation (frozen cell method)

To prepare frozen competent yeast cells, several colonies were picked from a freshly grown plate and grown overnight in YPDA at 30 °C with shaking. The following morning, the overnight culture was diluted to an OD_{600} of 0.15 in fresh medium and grown at 30 °C to an OD_{600} of 0.5 – 0.6 (1.2 – 1.5 x 10^7 cells). The cells were then harvested at 3000 rpm for 2 minutes at room temperature in a Heraeus centrifuge. The cells were then washed in one half culture volume sterile water and spun as before. The cells were then resuspended in $1/8^{th}$ culture volume of LiSorb (100 mM LiOAc, 10 mM Tris-HCl pH 8.0, 1 mM EDTA pH 8.0, 1 M sorbitol (molecular biology quality) filter sterilized). The resuspended pellet was incubated for 5 minutes at room temperature before being spun as before. The cell pellet was again resuspended in LiSorb (600 μl per 100 ml original culture). Single stranded carrier DNA was added (10 μl per 100 μl yeast of 10 mg/ml salmon sperm DNA (Gibco), heat-treated at 95 °C for 5 minutes). Cells were then aliquoted and frozen directly in a – 80 °C freezer where they were stored until use.

To transform frozen competent yeast cells, the cells were thawed at room temperature. 25 μl cells were used per transformation. 0.5 μl plasmid DNA (approx. 100 ng) was added to the cells, followed by 150 μl LiPEG (100 mM LiOAc, 10 mM Tris-HCl pH 8.0, 1 mM EDTA pH 8.0, 40 % PEG3350, filter sterilized). The cells were then vortexed and incubated for 20 minutes at room temperature. 17.5 μl DMSO was added and the cells were heat-shocked for 15 minutes in a 42 °C waterbath. The cells were then pelleted at 400 g in a microfuge, the supernatant removed, and the cells resuspended in 500 μl sterile water. 100 μl were the plated onto appropriate selective plates and grown at 30 °C.

In the case of directed yeast two-hybrid experiments, transformed cells were originally grown on SC-Leu/-Trp plates to select for both the bait and prey plasmids. After 2 –3 days growth, colonies were picked and restreaked onto SC-Leu/-Trp and SC-Leu/-Trp/-His/-Ade plates to assess the two-hybrid interaction.

5.5.3 Plasmid DNA minipreps from yeast cells

To prepare plasmid DNA from yeast cells, a matchhead-sized ball of cells scraped from a fresh plate into 1 ml water, was pelleted at 400 g in a microfuge. The cell pellet was resuspended in 500 μl buffer S (10 mM K_2HPO_4 pH 7.2, 10 mM EDTA, 50 mM β-mercaptoethanol (i.e. 100 μl per 25 ml added immediately prior to use), and 50 μg/ml zymolyase). The cells were then incubated at 37 °C for at least 1 hour. After that 100 μl lysis buffer (25 mM Tris-HCl pH 7.5, 25 mM EDTA, 2.5 % (w/v) SDS) was added, vortexed, and the lysate incubated at 65 °C for 30 minutes or longer until the mixture cleared. 166 μl 3 M KOAc pH 5.5 was then added to stop

the lysis reaction, tubes were inverted to mix, and incubated on ice for 10 minutes. They were then centrifuged at 20000 x g in a microfuge at 4 °C for 15 minutes and the supernatant was transferred to a clean Eppendorf tube. 800 μl cold ethanol was added, tubes were inverted to mix, and incubated on ice for 10 minutes before centrifugation as before for a further 10 minutes. The supernatant was removed and the pellet washed in 1 ml 70% ethanol. The pellet was allowed to air dry before resuspension in 40 μl sterile water.

5.6 Mammalian cell methods

5.6.1 Cell culture

HeLa L cells were cultured at 37 °C and 5 % CO_2 atmosphere in Dulbeccos Modified Eagle Medium (DMEM) containing 10 % fetal calf serum, 100 U/ml penicillin and 100 μg/ml streptomycin (GIBCO, Invitrogen)

5.6.2 Immunofluorescence

For immunofluorescence, cells were normally cultured on ethanol-flamed 15 mm coverslips in 6-well plates. For paraformaldehyde fixation, 3 % paraformaldehyde was prepared by dissolving 3 g paraformaldehyde in 100 ml PBS at 80 °C in a fume hood. 10 μl 1 M $CaCl_2$ and 10 μl 1 M $MgCl_2$ were added while stirring before the solution was allowed to cool to room temperature and pH adjusted to 7.4. The solution was then vacuum-filtered through a 0.45 μm filter and 15 ml aliquots were stored at – 20 °C. Coverslips were washed twice in 2 ml PBS and then fixed in 3% paraformaldehyde for 20 minutes. Coverslips were then washed once in 2 ml quench solution (50 mM NH_4Cl in PBS made freshly prior to use) before incubation in a further 2 ml quench solution for 10 minutes. The coverslips were then washed in 3 x 2ml PBS. If the cells were to be permeabilised, the coverslips were incubated for 5 minutes in permeabilisation solution (0.2% TX100 in PBS) before washing in 3 x 2ml PBS.

For antibody labeling, primary antibodies were diluted appropriately in PBS. A strip of parafilm was placed on a flat surface and 50 μl drops of the antibody solution were placed on the strip. Coverslips with fixed cells were then transferred, cell face down, onto the antibody drops. The coverslips were then covered with a moist, dark chamber and left for 1 hour at room temperature. After this incubation they were washed in 3 x 2ml PBS. The same procedure was then followed for incubation with secondary antibodies conjugated to appropriate fluorophores. After washing in PBS for the final time, coverslips were mounted onto clean microscope slides by placing them, cell face down, onto a 10 μl drop of Moviol mounting medium (Prepared as follows: 2.4 g Moviol 4-88 added to 6 g analytical grade glycerol while stirring. 6 ml of ddH_2O then added and the solution was left for 2 hours at room temperature. 12 ml of 0.2 M Tris-HCl pH 8.5 was then added while stirring and the solution was mixed for 10 minutes at 50 °C. The Moviol solution was then clarified by centrifugation at 3000 x g for 15 minutes and stored at – 20 °C aliquoted into glass vials.). The mounting medium used usually contained 1 μg/ml DAPI stain. The coverslips were then left overnight at room temperature to allow the Moviol to dry.

Images were collected using an Axioskop-2 with a 63x Plan Apochromat oil immersion objective of NA 1.4, standard filter sets (Carl Zeiss, Göttingen, Germany),

a 1300 by 1030 pixel cooled-CCD camera (model #CCD-1300-Y, Princeton Instruments, Trenton, NY) and Metavue software (Visitron Systems, Puchheim, Germany). Images were cropped in Adobe Photoshop 7.0 then sized and placed using Adobe Illustrator 10.0 (Adobe Systems, San Jose, CA).

5.6.3 Cell extracts and immunoprecipitation

In order to detach cells from the cell culture dishes, HeLa or Hek293T cells were treated with PBS containing 1 mM EDTA for 10 minutes at 37 °C, then gently pipetted off from the cell culture dishes into clean plastic vials and centrifuged for 5 minutes at 400 g. Total cell extracts were prepared from cell pellets by addition of ice-cold lysis buffer (e.g. RIPA or TNTE, see 5.1.3) containing 1 tablet of complete mini protease inhibitor (Roche, Mannheim, Germany) per 10 ml solution and pipetting up and down several times. After 20 minutes incubation on ice the lysate was centrifuged at 20000 g at 4 °C. The supernatant was transferred to a clean Eppendorf and the protein concentration of the extract was determined as described in 5.4.4.

For immunoprecipitation (IP) cell extracts were incubated with antibodies in an appropriate volume of lysis buffer. Small scale IPs for detection of proteins on Western blot were usually performed with cell extracts from one 10 cm dish and 1 µg purified antibody in a total volume of 1 ml. After 1 hour incubation on a roller at 4 °C the antibody-antigen complex was precipitated by adding 15 µl of either proteinA- (for rabbit polyclonal or mouse monoclonal antibodies) or proteinG-sepharose (for sheep polyclonal antibodies) (both Amersham) and incubating for another 30 minutes while rolling at 4 °C. Then, the complex on beads was centrifuged at 400 g at 4 °C, washed three times with 1 ml lysis buffer and eluted with 1.5x SDS sample buffer.

For big scale IPs, that means for detection of interacting proteins on CBB stained SDS-PAGE gels, cell extract of 20 x 15 cm dishes and 5 µg antibody was used in a total volume of 15 ml. In order to avoid a massive band of the antibody heavy chain (55 kDa) on the CBB stained gel the antibody was cross-linked to proteinA- or proteinG-sepharose using the bifunctional coupling reagent dimethyl pimelidate (DMP) before being used for IP reactions. The protocol followed is described in detail in (Harlow and Lane, 1998). In short, the antibody-sepharose complex was washed in 10 volumes of 0.2 M sodium borate pH 9.0 and centrifuged at 3000 g for 5 minutes. The antibody beads were resuspended in 10 volumes of 0.2 M sodium borate pH 9.0 and solid DMP was added to a final concentration of 20 mM. The slurry was incubated for 30 minutes at room temperature with gentle mixing, then the reaction was stopped by washing the beads once in 0.2 M ethanolamine pH 8.0, following incubation for 2 hours at room temperature in 0.2 M ethanolamine pH 8.0 with gentle mixing. After that beads were washed in PBS once, resuspended in PBS and used immediately or stored at 4 °C for further usage.

5.6.4 Transient transfection of mammalian cells

HeLa cells were transiently transfected with DNA constructs using the lipid-based transfection reagent FuGENE6 (Roche). The cells were seeded 24 hours before transfection to give 70% confluency at the start of transfection (approx. 70.000 to 100.000 cells seeded per well of a 6-well plate). Usually, per single well of a 6-well plate 1 µg plasmid DNA was used in complex with 3 µl FuGene6 diluted in 100 µl

OptiMEM medium (Invitrogen). After gentle mixing and complex formation for 25 minutes at room temperature the mixture was added drop-wise to the cells which were then incubated at 37 °C, 5 % CO_2 in 2 ml DMEM until being processed for IP, Western blotting or immunofluorescence.

5.6.5 RNA interference

In order to selectively knockdown the expression levels of particular proteins, small interfering RNA duplexes (siRNAs) were transfected into cultured Hela cells. The protocol used was essentially that of (Elbashir et al., 2001). 21 nucleotide siRNA duplexes with a 2 nucleotide 3' overhang were designed and produced by Dharmacon Inc (see 5.1.5). The lyophilised and already annealed siRNA duplexes were diluted to a stock solution of 100 μM and stored at – 80 °C.

Hela cells were seeded 24 hours before transfection with the siRNA duplex (approx. 20.000 to 30.000 cells seeded per well of a 6-well plate for a 72 hours siRNA time course). For transfection, the lipid-based transfection reagent Oligofectamine (Invitrogen) was used. For the transfection of a single well of a 6-well plate, the following amounts were used: 3 μl Oligofectamine and 3 μl of 20 μM siRNA duplex were added to 200 μl OptiMEM medium (Invitrogen) in a clean, RNAse-free Eppendorf tube. The mixture was mixed gently and left for 25 minutes at room temperature. The entire mixture was then added drop-wise to the cells which were then incubated at 37 °C, 5 % CO_2 in 2 ml DMEM until being processed for Western blotting or immunofluorescence.

5.7 Functional assays

5.7.1 STxB purification and endocytosis

Shiga toxin B-subunit (in vector pTrc99A, gift from Dr. Misumi, Fukuoka University School of Medicine, Fukuoka, Japan) was purified from periplasm of *E. coli* BL21. A single colony was picked from a fresh plate of transformed *E. coli*, used to inoculate 25 ml of LB plus ampicillin and grown overnight at 30 °C with shaking. 1 ml of the overnight culture was then used to inoculate 1 l of fresh LB plus ampicillin, and grown at 30 °C until an OD_{600} of 0.5 – 0.6 was reached, before being induced with 0.5 mM Isopropyl β-D-thiogalactoside (IPTG) from a 1 M stock for 14 hours. Bacteria were then harvested by centrifugation at 3000 x g for 15 minutes at 4 °C, washed once with ice-cold PBS and the cell pellet was resuspended in 20 ml ice cold 20 mM Tris-HCl pH 7,5, 150 mM NaCl. Polymixin B was added to a final concentration of 0.1 mg/ml and the suspension was incubated for 30 min on the roller at 4 °C. After sonication (2 x 10 s at 70 % intensity), the periplasm lysate was cleared by centrifugation at 13000 x g for 15 minutes at 4 °C. The supernatant was cleared again by centrifugation at 90000 x g for 35 minutes at 4 °C, then diluted to roughly 50 mM NaCl with 20 mM Tris-HCl pH 7,5 and loaded onto a 5 ml HiTrapQ anion exchange column (Amersham-Pharmacia). After washes with 20 ml 20 mM Tris-HCl pH 7,5, protein was eluted with 50 ml of a linear gradient from 0 mM to 600 mM NaCl in 20 mM Tris-HCl pH 7,5 with a flow rate of 2 ml/min. 2.5 ml fractions were collected and analysed by SDS-PAGE. Fractions of interest were pooled

(which gave 15 ml of approx. 1 mg/ml protein) and concentrated in a centricon spin concentrator 10K (Millipore, Billerica, MA, USA) at 4 °C at 3000 x g to reach more or less 5 mg/ml total protein concentration. Then, 500 μl (approx. 2.5 mg) of this solution were loaded on a Superose 12 column (Amersham-Pharmacia) for gel filtraton in PBS with a flow rate of 0.15 ml/min. 1 ml fractions were collected and analysed by SDS-PAGE.

To label purified Shiga Toxin B-subunit on amine residues with an N-hydroxysuccinimidyl ester of Cy3 dye one STxB peak fraction of approx. 1.1 mg/ml protein was added to one vial of Cy3 Mono-Reactive Dye Pack (GE Healthcare, Munich, Germany), mixed by gentle shaking and left at room temperature for 5 minutes. The labelling reaction was stopped by addition of 100 μl 1M Tris-HCl pH 8.0 and everything passed through a PD10 desalting column (Amersham-Pharmacia) in order to separate the labelled protein from excess, unconjugated dye. 500 μl fractions in PBS were collected and the absorption at 280 nm and 552 nm wavelength was measured in a spectrophotometer for each fraction. The two fractions with highest protein concentration (fraction 8 and 9) were pooled and molar concentrations of dye and protein were calculated using the molar extincition coefficient of 150000 $M^{-1}cm^{-1}$ at 552 nm for the Cy3 dye and 170000 $M^{-1}cm^{-1}$ at 280 nm for the pentameric Shiga toxin B-subunit. The calculation was corrected for the absorbance of the dye at 280 nm, which is approximately 8 % of the absorbance at 552 nm. Finally, this lead to a stoichiometry of 5 Cy3 dye molecules per pentamer of STxB and a protein concentration of 0.7 mg/ml in 1 ml solution.

For uptake assays, HeLa cells plated on glass coverslips at a density of 70000 cells/ well of a 6-well plate and, as indicated in the figures transfected for 24 hours with DNA plasmids, were washed three-times in ice cold PBS, and placed on 40 μl drops of uptake medium (DME, 2% (w/v) bovine serum albumin, 20 mM HEPES-NaOH pH 7.5) and 0.7 μg/ml Cy3-STxB on an ice cold metal plate covered in Parafilm (Pechiney Plastic Packaging, Menasha, WI). After 30 minutes incubation the coverslips were washed three-times in ice cold PBS to remove excess ligand. One coverslip was fixed to give the total bound ligand, while the remaining coverslips were transferred to a 6-well plate containing pre-warmed growth medium and incubated at 37 °C and 5 % CO_2. At the time points indicated in the figures coverslips were fixed and processed for immune fluorescence microscopy (see 5.6.2).

5.7.2 Shiga-like toxin 1 cytotoxicity assay

Cytotoxicity was defined as a decrease in the ability of cells to incorporate [^{35}S]-methionine into acid-precipitable material after Shiga-like toxin 1 treatment using an established method (Spooner et al., 2004). HeLa cells were plated at a density of 150.000 cells/well in a 6-well plate and, the next day, transiently transfected with either wild-type or RA-mutant RabGAPs for 10 hours using FuGene6 like described in 5.6.4. Then, the cells were detached from the dish using PBS containing 1 mM EDTA, re-plated in 96-well plates at a density of 15.000 cells/well and left for another 14 hours. After washing with PBS, cells were incubated for 1 hour with 100 μl DMEM/FCS containing serial 2-fold dilutions from 50 ng/ml to 0.05 ng/ml of Shiga-like toxin 1. Subsequently, cells were washed with PBS and incubated in PBS containing 50 μCi/ml [^{35}S]-methionine for 30 minutes. Labelled proteins were precipitated with three washes in 5 % (w/v) trichloroacetic acid, the wells were

washed twice with PBS, then 50 μl of scintillation fluid were added, and the amount of radiolabel incorporated was determined in a Wallac MicroBeta Trilux counter (Perkin-Elmer). For each condition, the concentration giving 50 % inhibition (IC_{50}) for Shiga-like toxin 1 was calculated from the toxin titration.

5.7.3 EGF uptake assay

EGF coupled to Alexa Fluor 488 or Alex Fluor 555 (40x stock, 200 µg/ml) (Molecular Probes, Invitrogen) were stored as stock solutions in PBS at – 20 °C. For uptake assays, HeLa cells plated on glass coverslips at a density of 70.000 cells/ well of a 6-well plate were washed three times with serum-free growth medium 36 hours after plating, and then incubated in serum free growth medium for 12 to 14 hours at 37 °C and 5 % CO_2. Coverslips were then washed three-times in ice cold PBS, and placed on 40 µl drops of uptake medium (DME, 2% (w/v) bovine serum albumin, 20 mM HEPES-NaOH pH 7.5) and 5 µg/ml EGF on an ice cold metal plate covered in Parafilm (Pechiney Plastic Packaging, Menasha, WI). After 30 minutes incubation the coverslips were washed three-times in ice cold PBS to remove excess ligand. One coverslip was fixed to give the total bound ligand, while the remaining coverslips were transferred to a 6-well plate containing pre-warmed growth medium and incubated at 37 °C and 5 % CO_2. At the time points indicated in the figures coverslips were fixed and processed for immune fluorescence microscopy (see 5.6.2).

For combined EGF and STxB assays, both ligands were mixed and bound simultaneously to the cell surface, and then the standard procedure was followed.

5.7.4 GTP-hydrolysis assay

To measure GTP-hydrolysis of a Rab together with a certain GAP Rab proteins were loaded with [γ-^{32}P]GTP and incubated with the GAP. GTP hydrolysis was measured counting free inorganic phosphate [γ-^{32}P] in the supernatant of GAP and control reactions after charcoal extraction.

Before, GTP-binding was measured using a nitrocellulose filter-binding assay (Du and Novick, 2001). To monitor Rab GTP loading 10 µl of 10x assay buffer (500 mM Hepes-NaOH pH 6.8, 10 mg/ml BSA, 10 mM DTT), 73 µl ddH$_2$O, 5 µl 10 mM EDTA pH 8.0, 5 µl 1 mM GTP, 2 µl of [γ-^{32}P]GTP (Amersham, PB10244, 10 mCi/ml; 5000 Ci/mmol) and 100 pmoles Rab protein, diluted with 1x assay buffer to 5 µl, were mixed on ice and then incubated in a 30 °C water bath. Every 5 minutes, a 20 µl aliquot of the loading mixture was taken and pipetted immediately onto a nitrocellulose filter sitting on top of a vacuum flask. The filter was washed twice with assay buffer (without BSA) and then dried on Whatman paper, before being transferred to a scintillation vial containing 4 ml of Ultima Gold scintillation liquid (Perkin-Elmer) and scintillation counted.

For the GTP-hydrolysis reaction together with the GAP, Rab proteins were loaded with GTP in the same reaction mix (10 µl of 10x assay buffer, 73 µl ddH$_2$O, 5 µl 10 mM EDTA pH 8.0, 5 µl 1 mM GTP, 2 µl of [γ-^{32}P]GTP (Amersham, PB10244, 10 mCi/ml; 5000 Ci/mmol) and 100 pmoles Rab protein, diluted with 1x assay buffer to 5 µl). After 15 minutes incubation at 30 °C in a waterbath the reaction mix with the loaded Rab was split into two and kept on ice. A 2.5 µl aliquot of the assay mix was scintillation counted to measure the specific activity in cpm/pmole GTP. GAP

reactions were started by the addition of 0.5 pmoles of the RabGAP to one vial (+ GAP) and assay buffer to the other vial (- GAP). Reactions were then incubated at 30 °C for 60 minutes, then stopped on ice. 5 µl samples were taken in duplicate. These aliquots were immediately added to 795 µl of ice cold 5% (w/v) activated charcoal slurry in 50 mM NaH$_2$PO$_4$, vortexed to mix thoroughly and left on ice for 1 h. Then the samples were centrifuged for 5 minutes at 16100 g in a benchtop microfuge to pellet the charcoal. A 400 µl aliquot of the supernatant was transferred into a scintillation vial containing 4 ml of Ultima Gold scintillation liquid (Perkin-Elmer) and scintillation counted.

The amount of GTP hydrolysed in each reaction was calculated from the specific activity of the reaction mixture. First, the measured specific activity from the 2.5 µl aliquot (cpm/ 2,5 µl) was multiplied by 40 to get the specific activity for the full assay (100 µl). This value was then divided by the amount of total GTP in the reaction mixture (5000 pmol) to get the specific activity in cpm/pmole GTP. The double counted cpm values from the 5 µl aliquots taken from each reaction after 60 minutes incubation were averaged and then multiplied by 2 (factor for 400 µl out of 800 µl charcoal mix) and by 20 (factor for 5 µl out of 100 µl total reaction mix). To calculate how much GTP in pmole was hydrolysed, the corrected cpm activity values were divided by the specific activity per pmole GTP (cpm/pmole). For comparison in the diagram the amount of hydrolysed GTP of the minus GAP reactions were substracted from the plus GAP reactions and plotted as pmol hydrolysed GTP/ hour.

Abbreviations

CC	coiled-coil
CGN	*cis* Golgi network
EEA1	early endosomal antigen 1
EGF	epidermal growth factor
EGFR	EGF receptor
ER	endoplasmic reticulum
ERGIC	ER-to-Golgi intermediate compartment
ESCRT	endosomal sorting complex required for transport
GAP	GTPase-activating protein
Gb3	globotriasoyl ceramide
GDF	GDI displacement factor
GDI	GDP dissociation inhibitor
GDP	guanosine diphosphate
GEF	guanine nucleotide exchange factor
GPI	glycosylphosphatidylinositol
GTP	guanosine triphosphate
GTPase	guanosine triphosphatase
IC_{50}	inhibitory concentration required for 50 % inhibition
NSF	N-ethylmaleimide sensitive fusion protein
MPR	mannose 6-phosphate receptor
MVB	multivesicular body
QDO	quadrupel drop-out
siRNA	small interfering RNA
SNARE	soluble NSF attachment receptor
STxB	Shiga toxin B-subunit
TfR	transferrin receptor
TGN	*trans* Golgi network
VTC	vesicular tubular cluster
Y2H	yeast two-hybrid

References

Acharya, U., A. Mallabiabarrena, J.K. Acharya, and V. Malhotra. 1998. Signaling via mitogen-activated protein kinase kinase (MEK1) is required for Golgi fragmentation during mitosis. *Cell*. 92:183-92.

Aivazian, D., R.L. Serrano, and S. Pfeffer. 2006. TIP47 is a key effector for Rab9 localization. *J Cell Biol*. 173:917-26.

Albert, S., and D. Gallwitz. 1999. Two new members of a family of Ypt/Rab GTPase activating proteins. Promiscuity of substrate recognition. *J Biol Chem*. 274:33186-9.

Alexander, A. 1998. Endocytosis and intracellular sorting of receptor tyrosine kinases. *Front Biosci*. 3:d729-38.

Allan, B.B., B.D. Moyer, and W.E. Balch. 2000. Rab1 recruitment of p115 into a cis-SNARE complex: programming budding COPII vesicles for fusion. *Science*. 289:444-8.

Altan-Bonnet, N., R. Sougrat, W. Liu, E.L. Snapp, T. Ward, and J. Lippincott-Schwartz. 2006. Golgi inheritance in mammalian cells is mediated through endoplasmic reticulum export activities. *Mol Biol Cell*. 17:990-1005.

Amessou, M., A. Fradagrada, T. Falguieres, J.M. Lord, D.C. Smith, L.M. Roberts, C. Lamaze, and L. Johannes. 2007. Syntaxin 16 and syntaxin 5 are required for efficient retrograde transport of several exogenous and endogenous cargo proteins. *J Cell Sci*. 120:1457-68.

Appenzeller-Herzog, C., and H.P. Hauri. 2006. The ER-Golgi intermediate compartment (ERGIC): in search of its identity and function. *J Cell Sci*. 119:2173-83.

Aridor, M., and L.A. Hannan. 2000. Traffic jam: a compendium of human diseases that affect intracellular transport processes. *Traffic*. 1:836-51.

Aridor, M., and L.A. Hannan. 2002. Traffic jams II: an update of diseases of intracellular transport. *Traffic*. 3:781-90.

Axelsson, M.A., and G. Warren. 2004. Rapid, endoplasmic reticulum-independent diffusion of the mitotic Golgi haze. *Mol Biol Cell*. 15:1843-52.

Bahadoran, P., E. Aberdam, F. Mantoux, R. Busca, K. Bille, N. Yalman, G. de Saint-Basile, R. Casaroli-Marano, J.P. Ortonne, and R. Ballotti. 2001. Rab27a: A key to melanosome transport in human melanocytes. *J Cell Biol*. 152:843-50.

Bananis, E., S. Nath, K. Gordon, P. Satir, R.J. Stockert, J.W. Murray, and A.W. Wolkoff. 2004. Microtubule-dependent movement of late endocytic vesicles in vitro: requirements for Dynein and Kinesin. *Mol Biol Cell*. 15:3688-97.

Barr, F.A., and B. Short. 2003. Golgins in the structure and dynamics of the Golgi apparatus. *Curr Opin Cell Biol*. 15:405-13.

Behnia, R., and S. Munro. 2005. Organelle identity and the signposts for membrane traffic. *Nature*. 438:597-604.

Bentivoglio, M., and P. Mazzarello. 1998. One hundred years of the Golgi apparatus: history of a disputed cell organelle. *Ital J Neurol Sci*. 19:241-7.

Bergbrede, T., O. Pylypenko, A. Rak, and K. Alexandrov. 2005. Structure of the extremely slow GTPase Rab6A in the GTP bound form at 1.8A resolution. *J Struct Biol*. 152:235-8.

Bonifacino, J.S., and B.S. Glick. 2004. The mechanisms of vesicle budding and fusion. *Cell*. 116:153-66.

Burkhard, P., J. Stetefeld, and S.V. Strelkov. 2001. Coiled coils: a highly versatile protein folding motif. *Trends Cell Biol*. 11:82-8.

Carroll, K.S., J. Hanna, I. Simon, J. Krise, P. Barbero, and S.R. Pfeffer. 2001. Role of Rab9 GTPase in facilitating receptor recruitment by TIP47. *Science*. 292:1373-6.

Charest, A., K. Lane, K. McMahon, and D.E. Housman. 2001. Association of a novel PDZ domain-containing peripheral Golgi protein with the Q-SNARE (Q-soluble N-ethylmaleimide-sensitive fusion protein (NSF) attachment protein receptor) protein syntaxin 6. *J Biol Chem*. 276:29456-65.

Charest, A., K. Lane, K. McMahon, J. Park, E. Preisinger, H. Conroy, and D. Housman. 2003. Fusion of FIG to the receptor tyrosine kinase ROS in a glioblastoma with an interstitial del(6)(q21q21). *Genes Chromosomes Cancer*. 37:58-71.

Chen, A., R.J. AbuJarour, and R.K. Draper. 2003. Evidence that the transport of ricin to the cytoplasm is independent of both Rab6A and COPI. *J Cell Sci*. 116:3503-10.

Chen, Y.A., and R.H. Scheller. 2001. SNARE-mediated membrane fusion. *Nat Rev Mol Cell Biol*. 2:98-106.

Cheng, J., B.D. Moyer, M. Milewski, J. Loffing, M. Ikeda, J.E. Mickle, G.R. Cutting, M. Li, B.A. Stanton, and W.B. Guggino. 2002. A Golgi-associated PDZ domain protein modulates cystic fibrosis transmembrane regulator plasma membrane expression. *J Biol Chem*. 277:3520-9.

Cheng, J., H. Wang, and W.B. Guggino. 2004. Modulation of mature cystic fibrosis transmembrane regulator protein by the PDZ domain protein CAL. *J Biol Chem*. 279:1892-8.

Cheng, J., H. Wang, and W.B. Guggino. 2005. Regulation of cystic fibrosis transmembrane regulator trafficking and protein expression by a Rho family small GTPase TC10. *J Biol Chem*. 280:3731-9.

Choudhury, R., A. Diao, F. Zhang, E. Eisenberg, A. Saint-Pol, C. Williams, A. Konstantakopoulos, J. Lucocq, L. Johannes, C. Rabouille, L.E. Greene, and M. Lowe. 2005. Lowe syndrome protein OCRL1 interacts with clathrin and regulates protein trafficking between endosomes and the trans-Golgi network. *Mol Biol Cell*. 16:3467-79.

Corda, D., A. Colanzi, and A. Luini. 2006. The multiple activities of CtBP/BARS proteins: the Golgi view. *Trends Cell Biol*. 16:167-73.

Corthesy-Theulaz, I., A. Pauloin, and S.R. Pfeffer. 1992. Cytoplasmic dynein participates in the centrosomal localization of the Golgi complex. *J Cell Biol*. 118:1333-45.

Cuif, M.H., F. Possmayer, H. Zander, N. Bordes, F. Jollivet, A. Couedel-Courteille, I. Janoueix-Lerosey, G. Langsley, M. Bornens, and B. Goud. 1999. Characterization of GAPCenA, a GTPase activating protein for Rab6, part of which associates with the centrosome. *Embo J*. 18:1772-82.

Del Nery, E., S. Miserey-Lenkei, T. Falguieres, C. Nizak, L. Johannes, F. Perez, and B. Goud. 2006. Rab6A and Rab6A' GTPases play non-overlapping roles in membrane trafficking. *Traffic*. 7:394-407.

Delprato, A., E. Merithew, and D.G. Lambright. 2004. Structure, exchange determinants, and family-wide rab specificity of the tandem helical bundle and Vps9 domains of Rabex-5. *Cell*. 118:607-17.

Diao, A., D. Rahman, D.J. Pappin, J. Lucocq, and M. Lowe. 2003. The coiled-coil membrane protein golgin-84 is a novel rab effector required for Golgi ribbon formation. *J Cell Biol*. 160:201-12.

Dikic, I. 2003. Mechanisms controlling EGF receptor endocytosis and degradation. *Biochem Soc Trans*. 31:1178-81.

Dong, G., M. Medkova, P. Novick, and K.M. Reinisch. 2007. A catalytic coiled coil: structural insights into the activation of the Rab GTPase Sec4p by Sec2p. *Mol Cell*. 25:455-62.

Driskell, O.J., A. Mironov, V.J. Allan, and P.G. Woodman. 2007. Dynein is required for receptor sorting and the morphogenesis of early endosomes. *Nat Cell Biol*. 9:113-20.

Du, L.L., and P. Novick. 2001. Purification and properties of a GTPase-activating protein for yeast Rab GTPases. *Methods Enzymol*. 329:91-9.

Duden, R. 2003. ER-to-Golgi transport: COP I and COP II function (Review). *Mol Membr Biol*. 20:197-207.

Echard, A., F. Jollivet, O. Martinez, J.J. Lacapere, A. Rousselet, I. Janoueix-Lerosey, and B. Goud. 1998. Interaction of a Golgi-associated kinesin-like protein with Rab6. *Science*. 279:580-5.

Echard, A., F.J. Opdam, H.J. de Leeuw, F. Jollivet, P. Savelkoul, W. Hendriks, J. Voorberg, B. Goud, and J.A. Fransen. 2000. Alternative splicing of the human Rab6A gene generates two close but functionally different isoforms. *Mol Biol Cell*. 11:3819-33.

Elbashir, S.M., J. Harborth, W. Lendeckel, A. Yalcin, K. Weber, and T. Tuschl. 2001. Duplexes of 21-nucleotide RNAs mediate RNA interference in cultured mammalian cells. *Nature*. 411:494-8.

Elbashir, S.M., J. Harborth, K. Weber, and T. Tuschl. 2002. Analysis of gene function in somatic mammalian cells using small interfering RNAs. *Methods*. 26:199-213.

Farquhar, M.G., and G.E. Palade. 1981. The Golgi apparatus (complex)-(1954-1981)-from artifact to center stage. *J Cell Biol*. 91:77s-103s.

Fridmann-Sirkis, Y., S. Siniossoglou, and H.R. Pelham. 2004. TMF is a golgin that binds Rab6 and influences Golgi morphology. *BMC Cell Biol*. 5:18.

Fritzler, M.J., J.C. Hamel, R.L. Ochs, and E.K. Chan. 1993. Molecular characterization of two human autoantigens: unique cDNAs encoding 95- and 160-kD proteins of a putative family in the Golgi complex. *J Exp Med*. 178:49-62.

Ganley, I.G., K. Carroll, L. Bittova, and S. Pfeffer. 2004. Rab9 GTPase regulates late endosome size and requires effector interaction for its stability. *Mol Biol Cell*. 15:5420-30.

Ghosh, P., and S. Kornfeld. 2004. The GGA proteins: key players in protein sorting at the trans-Golgi network. *Eur J Cell Biol*. 83:257-62.

Gillingham, A.K., and S. Munro. 2003. Long coiled-coil proteins and membrane traffic. *Biochim Biophys Acta*. 1641:71-85.

Girod, A., B. Storrie, J.C. Simpson, L. Johannes, B. Goud, L.M. Roberts, J.M. Lord, T. Nilsson, and R. Pepperkok. 1999. Evidence for a COP-I-independent

transport route from the Golgi complex to the endoplasmic reticulum. *Nat Cell Biol*. 1:423-30.

Glebov, O.O., N.A. Bright, and B.J. Nichols. 2006. Flotillin-1 defines a clathrin-independent endocytic pathway in mammalian cells. *Nat Cell Biol*. 8:46-54.

Golgi, C. 1898. *Boll. Soc. Med. Chir. Pavia*. 13:3-16.

Goud, B., A. Zahraoui, A. Tavitian, and J. Saraste. 1990. Small GTP-binding protein associated with Golgi cisternae. *Nature*. 345:553-6.

Griffith, K.J., E.K. Chan, C.C. Lung, J.C. Hamel, X. Guo, K. Miyachi, and M.J. Fritzler. 1997. Molecular cloning of a novel 97-kd Golgi complex autoantigen associated with Sjogren's syndrome. *Arthritis Rheum*. 40:1693-702.

Grosshans, B.L., D. Ortiz, and P. Novick. 2006. Rabs and their effectors: achieving specificity in membrane traffic. *Proc Natl Acad Sci U S A*. 103:11821-7.

Haas, A.K., E. Fuchs, R. Kopajtich, and F.A. Barr. 2005. A GTPase-activating protein controls Rab5 function in endocytic trafficking. *Nat Cell Biol*. 7:887-93.

Habermann, A., T.A. Schroer, G. Griffiths, and J.K. Burkhardt. 2001. Immunolocalization of cytoplasmic dynein and dynactin subunits in cultured macrophages: enrichment on early endocytic organelles. *J Cell Sci*. 114:229-240.

Harlow, E., and D. Lane. 1998. Using Antibodies: A Laboratory Manual. *Cold Spring Harbor Laboratory Press*.

Harris, B.Z., and W.A. Lim. 2001. Mechanism and role of PDZ domains in signaling complex assembly. *J Cell Sci*. 114:3219-31.

Hassel, B., M. Schreff, E.M. Stube, U. Blaich, and S. Schumacher. 2003. CALEB/NGC interacts with the Golgi-associated protein PIST. *J Biol Chem*. 278:40136-43.

Hicks, S.W., and C.E. Machamer. 2002. The NH2-terminal domain of Golgin-160 contains both Golgi and nuclear targeting information. *J Biol Chem*. 277:35833-9.

Hicks, S.W., and C.E. Machamer. 2005. Isoform-specific interaction of golgin-160 with the Golgi-associated protein PIST. *J Biol Chem*. 280:28944-51.

Hino, Y., A. Asano, R. Sato, and S. Shimizu. 1978. Biochemical studies of rat liver Golgi apparatus. I. Isolation and preliminary characterization. *J Biochem (Tokyo)*. 83:909-23.

Hoogenraad, C.C., A. Akhmanova, S.A. Howell, B.R. Dortland, C.I. De Zeeuw, R. Willemsen, P. Visser, F. Grosveld, and N. Galjart. 2001. Mammalian Golgi-associated Bicaudal-D2 functions in the dynein-dynactin pathway by interacting with these complexes. *Embo J*. 20:4041-54.

Hume, A.N., L.M. Collinson, A. Rapak, A.Q. Gomes, C.R. Hopkins, and M.C. Seabra. 2001. Rab27a regulates the peripheral distribution of melanosomes in melanocytes. *J Cell Biol*. 152:795-808.

Hurley, J.H., and S.D. Emr. 2006. The ESCRT complexes: structure and mechanism of a membrane-trafficking network. *Annu Rev Biophys Biomol Struct*. 35:277-98.

Hyvola, N., A. Diao, E. McKenzie, A. Skippen, S. Cockcroft, and M. Lowe. 2006. Membrane targeting and activation of the Lowe syndrome protein OCRL1 by rab GTPases. *Embo J*. 25:3750-61.

Ito, C., F. Suzuki-Toyota, M. Maekawa, Y. Toyama, R. Yao, T. Noda, and K. Toshimori. 2004. Failure to assemble the peri-nuclear structures in GOPC

deficient spermatids as found in round-headed spermatozoa. *Arch Histol Cytol*. 67:349-60.

Ito, H., I. Iwamoto, R. Morishita, Y. Nozawa, T. Asano, and K. Nagata. 2006. Identification of a PDZ protein, PIST, as a binding partner for Rho effector Rhotekin: biochemical and cell-biological characterization of Rhotekin-PIST interaction. *Biochem J*. 397:389-98.

James, P., J. Halladay, and E.A. Craig. 1996. Genomic libraries and a host strain designed for highly efficient two-hybrid selection in yeast. *Genetics*. 144:1425-36.

Jones, S., C. Newman, F. Liu, and N. Segev. 2000. The TRAPP complex is a nucleotide exchanger for Ypt1 and Ypt31/32. *Mol Biol Cell*. 11:4403-11.

Kim, Y.G., S. Raunser, C. Munger, J. Wagner, Y.L. Song, M. Cygler, T. Walz, B.H. Oh, and M. Sacher. 2006. The architecture of the multisubunit TRAPP I complex suggests a model for vesicle tethering. *Cell*. 127:817-30.

Kim, Y.G., E.J. Sohn, J. Seo, K.J. Lee, H.S. Lee, I. Hwang, M. Whiteway, M. Sacher, and B.H. Oh. 2005. Crystal structure of bet3 reveals a novel mechanism for Golgi localization of tethering factor TRAPP. *Nat Struct Mol Biol*. 12:38-45.

Klumperman, J. 2000. Transport between ER and Golgi. *Curr Opin Cell Biol*. 12:445-9.

Kupfer, A., D. Louvard, and S.J. Singer. 1982. Polarization of the Golgi apparatus and the microtubule-organizing center in cultured fibroblasts at the edge of an experimental wound. *Proc Natl Acad Sci U S A*. 79:2603-7.

Lanzetti, L., V. Rybin, M.G. Malabarba, S. Christoforidis, G. Scita, M. Zerial, and P.P. Di Fiore. 2000. The Eps8 protein coordinates EGF receptor signalling through Rac and trafficking through Rab5. *Nature*. 408:374-7.

Lauvrak, S.U., M.L. Torgersen, and K. Sandvig. 2004. Efficient endosome-to-Golgi transport of Shiga toxin is dependent on dynamin and clathrin. *J Cell Sci*. 117:2321-31.

Leelavathi, D.E. 1970. Isolation of a Golgi-rich fraction from rat liver. *Biochimica et Biophysica Acta (BBA) - Biomembranes*. 211:124-138.

Liewen, H., I. Meinhold-Heerlein, V. Oliveira, R. Schwarzenbacher, G. Luo, A. Wadle, M. Jung, M. Pfreundschuh, and F. Stenner-Liewen. 2005. Characterization of the human GARP (Golgi associated retrograde protein) complex. *Exp Cell Res*. 306:24-34.

Lowe, M., C. Rabouille, N. Nakamura, R. Watson, M. Jackman, E. Jamsa, D. Rahman, D.J. Pappin, and G. Warren. 1998. Cdc2 kinase directly phosphorylates the cis-Golgi matrix protein GM130 and is required for Golgi fragmentation in mitosis. *Cell*. 94:783-93.

Lu, L., G. Tai, and W. Hong. 2004. Autoantigen Golgin-97, an effector of Arl1 GTPase, participates in traffic from the endosome to the trans-golgi network. *Mol Biol Cell*. 15:4426-43.

Luzio, J.P., B. Brake, G. Banting, K.E. Howell, P. Braghetta, and K.K. Stanley. 1990. Identification, sequencing and expression of an integral membrane protein of the trans-Golgi network (TGN38). *Biochem J*. 270:97-102.

Maag, R.S., M. Mancini, A. Rosen, and C.E. Machamer. 2005. Caspase-resistant Golgin-160 disrupts apoptosis induced by secretory pathway stress and ligation of death receptors. *Mol Biol Cell*. 16:3019-27.

Mallard, F., B.L. Tang, T. Galli, D. Tenza, A. Saint-Pol, X. Yue, C. Antony, W. Hong, B. Goud, and L. Johannes. 2002. Early/recycling endosomes-to-TGN transport involves two SNARE complexes and a Rab6 isoform. *J Cell Biol*. 156:653-64.

Mancini, M., C.E. Machamer, S. Roy, D.W. Nicholson, N.A. Thornberry, L.A. Casciola-Rosen, and A. Rosen. 2000. Caspase-2 is localized at the Golgi complex and cleaves golgin-160 during apoptosis. *J Cell Biol*. 149:603-12.

Martinez, O., C. Antony, G. Pehau-Arnaudet, E.G. Berger, J. Salamero, and B. Goud. 1997. GTP-bound forms of rab6 induce the redistribution of Golgi proteins into the endoplasmic reticulum. *Proc Natl Acad Sci U S A*. 94:1828-33.

Martinez, O., A. Schmidt, J. Salamero, B. Hoflack, M. Roa, and B. Goud. 1994. The small GTP-binding protein rab6 functions in intra-Golgi transport. *J Cell Biol*. 127:1575-88.

Matanis, T., A. Akhmanova, P. Wulf, E. Del Nery, T. Weide, T. Stepanova, N. Galjart, F. Grosveld, B. Goud, C.I. De Zeeuw, A. Barnekow, and C.C. Hoogenraad. 2002. Bicaudal-D regulates COPI-independent Golgi-ER transport by recruiting the dynein-dynactin motor complex. *Nat Cell Biol*. 4:986-92.

Maxfield, F.R., and T.E. McGraw. 2004. Endocytic recycling. *Nat Rev Mol Cell Biol*. 5:121-32.

Mayer, T., N. Touchot, and Z. Elazar. 1996. Transport between cis and medial Golgi cisternae requires the function of the Ras-related protein Rab6. *J Biol Chem*. 271:16097-103.

Miserey-Lenkei, S., A. Couedel-Courteille, E. Del Nery, S. Bardin, M. Piel, V. Racine, J.B. Sibarita, F. Perez, M. Bornens, and B. Goud. 2006. A role for the Rab6A' GTPase in the inactivation of the Mad2-spindle checkpoint. *Embo J*. 25:278-89.

Misumi, Y., M. Sohda, A. Yano, T. Fujiwara, and Y. Ikehara. 1997. Molecular characterization of GCP170, a 170-kDa protein associated with the cytoplasmic face of the Golgi membrane. *J Biol Chem*. 272:23851-8.

Monier, S., F. Jollivet, I. Janoueix-Lerosey, L. Johannes, and B. Goud. 2002. Characterization of novel Rab6-interacting proteins involved in endosome-to-TGN transport. *Traffic*. 3:289-97.

Mousavi, S.A., L. Malerod, T. Berg, and R. Kjeken. 2004. Clathrin-dependent endocytosis. *Biochem J*. 377:1-16.

Moyer, B.D., B.B. Allan, and W.E. Balch. 2001. Rab1 interaction with a GM130 effector complex regulates COPII vesicle cis--Golgi tethering. *Traffic*. 2:268-76.

Mukhopadhyay, D., and H. Riezman. 2007. Proteasome-independent functions of ubiquitin in endocytosis and signaling. *Science*. 315:201-5.

Munro, S. 2002. Organelle identity and the targeting of peripheral membrane proteins. *Curr Opin Cell Biol*. 14:506-14.

Murray, R.Z., F.G. Wylie, T. Khromykh, D.A. Hume, and J.L. Stow. 2005. Syntaxin 6 and Vti1b form a novel SNARE complex, which is up-regulated in activated macrophages to facilitate exocytosis of tumor necrosis Factor-alpha. *J Biol Chem*. 280:10478-83.

Nakamura, N., C. Rabouille, R. Watson, T. Nilsson, N. Hui, P. Slusarewicz, T.E. Kreis, and G. Warren. 1995. Characterization of a cis-Golgi matrix protein, GM130. *J Cell Biol*. 131:1715-26.

Neudauer, C.L., G. Joberty, and I.G. Macara. 2001. PIST: a novel PDZ/coiled-coil domain binding partner for the rho-family GTPase TC10. *Biochem Biophys Res Commun*. 280:541-7.

Nichols, B. 2003. Caveosomes and endocytosis of lipid rafts. *J Cell Sci*. 116:4707-14.

Nichols, B.J., A.K. Kenworthy, R.S. Polishchuk, R. Lodge, T.H. Roberts, K. Hirschberg, R.D. Phair, and J. Lippincott-Schwartz. 2001. Rapid cycling of lipid raft markers between the cell surface and Golgi complex. *J Cell Biol*. 153:529-41.

Nourry, C., S.G. Grant, and J.P. Borg. 2003. PDZ domain proteins: plug and play! *Sci STKE*. 2003:RE7.

O'Loughlin, E.V., and R.M. Robins-Browne. 2001. Effect of Shiga toxin and Shiga-like toxins on eukaryotic cells. *Microbes Infect*. 3:493-507.

Olkkonen, V.M., and E. Ikonen. 2006. When intracellular logistics fails--genetic defects in membrane trafficking. *J Cell Sci*. 119:5031-45.

Opdam, F.J., A. Echard, H.J. Croes, J.A. van den Hurk, R.A. van de Vorstenbosch, L.A. Ginsel, B. Goud, and J.A. Fransen. 2000. The small GTPase Rab6B, a novel Rab6 subfamily member, is cell-type specifically expressed and localised to the Golgi apparatus. *J Cell Sci*. 113 (Pt 15):2725-35.

Ostermeier, C., and A.T. Brunger. 1999. Structural basis of Rab effector specificity: crystal structure of the small G protein Rab3A complexed with the effector domain of rabphilin-3A. *Cell*. 96:363-74.

Pan, X., S. Eathiraj, M. Munson, and D.G. Lambright. 2006. TBC-domain GAPs for Rab GTPases accelerate GTP hydrolysis by a dual-finger mechanism. *Nature*. 442:303-6.

Pecot, M.Y., and V. Malhotra. 2004. Golgi membranes remain segregated from the endoplasmic reticulum during mitosis in mammalian cells. *Cell*. 116:99-107.

Pecot, M.Y., and V. Malhotra. 2006. The Golgi apparatus maintains its organization independent of the endoplasmic reticulum. *Mol Biol Cell*. 17:5372-80.

Pelham, H. 2000. Getting stuck in the Golgi. *Traffic*. 1:191-2.

Pelham, H.R. 1996. The dynamic organisation of the secretory pathway. *Cell Struct Funct*. 21:413-9.

Pelham, H.R. 2001. SNAREs and the specificity of membrane fusion. *Trends Cell Biol*. 11:99-101.

Pereira, G., T.U. Tanaka, K. Nasmyth, and E. Schiebel. 2001. Modes of spindle pole body inheritance and segregation of the Bfa1p-Bub2p checkpoint protein complex. *Embo J*. 20:6359-70.

Pereira-Leal, J.B., and M.C. Seabra. 2000. The mammalian Rab family of small GTPases: definition of family and subfamily sequence motifs suggests a mechanism for functional specificity in the Ras superfamily. *J Mol Biol*. 301:1077-87.

Pereira-Leal, J.B., and M.C. Seabra. 2001. Evolution of the Rab family of small GTP-binding proteins. *J Mol Biol*. 313:889-901.

Perera, H.K., M. Clarke, N.J. Morris, W. Hong, L.H. Chamberlain, and G.W. Gould. 2003. Syntaxin 6 regulates Glut4 trafficking in 3T3-L1 adipocytes. *Mol Biol Cell*. 14:2946-58.

Pfeffer, S. 2003. Membrane domains in the secretory and endocytic pathways. *Cell*. 112:507-17.

Pfeffer, S. 2005a. A model for Rab GTPase localization. *Biochem Soc Trans*. 33:627-30.

Pfeffer, S., and D. Aivazian. 2004. Targeting Rab GTPases to distinct membrane compartments. *Nat Rev Mol Cell Biol*. 5:886-96.

Pfeffer, S.R. 2001. Rab GTPases: specifying and deciphering organelle identity and function. *Trends Cell Biol*. 11:487-91.

Pfeffer, S.R. 2005b. Structural clues to Rab GTPase functional diversity. *J Biol Chem*. 280:15485-8.

Ponnambalam, S., M. Girotti, M.L. Yaspo, C.E. Owen, A.C. Perry, T. Suganuma, T. Nilsson, M. Fried, G. Banting, and G. Warren. 1996. Primate homologues of rat TGN38: primary structure, expression and functional implications. *J Cell Sci*. 109 (Pt 3):675-85.

Ponting, C.P., C. Phillips, K.E. Davies, and D.J. Blake. 1997. PDZ domains: targeting signalling molecules to sub-membranous sites. *Bioessays*. 19:469-79.

Preisinger, C., and F.A. Barr. 2005. Kinases regulating Golgi apparatus structure and function. *Biochem Soc Symp*:15-30.

Preisinger, C., B. Short, V. De Corte, E. Bruyneel, A. Haas, R. Kopajtich, J. Gettemans, and F.A. Barr. 2004. YSK1 is activated by the Golgi matrix protein GM130 and plays a role in cell migration through its substrate 14-3-3zeta. *J Cell Biol*. 164:1009-20.

Pylypenko, O., A. Rak, T. Durek, S. Kushnir, B.E. Dursina, N.H. Thomae, A.T. Constantinescu, L. Brunsveld, A. Watzke, H. Waldmann, R.S. Goody, and K. Alexandrov. 2006. Structure of doubly prenylated Ypt1:GDI complex and the mechanism of GDI-mediated Rab recycling. *Embo J*. 25:13-23.

Raiborg, C., T.E. Rusten, and H. Stenmark. 2003. Protein sorting into multivesicular endosomes. *Curr Opin Cell Biol*. 15:446-55.

Reynolds, A., D. Leake, Q. Boese, S. Scaringe, W.S. Marshall, and A. Khvorova. 2004. Rational siRNA design for RNA interference. *Nat Biotechnol*. 22:326-30.

Richardson, P.M., and L.I. Zon. 1995. Molecular cloning of a cDNA with a novel domain present in the tre-2 oncogene and the yeast cell cycle regulators BUB2 and cdc16. *Oncogene*. 11:1139-48.

Robbins, E., and N.K. Gonatas. 1964. Histochemical and Ultrastructural Studies on Hela Cell Cultures Exposed to Spindle Inhibitors with Special Reference to the Interphase Cell. *J Histochem Cytochem*. 12:704-11.

Rodriguez-Boulan, E., and A. Musch. 2005. Protein sorting in the Golgi complex: shifting paradigms. *Biochim Biophys Acta*. 1744:455-64.

Rogalski, A.A., J.E. Bergmann, and S.J. Singer. 1984. Effect of microtubule assembly status on the intracellular processing and surface expression of an integral protein of the plasma membrane. *J Cell Biol*. 99:1101-9.

Roh, M.H., and B. Margolis. 2003. Composition and function of PDZ protein complexes during cell polarization. *Am J Physiol Renal Physiol*. 285:F377-87.

Rosing, M., E. Ossendorf, A. Rak, and A. Barnekow. 2007. Giantin interacts with both the small GTPase Rab6 and Rab1. *Exp Cell Res*.

Roth, M.G. 2006. Clathrin-mediated endocytosis before fluorescent proteins. *Nat Rev Mol Cell Biol*. 7:63-8.

Sambrook, J., and D.W. Russel. 2001. Molecular Cloning: A Laboratory Manual. *Cold Spring Harbor Laboratory Press*.

Sandvig, K., S. Grimmer, S.U. Lauvrak, M.L. Torgersen, G. Skretting, B. van Deurs, and T.G. Iversen. 2002. Pathways followed by ricin and Shiga toxin into cells. *Histochem Cell Biol*. 117:131-41.

Sandvig, K., S. Olsnes, J.E. Brown, O.W. Petersen, and B. van Deurs. 1989. Endocytosis from coated pits of Shiga toxin: a glycolipid-binding protein from Shigella dysenteriae 1. *J Cell Biol*. 108:1331-43.

Sandvig, K., and B. van Deurs. 2002. Transport of protein toxins into cells: pathways used by ricin, cholera toxin and Shiga toxin. *FEBS Lett*. 529:49-53.

Sato, Y., R. Shirakawa, H. Horiuchi, N. Dohmae, S. Fukai, and O. Nureki. 2007. Asymmetric coiled-coil structure with Guanine nucleotide exchange activity. *Structure*. 15:245-52.

Seabra, M.C., and E. Coudrier. 2004. Rab GTPases and myosin motors in organelle motility. *Traffic*. 5:393-9.

Shan, J., J.M. Mason, L. Yuan, M. Barcia, D. Porti, A. Calabro, D. Budman, V. Vinciguerra, and H. Xu. 2000. Rab6c, a new member of the rab gene family, is involved in drug resistance in MCF7/AdrR cells. *Gene*. 257:67-75.

Shevchenko, A., M. Wilm, O. Vorm, and M. Mann. 1996. Mass spectrometric sequencing of proteins silver-stained polyacrylamide gels. *Anal Chem*. 68:850-8.

Short, B., A. Haas, and F.A. Barr. 2005. Golgins and GTPases, giving identity and structure to the Golgi apparatus. *Biochim Biophys Acta*. 1744:383-95.

Short, B., C. Preisinger, J. Schaletzky, R. Kopajtich, and F.A. Barr. 2002. The Rab6 GTPase regulates recruitment of the dynactin complex to Golgi membranes. *Curr Biol*. 12:1792-5.

Sigismund, S., T. Woelk, C. Puri, E. Maspero, C. Tacchetti, P. Transidico, P.P. Di Fiore, and S. Polo. 2005. Clathrin-independent endocytosis of ubiquitinated cargos. *Proc Natl Acad Sci U S A*. 102:2760-5.

Sivars, U., D. Aivazian, and S.R. Pfeffer. 2003. Yip3 catalyses the dissociation of endosomal Rab-GDI complexes. *Nature*. 425:856-9.

Spiro, R.G. 2002. Protein glycosylation: nature, distribution, enzymatic formation, and disease implications of glycopeptide bonds. *Glycobiology*. 12:43R-56R.

Spooner, R.A., D.C. Smith, A.J. Easton, L.M. Roberts, and J.M. Lord. 2006. Retrograde transport pathways utilised by viruses and protein toxins. *Virol J*. 3:26.

Spooner, R.A., P.D. Watson, C.J. Marsden, D.C. Smith, K.A. Moore, J.P. Cook, J.M. Lord, and L.M. Roberts. 2004. Protein disulphide-isomerase reduces ricin to its A and B chains in the endoplasmic reticulum. *Biochem J*. 383:285-93.

Sutterlin, C., C.Y. Lin, Y. Feng, D.K. Ferris, R.L. Erikson, and V. Malhotra. 2001. Polo-like kinase is required for the fragmentation of pericentriolar Golgi stacks during mitosis. *Proc Natl Acad Sci U S A*. 98:9128-32.

Teber, I., F. Nagano, J. Kremerskothen, K. Bilbilis, B. Goud, and A. Barnekow. 2005. Rab6 interacts with the mint3 adaptor protein. *Biol Chem*. 386:671-7.

Tsai, B., Y. Ye, and T.A. Rapoport. 2002. Retro-translocation of proteins from the endoplasmic reticulum into the cytosol. *Nat Rev Mol Cell Biol*. 3:246-55.

Urbe, S. 2005. Ubiquitin and endocytic protein sorting. *Essays Biochem*. 41:81-98.

Valetti, C., D.M. Wetzel, M. Schrader, M.J. Hasbani, S.R. Gill, T.E. Kreis, and T.A. Schroer. 1999. Role of dynactin in endocytic traffic: effects of dynamitin overexpression and colocalization with CLIP-170. *Mol Biol Cell*. 10:4107-20.

Vaughan, P.S., P. Miura, M. Henderson, B. Byrne, and K.T. Vaughan. 2002. A role for regulated binding of p150(Glued) to microtubule plus ends in organelle transport. *J Cell Biol*. 158:305-19.

Watson, P., R. Forster, K.J. Palmer, R. Pepperkok, and D.J. Stephens. 2005. Coupling of ER exit to microtubules through direct interaction of COPII with dynactin. *Nat Cell Biol*. 7:48-55.

Watson, P., and D.J. Stephens. 2006. Microtubule plus-end loading of p150(Glued) is mediated by EB1 and CLIP-170 but is not required for intracellular membrane traffic in mammalian cells. *J Cell Sci*. 119:2758-67.

Weide, T., M. Bayer, M. Koster, J.P. Siebrasse, R. Peters, and A. Barnekow. 2001. The Golgi matrix protein GM130: a specific interacting partner of the small GTPase rab1b. *EMBO Rep*. 2:336-41.

Wendler, F., and S. Tooze. 2001. Syntaxin 6: the promiscuous behaviour of a SNARE protein. *Traffic*. 2:606-11.

Wennerberg, K., K.L. Rossman, and C.J. Der. 2005. The Ras superfamily at a glance. *J Cell Sci*. 118:843-6.

Wente, W., T. Stroh, A. Beaudet, D. Richter, and H.J. Kreienkamp. 2005. Interactions with PDZ domain proteins PIST/GOPC and PDZK1 regulate intracellular sorting of the somatostatin receptor subtype 5. *J Biol Chem*. 280:32419-25.

White, J., L. Johannes, F. Mallard, A. Girod, S. Grill, S. Reinsch, P. Keller, B. Tzschaschel, A. Echard, B. Goud, and E.H. Stelzer. 1999. Rab6 coordinates a novel Golgi to ER retrograde transport pathway in live cells. *J Cell Biol*. 147:743-60.

Williams, R.L., and S. Urbe. 2007. The emerging shape of the ESCRT machinery. *Nat Rev Mol Cell Biol*. 8:355-68.

Woodman, P.G. 2000. Biogenesis of the sorting endosome: the role of Rab5. *Traffic*. 1:695-701.

Wu, X., K. Rao, M.B. Bowers, N.G. Copeland, N.A. Jenkins, and J.A. Hammer, 3rd. 2001. Rab27a enables myosin Va-dependent melanosome capture by recruiting the myosin to the organelle. *J Cell Sci*. 114:1091-100.

Yao, R., C. Ito, Y. Natsume, Y. Sugitani, H. Yamanaka, S. Kuretake, K. Yanagida, A. Sato, K. Toshimori, and T. Noda. 2002. Lack of acrosome formation in mice lacking a Golgi protein, GOPC. *Proc Natl Acad Sci U S A*. 99:11211-6.

Yao, R., T. Maeda, S. Takada, and T. Noda. 2001. Identification of a PDZ domain containing Golgi protein, GOPC, as an interaction partner of frizzled. *Biochem Biophys Res Commun*. 286:771-8.

Young, J., T. Stauber, E. del Nery, I. Vernos, R. Pepperkok, and T. Nilsson. 2005. Regulation of microtubule-dependent recycling at the trans-Golgi network by Rab6A and Rab6A'. *Mol Biol Cell*. 16:162-77.

Yu, M., and D.B. Haslam. 2005. Shiga toxin is transported from the endoplasmic reticulum following interaction with the luminal chaperone HEDJ/ERdj3. *Infect Immun*. 73:2524-32.

Zahraoui, A., N. Touchot, P. Chardin, and A. Tavitian. 1989. The human Rab genes encode a family of GTP-binding proteins related to yeast YPT1 and SEC4 products involved in secretion. *J Biol Chem*. 264:12394-401.

Zerial, M., and H. McBride. 2001. Rab proteins as membrane organizers. *Nat Rev Mol Cell Biol*. 2:107-17.

Publications

Parts of this work are published in:

Articles:

Fuchs E, Short B, Barr FA. *Assay and properties of Rab6 interaction with Dynein-dynactin complexes.* **Methods Enzymol.** 2005;403:607-18.

Haas AK, **Fuchs E**, Kopajtich R, Barr FA. *A GTPase-activating protein controls Rab5 function in endocytic trafficking.* **Nat Cell Biol.** 2005 Sep;7(9):887-93.

Fuchs E, Haas AK, Spooner RA, Yoshimura S, Lord JM, Barr FA. *Specific Rab GTPase-activating proteins define the Shiga toxin and epidermal growth factor uptake pathways.* **J Cell Biol.** 2007 Jun 11;177(6):1133-43

Haas AK, Yoshimura S, Stephens D, Preisinger C, **Fuchs E**, Barr FA. *Rab1 and Rab43 are the key Rabs required for the biogenesis and maintenance of a functional Golgi in human cells.* **J Cell Sci.** 2007 Aug 7; (Epub ahead of print)

Poster presentation:

Fuchs E, Haas AK, Yoshimura S, Barr FA. *Specific Rab GTPase-activating proteins define the Shiga toxin and epidermal growth factor uptake pathways.* ASCB Annual Meeting 2006, San Diego, USA

Acknowledgements

I would like to thank Prof. Francis Barr for giving me the opportunity to work in his lab and for his support through all the years. In his lab I learned many interesting methods and aspects of biochemistry and cell biology.

I would like to express my gratitude to Prof. Erich Nigg for generously agreeing to lead my PhD committee. I always appreciated the possibility to use the departmental facilities and to be a member of the Nigg department.

I am grateful to PD Dr. Angelika Böttger for agreeing to be the second referee for this thesis. I would like to thank all the members of my thesis committee for their time.

My special thanks go to Prof. Mike Lord at the University of Warwick for giving me the opportunity to carry out my very last but very important experiment for the thesis in his lab. Thanks to the toxin lab for the very pleasant time in Warwick, especially to Robert Spooner for his advice on cytotox assays and for the beer in the Virgin.

I would like to thank all present and former members of the Barr lab for the good team spirit and the funny lab times we had together, especially Alexander Haas and Shin-ichiro Yoshimura for their tough persistence to close the last GAP in the "GAPome", Robert Kopajtich for really excellent technical assistance and for subcloning the "Rabome" and Anna-Maria "Annamiarl" Göbel for assistance in the fight for women's rights in the Barr lab.

Furthermore I would like to thank Roman Körner and Christian Preisinger for the training in MS sample preparation and for all their time spent in the basement during the measurements. I am grateful for the help of Albert Ries with computer issues and for his advice concerning radioactive work (Thanks for all the waste disposals!).

For the perfect organisation of the department and for numerous chats during breaks I would like to thank Alison Dalfovo, Marianne Siebert, Alicia Baskaya, Klaus Weber, Elena Nigg, Lidia Pinto and Monika Matzner. Thanks as well to all present and former members of the Nigg department for the friendly atmosphere and their interest in Golgi seminars.

I would like to thank Anja Hanisch, Kerstin Thein and Simone Heubes for their friendship and for the various non-lab activities and Monika Mayr for the relaxing walks with Parka and Taylor and the regular late hour taxi service.

My non-lab friends Insa Kather, Christine Epp and Martina Nesper-Brock deserve big thanks for their endurance through all the years of friendship even though I had barely time to meet them.

Ein grosses Dankeschön geht an meinen Bruder Rainer und meine Schwägerin Anita für ihre Unterstützung in allen Lebenslagen, sowie an den Rest meiner Verwandtschaft für die angenehme Zeit bei diversen Festen.

Der grösste Dank gilt meinen Eltern, auf die ich mich jederzeit verlassen kann und die mich tatkräftig und ideell unterstützen, egal wie, wo und wann. Vielen Dank dafür und für die erholsamen Auszeiten daheim!

Danke, Volker, für die kostbare Zeit mit Dir in München, London und Freiburg! Ich freue mich auf unsere gemeinsame Zukunft ohne regelmäßige Abschiede auf Flughäfen und Bahnhöfen!

Curriculum Vitae

Personal data

Name: Evelyn Fuchs
Date of Birth: 24th of November 1977
Place of Birth: Kösching, Germany

School education

1984 – 1988   Primary school Pondorf
1988 – 1997   Reuchlin-Gymnasium Ingolstadt
                  06/1997 Abitur, grade: 1,3 (1,3/ 1,0)

Academic education

1997 – 2002   Studies of biochemistry at the University of Bayreuth

04/2002 – 10/2002 Diploma thesis at Degussa AG, Dr. Volker Sieber and
                   Universtity of Bayreuth, Prof. Dr. Franz-Xaver Schmid
                   Topic: "Cloning, Recombinant Expression and Characterisation
                   of Sulfohydrolase2 of the Red Algae *Chondrus crispus*"

10/2002   Diploma examination, grade: 1,4 (1,4/ 1,0)
                   Subjects: Biochemistry, biophysics, genetics and plant
                   physiology

02/2003 – 08/2007 PhD thesis at the Max-Planck-Institute of Biochemistry,
                   Martinsried, Department of Cell Biology, Prof. Dr. Erich Nigg,
                   Junior group Intracellular Protein Transport, Dr. Francis Barr
                   Topic: "Regulation of Membrane Traffic at the Golgi apparatus
                   by Rab GTPases and their GAPs"

Professional development

12/2004   Biological safety course (according to German genetic
                   engineering safety regulations (§15 GenTSV)), Max-Planck-
                   Institute of Biochemistry, Martinsried, Germany

06/2005   EMBO practical course "Electron Microscopy and Stereology in
                   Cell Biology", Ceske Budejovice, Czech Republic

02/2007 – 03/2007 Visiting scientist in the laboratory of Prof. Lord, Molecular Cell
                   Biology, University of Warwick, UK

Publications

Articles:

1. **Fuchs E**, Short B, Barr FA. *Assay and properties of Rab6 interaction with Dynein-dynactin complexes.* **Methods Enzymol.** 2005;403:607-18.

2. Haas AK, **Fuchs E**, Kopajtich R, Barr FA. *A GTPase-activating protein controls Rab5 function in endocytic trafficking.* **Nat Cell Biol.** 2005 Sep;7(9):887-93.

3. **Fuchs E**, Haas AK, Spooner RA, Yoshimura S, Lord JM, Barr FA. *Specific Rab GTPase-activating proteins define the Shiga toxin and epidermal growth factor uptake pathways.* **J Cell Biol.** 2007 Jun 11;177(6):1133-43

4. Yoshimura S, Egerer J, **Fuchs E**, Haas AK, Barr FA. *Functional dissection of Rab GTPases involved in primary cilium formation.* **J Cell Biol.** 2007 Jul 30;178(3):363-9

5. Haas AK, Yoshimura S, Stephens D, Preisinger C, **Fuchs E**, Barr FA. *Analysis of GTPase-activating proteins: Rab1 and Rab43 are key Rabs required to maintain a functional Golgi complex in human cells.* **J Cell Sci.** 2007 Aug 7; (Epub ahead of print)

Seminar talks und poster presentation:

1. Ringberg Meeting – Intracellular Protein Transport. 2004, Ringberg Castle, Tegernsee, Germany (Seminar talk). *Rab6 effector proteins at the Golgi apparatus.*

2. ASCB Annual Meeting 2006, San Diego, USA (Poster presentation). *Specific Rab GTPase-activating proteins define the Shiga toxin and epidermal growth factor uptake pathways.*

3. Molecular Cell Biology Seminar Series 2007, University of Warwick, UK (Seminar talk as visiting scientist) *Specific Rab GTPase-activating proteins define the Shiga toxin and epidermal growth factor uptake pathways.*